APPENDIX E

Water Resources Engineering

US Army Corps of Engineers

SOUTH SAN FRANCISCO BAY SHORELINE STUDY PHASE 1, ALVISO ECONOMIC IMPACT AREA

Appendix E: Water Resources Engineering

DRAFT

29 September 2014

U.S. Army Corps of Engineers

San Francisco District

This page was intentionally left blank

CONTENTS

TABLES

FIGURES

ACRONYMS

ACE	Annual Chance of Exceedance
ADH	ADaptive Hydraulics Modeling system
AEHW	Annual Extreme High Water level
CDF	Cumulative Distribution Function
CEPD	Comprehensive Evaluation of Project Datums
cfs	cubic feet per second
DDR	Design Documentation Report
DTM	Direct Transfer Method
EAD	Equivalent (or Expected) Annual Damage
EC	Engineer Circular
EM	Engineer Manual
ENSO	El Nino-Southern Oscillation
ER	Engineer Regulation
HEC-FDA	Hydrologic Engineering Center-Flood Damage reduction Analysis
HEC-RAS	Hydrologic Engineering Center-River Analysis System
HEC-SSP	Hydrologic Engineering Center-Statistical Software Package
HUC	Hydrologic Unit Code
Ktons/yr	Kilo (thousand) tons per year
LPP	Locally Preferred Plan
MEHW	Monthly Extreme High Water level
MHW	Mean High Water tidal datum
MLLW	Mean Lower Low Water tidal datum
MTL	Mean Tide Level tidal datum
NAVD88	North American Vertical Datum of 1988
NED	National Economic Development
NOAA	National Oceanographic and Atmospheric Administration
NRC	National Research Council
PDO	Pacific Decadal Oscillation
PED	Preconstruction Engineering and Design
RT	Residual Tide
SCC	California State Coastal Conservancy
SCVWD	Santa Clara Valley Water District
SLC	Sea Level Change
SSC	Suspended Solids Concentration
USACE	United States Army Corps of Engineers
USGS	United States Geological Survey
VE	Value Engineering
WSE	Water Surface Elevation

1 INTRODUCTION

1.1 PURPOSE OF THIS REPORT

This report summarizes the water resource engineering analyses required to support the planning and Federal interest determination of a multi-purpose flood risk management, ecosystem restoration, and recreation civil works project in South San Francisco Bay. This project is referred to as the "South San Francisco Bay Shoreline Study Phase 1, Alviso Economic Impact Area", or more generically as the "study" or "study area" in this report [see Figure 1 (South San Francisco Bay Shoreline Interim Study Areas)]. The area considered in the water resource engineering analyses differs from the study area, going further south into the watershed. This area for water resource engineering analyses will be referred to throughout the report as the "hydrologic study area" and is also shown in Figure 1 (South San Francisco Bay Shoreline Interim Study Areas).

This report is written as an appendix to the "Shoreline Phase 1 Study Integrated Interim Feasibility Study and Environmental Impact Statement/Report", also referred to simply as the "Integrated Document". The water resources engineering analyses span a decade of effort (2004 to 2014) and some analyses have been previously released to the public. Where analyses have been previously released to the public, they are referenced in this report as appropriate. Analyses that have not been previously released to the public are included in the main text of this report, or as an annex to this report/appendix to the Integrated Document where applicable. One exception to the unreleased analyses being included in this report is the "Tidal Flood Risk Analysis Summary Report", which is included as its own separate appendix (Appendix F) to the Integrated Document. Significant work has been produced for this project over the last decade and some analyses are not included in the previously released documents, this report, or Appendix F to the Integrated Document; because they have been superseded by other analyses.

1.2 BACKGROUND

The larger shoreline study area was originally studied in the 1980s for the purpose of determining the feasibility of, and Federal interest in, providing flood risk reduction against tidal and tidal-related fluvial inundation for developed areas within the tidal floodplain of San Francisco Bay in southern Alameda and Santa Clara County. The study report (USACE, 1988) recommended no action at that time due to the benefit-to-cost ratios of all alternatives being less than 1.0. Based on Congressional authority in 2002, the San Francisco District reviewed the previous study and determined in September of 2004 (USACE, 2004) that there was now sufficient Federal interest to proceed into the feasibility phase. It was decided to divide the study into four interim studies, due to the very large geographic extent of the shoreline study area. The four interim study areas were designated as the "Alameda County Eden Landing", Alameda County Cargill Ponds", "Santa Clara County Alviso Pond Complex", and "San Mateo County Ravenswood Ponds" (see Figure 1). It was further decided to start with the "Santa Clara County Alviso Pond Complex" interim study area. Technical work on the Santa Clara County Alviso Pond Complex interim feasibility study area progressed from 2004 to 2011, which corresponded with the completion of the USACE Feasibility Scoping Meeting milestone.

In 2011 it was mutually decided by the San Francisco District and the study's local partners (the Santa Clara Valley Water District [SCVWD] and the California State Coastal Conservancy [SCC]) to re-scope the study into a smaller area, to produce a constructible project within a reasonable time and cost. The deaths and damages caused by Hurricanes Katrina and Rita in 2005 re-focused the USACE on making public safety paramount in all USACE future activities, resulting in more stringent enforcement of existing guidance and new guidance from 2006 to present. Some of the additional USACE guidance was of concern to our local partners, as they were not required for the study at its start in 2004. As part of the re-scoping effort, the San Francisco District in partnership with the SCVWD and SCC produced an issue paper (USACE, 2011a), which recommended some changes from accepted practice on some of the USACE guidance. The San Francisco District followed the technical guidance given in the issue paper from 2011 through the USACE Alternative Formulation Briefing milestone in 2013. These additional technical analyses are described in Appendix F of the Integrated Document (Tidal Flood Risk Analysis Summary Report) and excerpted and referenced herein as appropriate.

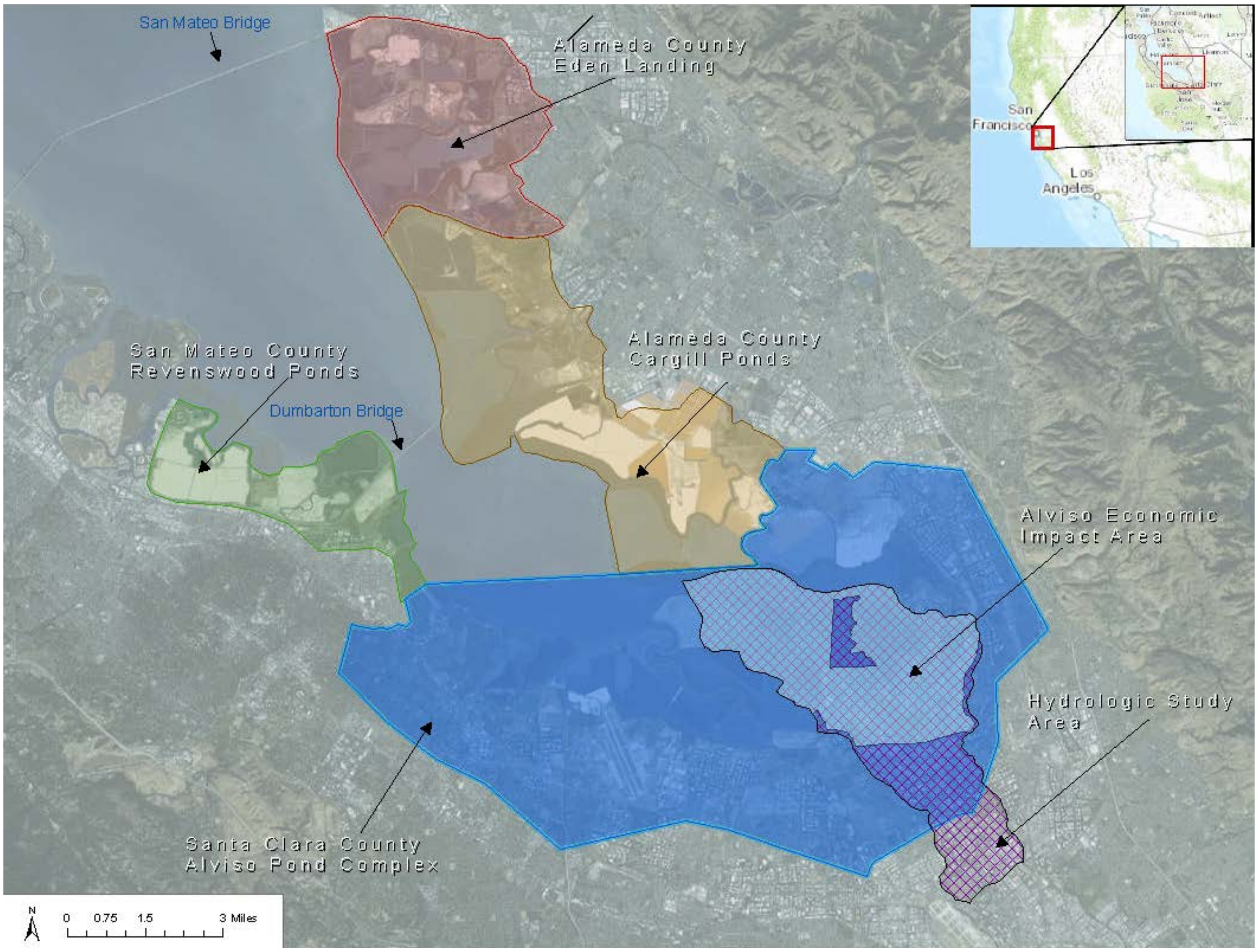

Figure 1. South San Francisco Bay Shoreline Interim Study Areas

The study's technical analyses can therefore be divided into three technical stages as given in Table 1 (The Technical Stages used in the South San Francisco Bay Shoreline Study, Phase 1). One of the significant differences between the technical stages is the treatment of sea level change (SLC). Past and current USACE policy requires that three SLC scenarios be considered when formulating and evaluating plans for a study, and was partially based on the three SLC curves given in (NRC, 1987). Typically, USACE has specified the local historical SLC for the low scenario, NRC I curve (or a modified version) for the intermediate scenario, and NRC III curve (or a modified version) for the high scenario. These National Research Council (NRC) SLC curves are shown in Figure 2-2 of (NRC, 1987); and the curves are based on a quadratic equation with the coefficients given in Table 2-4 of (NRC, 2012). The y-intercept passes through zero based on the start date for the equation; this start date varied depending on the guidance used.

Table 1. The Technical Stages used in the South San Francisco Bay Shoreline Study, Phase 1

Stage	Period	Milestone Reached	Extent - Remarks
Technical Stage I	2004 to 2011	Feasibility Scoping Meeting	Analyses covered the entire blue area in Figure 1.
Technical Stage II	2011 to 2013	Alternative Formulation Briefing	Study re-scoped so that analyses only cover the purple hatched area in Figure 1. Analyses followed guidance given in the issue paper (USACE, 2011a).
Technical Stage III	2013 to 2014	Will be included in the Public Draft Release	Analyses only cover the purple hatched area in Figure 1. Most Technical Stage II analyses were redone to meet USACE sea level change guidance.

For this report, the majority of analyses were updated during Technical Stage III to follow the latest USACE SLC guidance given in ER 1100-2-8162 (USACE, 2013). The SLC curves used during this stage were generated using the website: http://www.corpsclimate.us/ccaceslcurves.cfm. These scenarios are referred to as the USACE Low SLC scenario, USACE Intermediate SLC scenario, and USACE High SLC scenario. However, there are still some analyses being used from the previous technical stages related to the ecosystem restoration (available sediment) aspects of the project. During Technical Stage II, EC 1165-2-212 (USACE, 2011b) was followed and the Modified NRC Curve III was used in modeling the future with-project condition (see Annex 3 of this report). During Technical Stage I, (Brown, 2010) used the NRC I curve for his modeling and sediment budget analyses. The (Brown, 2010) and Annex 3 analyses were not updated to the latest SLC guidance because the uncertainty in future habitat change represents a larger uncertainty than the slight changes in SLC rates between the various guidance used. A summary of the SLC scenarios and nomenclature used in this report is given in Table 2.

With the completion of Technical Stage III, all water resources engineering technical work have been completed. All of the water resources engineering analyses needed for determination of a Federal interest and recommendation of a tentatively selected plan are now complete as of the release date of this report. No further water resources technical work is expected on this project until the Preconstruction Engineering and Design (PED) phase.

Table 2. Sea Level Change Curves and Nomenclature used in this Study

Equation for SLC Curves: $E(t) = a \times t + b \times t^2$ [ft]				
Reference - Curve	**Stage Used; Scenario/*Curve Name***	**Start date**	**a [ft/yr]**	**b [ft/yr^2]**
Historical Curve	Not Used	1986	0.00676	0
(NRC, 1987) NRC I	Technical Stage I; ***NRC I curve***	1986	0.0039	0.000092
(NRC, 1987) NRC II	Not Used	1986	0.0039	0.000217
(NRC, 1987) NRC III	Not Used	1986	0.0039	0.000344
Historical Curve	Not Used	1992	0.00676	0
(USACE, 2011b) Modified NRC Curve I	Technical Stage II; ***Modified NRC Curve I***	1992	0.0056	0.000089
(USACE, 2011b) Modified NRC Curve II	Not Used	1992	0.0056	0.000230
(USACE, 2011b) Modified NRC Curve III	Technical Stage II; ***Modified NRC Curve III***	1992	0.0056	0.000372
Historical Curve	Technical Stage III; ***USACE Low SLC scenario***	1992	0.00676	0
(USACE, 2013) Modified NRC Curve I	Technical Stage III; ***USACE Intermediate SLC scenario***	Same values as used in (USACE, 2011b), but generated from the website at: http://www.corpsclimate.us/ccaceslcurves.cfm		
(USACE, 2013) Modified NRC Curve II	Not Used			
(USACE, 2013) Modified NRC Curve III	Technical Stage III; ***USACE High SLC scenario***			

1.3 ORGANIZATION OF THIS REPORT

This report is organized into sections that provide the water resources engineering analyses in a logical order to support the project planning process. The major sections are organized by Existing Condition, Future Without-Project Condition, and Future With-project Condition. Under each major section are subsections based on technical disciplines or physical processes (watershed, hydrology, fluvial hydraulics, tidal hydraulics, and others). The report finishes with a Concluding Remarks section and References. Most of the material in this report comes from the analyses conducted during Technical Stage III, and are excerpted from Appendix F of the Integrated Document (Tidal Flood Risk Analysis Summary Report). Where appropriate material was also excerpted from other documents completed during Technical Stages I and II and other sources. Additional relevant information on analyses that have not been previously released to the public nor excerpted in this report is included in annexes to this report. Annexes 1, 3, and 4 are very large are referenced in this report, but are provided under their own separate cover, due to their size.

2 EXISTING CONDITION

2.1 WATERSHED

The hydrologic study area is contained within the downstream portion of the Coyote watershed and is bordered to the west by the Guadalupe watershed, where the Alviso Slough serves as the border between these two watersheds. The Coyote and Guadalupe watersheds, along with three other watersheds, all drain into South San Francisco Bay and make up the Coyote cataloging unit with the eight-digit USGS Hydrologic Unit Code (HUC) of 18050003. The HUC cataloging units are sometimes also referred to as watersheds. To avoid confusion throughout this report any reference to the Coyote watershed refers to the watershed and not the Coyote cataloging unit. The Coyote watershed drains approximately 325 square miles into San Francisco Bay.

The valley floor of the watershed once consisted of broad alluvial fans that were formed as streams emerged from the foothills, flattened, slowed and spread out, dropping out unconsolidated material. The watershed can now be characterized as a primarily flat valley area adjacent to San Francisco Bay, which has undergone rapid and extensive urbanization. The upstream foothills have undergone minor low density urbanization, while the steep mountainous regions have remained mostly rural, open space.

2.2 HYDROLOGY

Coyote Creek (eastern border) and Guadalupe River (Alviso Slough – western border) define the hydrologic boundaries of the hydrologic study area. The hydrology for these streams is derived from (USACE, 1977). This is the same hydrologic analysis used in the USACE's flood risk reduction projects. The 1977 results were updated for the year 2010 conditions for both Guadalupe River and Coyote Creek as described in the following paragraph. In November 2009 the District completed the Guadalupe Watershed Hydrologic Assessment (USACE, 2009) . The 2009 study updated the study methodology and results of the 1977 hydrology. The 2009 study results were found to be similar to the 1977 report. The peak discharge at the San Jose gage (USGS gage #11169000) for the 1% annual chance exceedance (ACE) event was estimated at 17,967 cubic feet per second [cfs] in 2009 and 17,000 cfs in the 1977 report, a 6% difference. The 2009 results are estimated for full built-out conditions. Since the difference in flow rates from 1977 to 2009 are so small, less than 10%, the changes in flow are not expected to change the results of the Guadalupe River hydraulics. The peak flood discharges for Guadalupe River, Coyote Creek, and Lower Penitencia Creek are shown in Table 3 (Guadalupe River, Coyote Creek, and Lower Penitencia Creek Peak Discharges). The hydrologic analyses reflect build-out conditions for each of the watersheds.

Table 3. Guadalupe River, Coyote Creek, and Lower Penitencia Creek Peak Discharges [cfs]

Location	Drainage Area [sq. mi.]	Percent Chance Exceedance / Peak Discharge [cfs]							
		50.0%	20.0%	10.0%	4.0%	2.0%	1.0%	0.4%	0.2%
Guadalupe River at San Jose (USACE, 1977)	144	2,700	4,500	6,700	9,700	13,500	17,000	21,000	32,000
Guadalupe River at San Jose (USACE, 2009)	146	3,317	6,059	7,712	10,463	14,251	17,967	22,431	27,942
Coyote Creek at Highway 237 (USACE, 1977)	321	3,300	6,200	8,400	10,500	13,000	14,500	16,000	18,000
Lower Penitencia Creek at Coyote Creek (NHC, 2006)	29	2,480	3,640	4,310	5,900	6,980	8,720	10,790	12,080

The hydrology presented above assumes that all of the flow is contained within the channel. This statement assumes that each creek contains the 50% thru the 0.2% Annual Chance Exceedance (ACE) flood events to the study limits. However, this does not represent the conditions out in the field. Where existing information was available the upstream channel capacities were taken into account and used in the Year 0 (2017) hydraulic analysis. The creeks where upstream capacity restrictions affect the Year 0 hydrology are presented in Table 4 (Guadalupe River and Coyote Creek Hydrology Based on Capacity Limitations) below. Comparing Table 3 and Table 4 shows that only the largest flow event (0.2%) differ at these locations, due to breakout of the flow upstream of the these locations.

Table 4. Guadalupe River and Coyote Creek Hydrology Based on Capacity Limitations [cfs]

Location	Drainage Area [sq. mi.]	Percent Annual Chance Exceedance / Peak Discharge [cfs]							
		50.0%	20.0%	10.0%	4.0%	2.0%	1.0%	0.4%	0.2%
Guadalupe River at San Jose	144	2,700	4,500	6,700	7009	13,500	17,000	21,000	24,050
Coyote Creek at Highway 237	320.89	3,300	6,200	8,400	10,500	13,000	14,500	16,000	17,000

Guadalupe River flow is lost between Los Gatos Creek and Hwy 880; 8,500-cfs is lost to the left flood plain and the channel capacity at Interstate highway 880 will be 24,050 cfs [see (USACE, 1991)]. The reduction of flow on Coyote Creek is limited to 17,000 cfs in the vicinity of Rock Springs Road; this is due to the loss of flow from the basin in the Canoas Creek area upstream [see (USACE, 2001)].

2.3 FLUVIAL HYDRAULICS

The two watercourses bordering the hydrologic study area are Coyote Creek and Guadalupe River (Alviso Slough). Both watercourses have had flood risk reduction projects constructed on them, with levels of performance to contain the 1-percent Annual Chance Exceedance (1% ACE) flood event, or equivalently known as a 100-year return period flood event. Existing conditions for events less than the 1% ACE are therefore contained within the watercourses. Events exceeding the 1% ACE were first modeled and calibrated using steady flow HEC-RAS models, which were subsequently modified to unsteady HEC-RAS models to determine breakout locations along the watercourses. A coincident frequency analysis was performed to determine the effects of coincidence of the peak tide and peak stream discharge and to determine the downstream boundary water surface levels. The coincident frequency analysis predicted the downstream boundary condition, influenced by tidal stage, for the unsteady HEC-RAS models. Breakout hydrographs from the unsteady HEC-RAS models were then used to model floodplain inundation using FLO-2D. Downstream boundary elevations from the coincidence frequency analysis and breakout peak outflow rates and volumes are presented in Table 5 (Existing Downstream Boundary Elevations and Peak Outflow Rates and Volumes). See Annex 1 of this report for more technical details related to the modeling efforts.

2.3.1 COYOTE CREEK

Coyote Creek originates in the Diablo Mountain Range and flows in a northeasterly direction though the cities of Morgan Hill, San Jose, and Milpitas before flowing into the San Francisco Bay. Coyote Creek is bounded by the Guadalupe River Watershed on the west and by the Diablo Mountain Range on the east. The USACE and the SCVWD built a flood risk reduction system on the lower portion of Coyote Creek. The USACE (Sacramento District) designed and built the reach upstream of Highway 237 and the SCVWD designed and built the reach downstream of Highway 237. The SCVWD is currently studying the upper portion of Coyote Creek, upstream of Montague Expressway; there may be other flow breakout locations in the upper Coyote Creek during flood events.

The Coyote Creek flood risk reduction project was designed to prevent flooding for a 1% ACE flood event downstream of Interstate Highway 880. The project consists of a bypass channel with levees, and alternate side overflow channels with offset levees and crossovers. During low flows the flows move along the natural channel to the bay. However during high flow events, the lower Coyote Creek bypass moves flood waters to the bay, bypassing the natural channel, just upstream of Lower Penitencia Creek. Flood flows from lower Coyote Creek spill into both the left (west) and right (east) floodplains. All of the flow breakout locations are concentrated downstream from Interstate highway 880 in the vicinity of Charcot Avenue. Overland flows occur in wide bands through predominantly commercial and industrial areas. On the left floodplain, the ground surface slopes away from Coyote Creek toward Guadalupe River. As a result, overland flows travel westerly and then northwesterly away from the creek. On the right floodplain, overland flows travel north between the Coyote Creek channel and Interstate Highway 880. The flow frequency curve for Coyote Creek at Highway 237 is given in Plate 17, coincident frequency (stage versus exceedance probability) results are given in Plate 43b, and the 0.2% ACE flood inundation map is shown in Plate 50, all of Annex 1 of this report (Riverine Hydraulics).

2.3.2 GUADALUPE RIVER (ALVISO SLOUGH)

Guadalupe River originates in the Santa Cruz Mountains and flows directly into San Francisco Bay, via Alviso Slough. The Guadalupe River basin is characterized by steep slopes in the mountains with a large, wide valley. The valley area is relatively flat and highly urbanized. The river flows though the heart of Silicon Valley and downtown San Jose. The drainage basin is approximately 160 square miles and 144 square miles at the confluence with Los Gatos Creek. Major tributaries to Guadalupe River include the Los Gatos Creek, Canoas Creek, Ross Creek, and Alamitos Creek watersheds.

The USACE downtown Guadalupe River flood risk reduction project includes approximately 2.5 miles of channel improvements and recreation trail for the reach of Guadalupe River between Interstate Highway 880 adjacent to downtown San Jose. This project was designed to prevent flooding for a 1% ACE flood event. Similarly, the SCVWD’s Lower Guadalupe River flood risk reduction project was constructed to contain the 1% ACE flood event and runs from Interstate Highway 880 to the bay.

The 0.5% and 0.2% ACE flood events will cause overland inundation of the floodplains. The 0.2% ACE flood event will cause widespread overland inundation on both left and right floodplains along Lower Guadalupe River. Overbank outflows from the river into the left (west) floodplain occur at two locations and into the right (east) floodplain at four locations. Left-side breakouts are located at San Jose International Airport and downstream of Montague Expressway. Right-side breakouts are all located between Montague Expressway and Tasman Drive. Flooded areas on the left floodplain include northern part of San Jose International Airport, residential and commercial areas generally located between Guadalupe River and Lafayette Street, as well as commercial and open areas in the vicinity of Highway 237; while on the right floodplain overland waters pond at Highway 237, spill over the highway between 1st Street and Zanker Road, inundate a vast area north of Highway 237 and pond behind high levees surrounding salt ponds. No water spills into the baylands from either floodplain. During the 0.2% ACE flood event, the maximum inundated area on the left floodplain is 739 acres, the mean inundation depth is 2.05 feet, and the maximum inundation depth is over 10 feet, with one isolated area at the airport deeper than 20 feet. The maximum area of inundation on the right floodplain is 1,233 acres, the mean inundation depth is 2.14 feet, and the maximum inundation depth is over 13 feet. The total inundated area (including both the left and right floodplains) is 1,972 acres.

The 0.5% ACE flood event causes localized flooding on the left (west) floodplain between the breakout location at the airport and Highway 101. The maximum overland inundation area is 42 acres, the mean inundation depth is 1.54 feet, and the maximum inundation depth is almost 20 feet.

The flow frequency curve for Guadalupe River in San Jose is given in Plate 16, coincident frequency (stage versus exceedance probability) results are given in Plate 43d, and the 0.2% ACE flood inundation maps are shown in Plates 54 and 55, of Annex 1 of this report (Riverine Hydraulics).

2.3.3 TABLE OF EXISTING BOUNDARY AND PEAK OUTFLOW CONDITIONS

Table 5. Existing Downstream Boundary Elevations and Peak Outflow Rates and Volumes*

Location	River Location	Percent Chance Exceedance / Elevation [ft NAVD88]							
		50%	20%	10%	4%	2%	1%	0.4%	0.2%
Coyote Creek	73 + 65	9.48	10.64	11.28	11.90	12.58	12.99	13.35	13.57
Guadalupe River	244 + 81	9.30	11.16	12.26	13.02	13.69	14.16	14.63	14.75

Breakout Location	Breakout Station	0.5%		0.2%	
		Flow [cfs]	Volume [ac-ft]	Flow [cfs]	Volume [ac-ft]
Coyote (East)	779+02	0	0	67	50
Coyote (West)	779+02	7	3	97	78
Guadalupe (East)	332+00	7	0.5	350	520
Guadalupe (East)	338+94	7	0.5	350	520
Guadalupe (East)	372+40	7	0.5	350	520
Guadalupe (East)	396+02	7	0.5	350	520
Guadalupe (West)	385+02	0	0	134	190
Guadalupe (West)	535+70	160	40	800	1200

*Data taken from Tables 21 and 24 of Annex 1 of this report (Riverine Hydraulics).

2.4 TIDAL HYDRAULICS

Tides and tide ranges are highly variable through the length of San Francisco Bay. Tides move through the narrow opening at the Golden Gate Bridge but are modified by bottom bathymetry, the shoreline, and the earth's rotation as they propagate throughout the San Francisco Bay estuary. Tides in San Francisco Bay are mixed semidiurnal, with two high and two low tides of unequal heights each day. The tides exhibit strong spring-neap variability, with the spring tides (larger tidal range) occurring approximately every two weeks during full and new moons. Neap tides (smaller tidal range) occur approximately every two weeks during the moon's quarter phases. The tides also vary on an annual cycle in which the strongest spring tides occur in late spring and early summer and then late fall and early winter (which may be commonly referred to by the public as king tides), and the weakest neap tides occur in spring and fall.

The South San Francisco Bay area (South Bay) has elevated tides relative to the Pacific Ocean and the rest of San Francisco Bay. The maximum tide levels generally increase with distance southward. As the tides propagate from the Pacific Ocean into San Francisco Bay, in the form of shallow water waves, the tide amplitudes and phases are modified by bathymetry, reflections from the shores, the earth's rotation and bottom friction. The enclosed nature of the bay creates a mix of progressive and standing-wave behavior for tides, meaning these waves are reflected back on themselves (Walters, et al., 1985), causing an amplification of the tides and an increase in tidal range with distance from the Golden Gate Bridge. The addition of the reflected wave to the original wave increases the tidal amplitude. Amplification causes the tidal range in the South Bay to increase southward as shown in Figure 2 (Tidal Ranges in South San Francisco Bay based on the last two National Tidal Datum Epochs). The tide range increases from 5.84 feet at the San Francisco tide gage to 9.28 feet at the Alviso Slough tide gage.

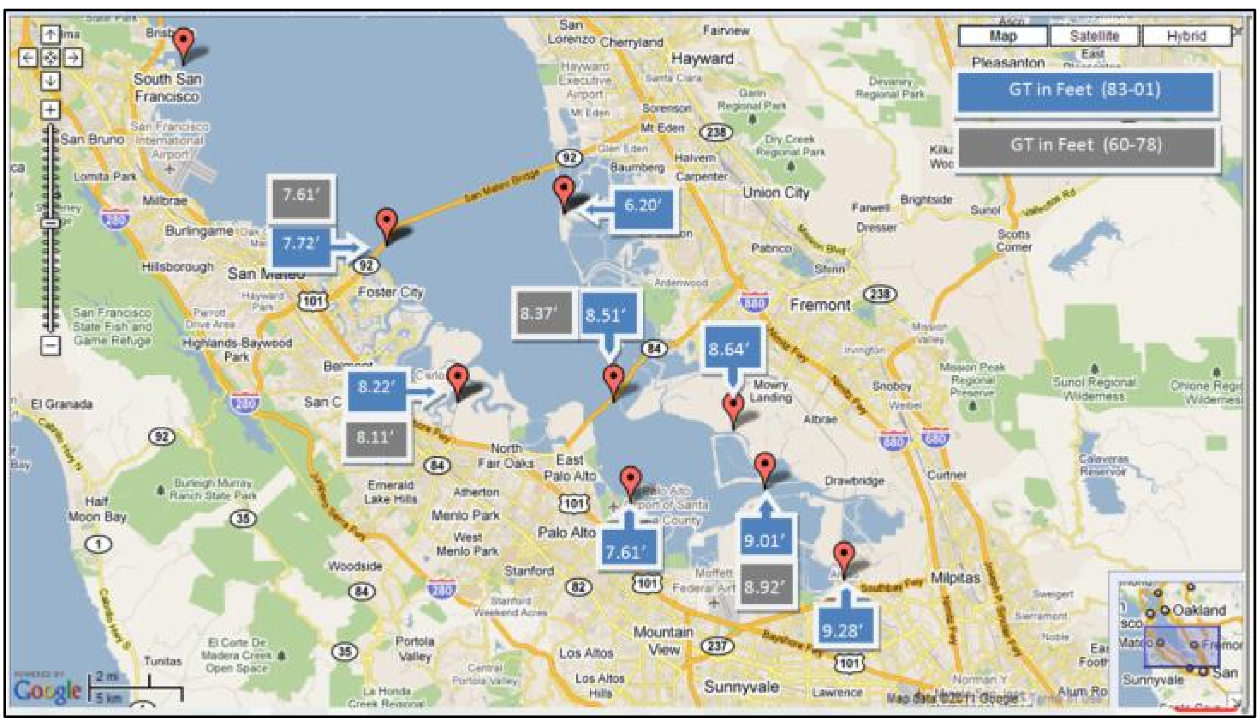

Figure 2. Tidal Ranges in South San Francisco Bay based on the last two National Tidal Datum Epochs

Tidal flood hazard analysis requires not only knowledge of astronomical tides, but also knowledge of residual tides. The residual tide is the difference between the measured water surface elevation and the water surface elevation predicted from the astronomical tide. Residual tides are commonly caused by storm events consisting of atmospheric pressure events or wind set-up. Storm events in San Francisco Bay commonly have durations of one to three days. Wind wave effects are not included in the residual tides, as they are higher frequency events that are filtered out of the tidal record.

The following subsections describe the available tidal data for San Francisco Bay, conversion of selected tidal data to the hydrologic study area, calculation of extreme water level statistics, and variability of the extreme water level statistics. The majority of information in this section comes from Appendix F of the Integrated Document (Tidal Flood Risk Analysis Summary Report); supplemented by Annexes 2 through 4 of this report (Documentation of Storm Data analysis, South San Francisco Bay Long Wave Modeling Report, and Monte Carlo Simulation Report), and [(Brown, 2010), (Sediment Analysis and Modeling for the South San Francisco Bay Shoreline Study)].

2.4.1 SAN FRANCISCO BAY TIDE DATA

There are approximately twenty active and historic water level (tide gages) measurement locations within San Francisco Bay. Tide data from two gages within the bay are used in this study (see Figure 3 (Water Level Stations used in this study)). The Coyote Creek gage (Station ID 9414575) is the closest gage to the hydrologic study area, but has a very short record length. The San Francisco gage (Station ID 9414290) has the longest continuous tide record in the United States, but is located over thirty miles from the hydrologic study area. Sections 2.4.2 (Tide Data Transfer to Hydrologic Study Area) and 2.4.3 (Extreme Water Level Statistics at the Hydrologic Study Area) describe how these two stations were used to develop the tidal data for the hydrologic study area.

Figure 3. Water Level Stations used in this study

105 years (1901 to 2005) of tide data from the San Francisco tide gage was used to identify significant storms (residual tides) and separate them from the astronomical tides. Over 500 high-water events were identified, from which forty-seven historical storm events were used to determine residual tide statistics (see Annex 2 and Figure 4). Other statistical results were also calculated from the San Francisco gage (see Appendix F (Tidal Flood Risk Analysis Summary Report) and Annex 2 (Documentation of Storm Data analysis, South San Francisco Bay Long Wave Modeling Report)). A comparison of vertical datum information between the San Francisco gage and the Coyote Creek gage is given in Table 6 (Comparison of Vertical Datum Information between the San Francisco and Coyote Creek Gages).

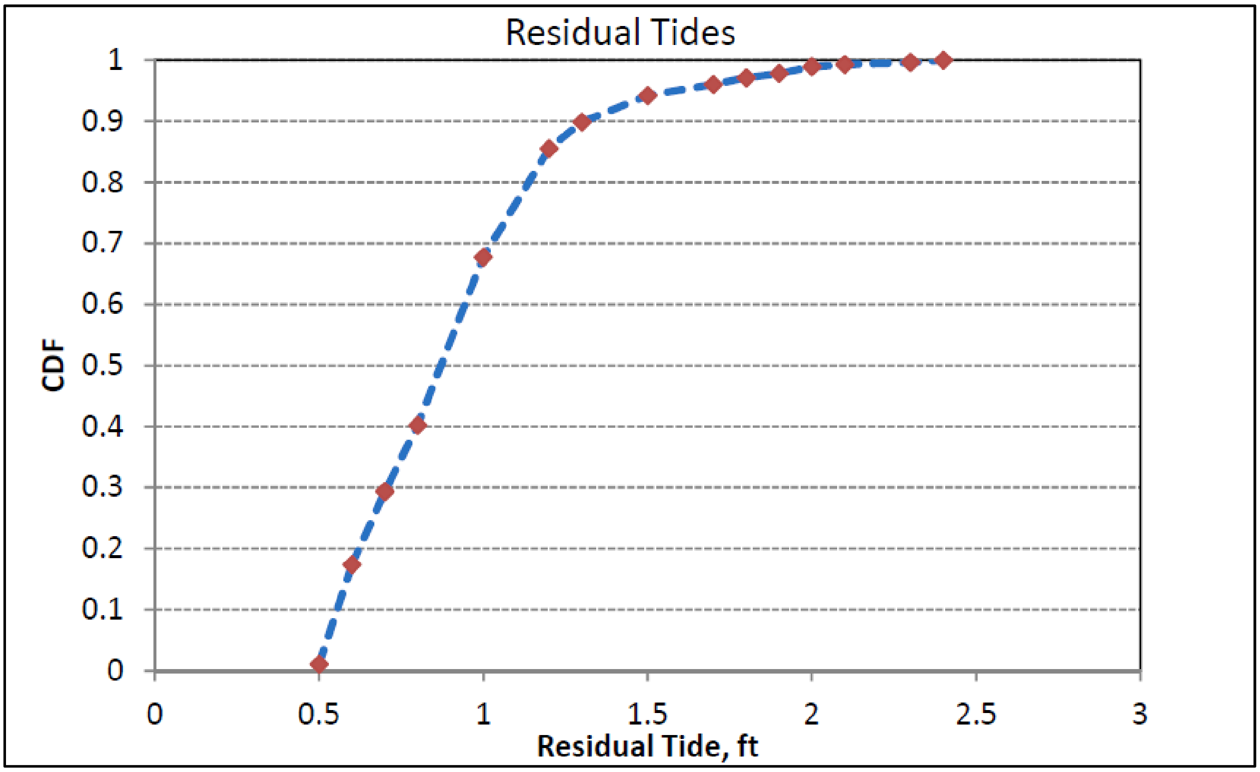

Figure 4. Cumulative Distribution Function for Residual Tides based on 47 events from gage 9414290

The Coyote Creek tide gage has been used intermittently since November 1974. A temporary National Oceanographic and Atmospheric Administration (NOAA) tide gage was deployed at Coyote Creek, Station ID 9414575, between March and August of 2011, and was used to update the tidal datum. The Mean Lower Low Water (MLLW) datum plane for the Coyote Creek tide gage was referenced to the North American Vertical Datum of 1988 (NAVD88), with some uncertainty due to difficulty in obtaining low water readings from the water level gages surveyed. The uncertainty in water surface flood elevations due to the Coyote Creek tidal datum conversion to NAVD88 has been recognized and accounted for in the water surface elevations developed for existing conditions. The project vertical datum must be the latest vertical reference frame of the National Spatial Reference System, currently NAVD88, to be held as constant for tide station comparisons, and a project datum diagram must be prepared per EM 1110-2-6056 (USACE, 2010). The Coyote Creek tide gage datum adjustment to NAVD88 will be reassessed in the PED phase, and adjustments will be made to design and other key information accordingly. A comparison of vertical datum information between the San Francisco gage and the Coyote Creek gage is given in Table 6 (Comparison of Vertical Datum Information between the San Francisco and Coyote Creek Gages).

Table 6. Comparison of Vertical Datum Information between the San Francisco and Coyote Creek s

Vertical Datum	San Francisco Gage	Coyote Creek Gage
	ID 9414290 [ft NAVD88]	ID 9414575 [ft NAVD88]
Highest Observed Water Level (27-JAN-1983)	8.72	N/A
Mean Higher High Water	5.90	7.64
Mean High Water	5.29	6.99
Mean Tide Level	3.24	3.48
Mean Sea Level	3.18	N/A
North American Vertical Datum of 1988	0.00	0.00
Mean Low Water	1.19	-0.07
Mean Lower Low Water	0.06	-1.35
Lowest Observed Water Level (17-DEC-1933)	-2.82	N/A

2.4.2 TIDE DATA TRANSFER TO HYDROLOGIC STUDY AREA

Two methods were used to transfer tide data from the San Francisco tide gage to the hydrologic study area. The first approach employed a direct transfer method between the San Francisco to Coyote Creek tide gages, where the Coyote Creek tide gage is used to represent hydrologic study area tidal conditions. The second approach used a numerical model of the San Francisco Bay – Sacramento-San Joaquin Delta system (UnTRIM Bay-Delta model, see Annex 3 (South San Francisco Bay Long Wave Modeling Report)), using twelve synthetic storm events to produce look-up tables at twenty-three predefined locations within the hydrologic study area. The look-up tables were then used as input into a Monte Carlo Simulation (MCS) program (see Annex 4 (Monte Carlo Simulation Report)) to determine water level statistics at the hydrologic study area from the San Francisco tide gage boundary condition/input. The numerical model – MCS approach was not used in the final analysis, due to changes in the geotechnical assumptions in the model and the significant increase in time and costs to re-run the simulations.

Extreme water statistics representative of coastal flood risk from high water levels in the South Bay area near the community of Alviso were developed by computing the tidal amplification factor between the predicted (astronomical) tide at the San Francisco tide gage and the Coyote Creek tide gage. Numerical modeling simulations were conducted to evaluate the change in residual tide recorded at the San Francisco tide gage as it propagated into South San Francisco Bay; these simulations indicate that residual tide varied minimally (see Annex 3 (South San Francisco Bay Long Wave Modeling Report)). Tidal residuals (observed – predicted tide) represent storm surge, and are therefore assumed to transfer directly to the South Bay. This method is referred to as the Direct Transfer Method (DTM).

Factors used to amplify the predicted tide at San Francisco are assumed to be linear and were computed by comparing predicted tide at the San Francisco tide gage to predicted tide at the Coyote Creek tide gage. The comparison indicated tidal amplification at Coyote Creek varied with predicted tide water surface elevation at the San Francisco tide gage. Four amplification factors were developed to account for the range of predicted tides, with a focus on the daily higher-high tide and are given in Table 7 (Tidal Amplification Factor from San

Francisco to Coyote Creek).

Table 7. Tidal Amplification Factor from San Francisco to Coyote Creek

Predicted Tide Range at San Francisco	Amplification Factor at Coyote Creek
Less than 4.94 feet MLLW	1.9
4.94 to 5.52 feet MLLW	1.6
5.53 to 6.15 feet MLLW	1.5
Greater than 6.15 feet MLLW	1.4

The DTM equations are given by:

$$MT_{CC} = PT_{CC} + RT_{SF} \quad \text{Equation 1.1}$$
$$PT_{CC} = (PT_{SF} - MTL_{SF}) \times A + MTL_{CC} \quad \text{Equation 1.2}$$
$$RT_{SF} = MT_{SF} - PT_{SF} \quad \text{Equation 1.3}$$

where:

MT_{CC} = Estimated Measured WSE at Coyote Creek (NAVD88)
RTSF = Residual Tide at San Francisco
PTCC = Predicted Tide at Coyote Creek
PTSF = Predicted Tide at San Francisco
MTLSF = Mean Tide Level at San Francisco (3.24’, MLLW)
A = Amplification Factor, Table 3
MTLCC = Mean Tide Level at Coyote Creek (3.48’, NAVD88)
MTSF = Measured WSE at San Francisco (MLLW)

Comparison of the derived water levels at Coyote Creek from the predicted daily higher-high tides at San Francisco showed good agreement, as seen in Figure 5 (Comparison of DTM Transferred WSE to Measured WSE at Coyote Creek) below.

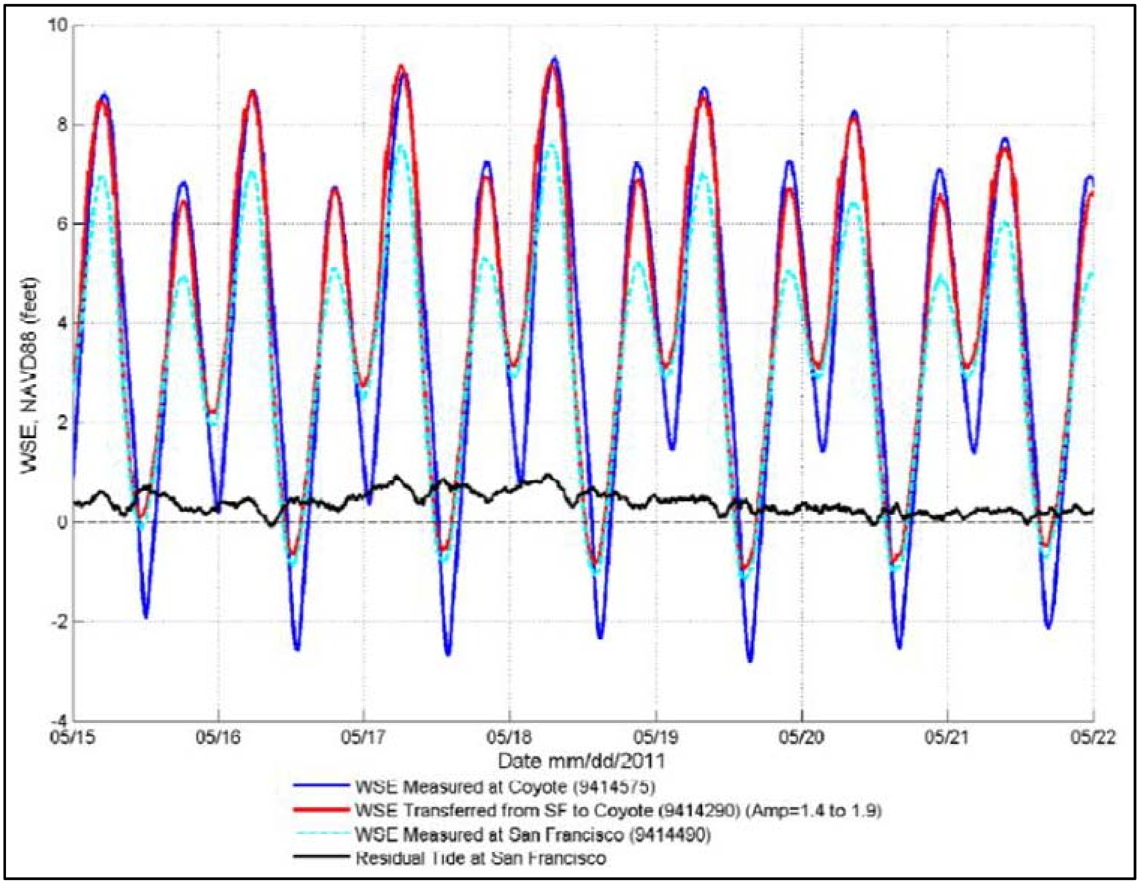

Figure 5. Comparison of DTM Transferred WSE to Measured WSE at Coyote Creek

2.4.3 EXTREME WATER LEVEL STATISTICS AT THE HYDROLOGIC STUDY AREA

Extreme water level statistics are calculated based on the DTM described in Section 2.4.2 (Tide Data Transfer to Hydrologic study area), by first computing the extreme water level statistics at the San Francisco tide gage, then applying the DTM to produce the derived Coyote Creek statistics. The results were computed using a 1992 base year, as the mid-point on which the time series data is detrended. The 1992 results are then progressed to Year 0 (2017) using the observed relative sea level rise of 0.0811 inches (2.06 millimeters) per year (an increase of 0.17 feet). For further details see Appendix F of the Integrated Document (Tidal Flood Risk Analysis Summary Report). The extreme water level statistics for both the San Francisco and Coyote Creek tide gages are given in Table 8 (Water Level Statistics for the San Francisco and Coyote Creek Tide Gages) below.

Table 8. ACE Water Levels for San Francisco and Coyote Creek Tide Gages, 1992 and 2017

	San Francisco Tide Gage (9414290)		Coyote Creek Tide Gage (9414575)	
	1992	2017	1992	2017
FREQ (%)	[feet MLLW]	[feet NAVD88]	[feet NAVD88]	[feet NAVD88]
99.99	6.89	7.12	8.25	8.42
50	7.48	7.71	9.08	9.25
20	7.81	8.04	9.54	9.71
10	8.01	8.24	9.82	9.99
4	8.25	8.48	10.15	10.32
2	8.41	8.64	10.38	10.55
1	8.56	8.79	10.59	10.76
0.4	8.75	8.98	10.85	11.02
0.2	8.88	9.11	11.04	11.21

While the numerical modeling - MCS approach was ultimately not used for transferring the San Francisco tide data to the hydrologic study area, it does provide a useful comparison and check of the results. A brief description of the numerical modeling approach is given herein. Sampling criteria and various statistical methods were developed to determine the probability input of astronomical and residual tides to the numerical model. Four scenarios were developed (three conditional sampling criteria and annual maximum) and analyzed using the extreme probability (Gumbel maximum distribution) and the joint probability methods. The results from the analyses indicated that Scenario 2 using the joint probability method provided the most reasonable results and was used for input to the Monte Carlo Simulation runs (see Annex 4 of this report (Monte Carlo Simulation Report)). The results for all four scenarios are shown in Table 9 (Water Levels for the Four Scenarios Considered for Numerical Modeling).

Table 9. Water Levels for the Four Scenarios Considered for Numerical Modeling [ft. NAVD88]

	Scenario 1	Scenario 2	Scenario 3	Scenario 4
Return Period	WSE ≥ 6.84 & RT ≥ 0.0	WSE ≥ 6.84 & RT ≥ 0.5	WSE ≥ 6.84 & RT ≥ 1.0	Annual Maximum
[years]	[ft NAVD88]	[ft NAVD88]	[ft NAVD88]	[ft NAVD88]
5	8.17	8.02	7.81	7.75
10	8.38	8.22	8.05	7.98
25	8.69	8.51	8.32	8.28
50	8.88	8.71	8.52	8.5
100	9.04	8.89	8.73	8.72
250	9.23	9.07	8.91	9.01
500	9.34	9.21	9.1	9.22

Scenario 2 using the joint probability method was selected as input in developing the look-up tables that were then used as input into the MCS model. The MCS model combined other factors such as wind speed, wind direction, and potential levee failure. While these other factors will affect the water level frequencies, they are of secondary influence when compared to the storm and tide inputs. Point 7 is the closest model output to the Coyote Creek tide gage and its results are shown in Table 10 (Water Level Frequency at Point 7 from Numerical Modeling) below.

Table 10. Water Level Frequency at Point 7 from Numerical Modeling*

Return Period [years]	Lower Bound (5%) [ft NAVD88]	Median (50%) [ft NAVD88]	Upper Bound (95%) [ft NAVD88]
2	9.51	9.55	9.58
5	9.78	9.84	9.88
10	9.97	10.05	10.14
25	10.22	10.33	10.46
50	10.35	10.53	10.65
100	10.51	10.69	10.81
250	10.68	10.85	11.05
500	10.78	10.96	11.15

*Data taken from Table 3-3 of Annex 4 of this report.

As a final check and to give better confidence in the results, the extreme water level statistic from this study was compared with results from prior studies; the comparison for the 1% ACE, or 100-year return period, is shown in Table 11 (Comparison of 1% ACE Water Level with Prior Studies).

Table 11. Comparison of 1% ACE Water Levels for San Francisco and Coyote Creek Tide Gages to Prior Studies

Gage	This Study [ft NAVD88]	Table 9 & Table 10 [ft NAVD88]	(USACE, 1984) [ft NAVD88]	(Knuuti, 1995) [ft NAVD88]	(PWA, 2007) [ft NAVD88]
San Francisco	8.79	8.89	8.69	8.89	8.72
Coyote Creek	10.76	10.69	10.99	-	11.02

Variation in the 1% ACE water levels may be attributed to many factors, such as methodology, record length and statistical methods. Accounting for these differences, the results are very consistent. The results of the current analysis, is based on an additional 7 to 31 years of data at the San Francisco tide gage. Interannual variations primarily due to El Nino-Southern Oscillation (ENSO) may influence statistics if an extreme is appended to the end of the record. Apparent SLC rates have been lower in the recent 5 to 10 years due to a neutral ENSO phase, and will account for some of the difference in the (PWA, 2007) and current result. Current SLC rates and coefficients used in the other studies have been updated in this study and account for some of the difference in results. One of the studies (PWA, 2007) contains a more in-depth discussion of the methods behind some of the other results cited.

2.4.4 NATURAL VARIABILITY, UNCERTAINTY IN COYOTE CREEK EXTREME WATER LEVEL STATISTICS

ACE statistics presented in Table 8 (Water Level Statistics for the San Francisco and Coyote Creek Tide Gages) represent the most likely or 50% occurrence. The bulk of natural variability is captured in the Cumulative Distribution Function (CDF) of tidal residuals [see Figure 4 (Cumulative Distribution Function for Residual Tides based on 47 events from gage 9414290)]. The 5 and 95 percent ACE water surface elevation estimates were computed using the DTM function and assume tidal residuals of 1.55 and 0.55 feet respectively. In the DTM formula, the residual is not amplified so the result is that the higher residual (1.55 feet) is used to compute the lower 5 percent and the lower residual (0.55 feet) is used to compute the upper 95 percent confidence interval [see Table 12 (Coyote Creek Tide Gage 2017 5, 50, 95 ACE Water Levels)]. The higher number is achieved due to a larger component of the tide is predicted or astronomical and thus subject to the amplification factor. The natural variability assumptions and computation are recognized to be a simplifying, coarse assumption, but accurate.

Combinations of water level components occurring concurrently such as high astronomical tide, storm surge residual, and extreme wind generated waves are possible, but would occur in the 95 to 99.99 percentile. The confidence interval range of the water surface elevation used in the HEC-FDA model to estimate flood damage is slightly greater than that shown in Table 12 (Coyote Creek Tide Gage 2017 5, 50, 95 ACE Water Levels). The FDA model uses order statistics to derive the confidence limit when using what is termed the "graphical method." As an example, the difference for the 50% ACE water surface elevation is about 0.1 feet, and the difference for the 0.2% ACE elevation is about 0.5 feet. Because of the small difference for the more likely events, and because the absolute value of the difference is generally symmetrical above and below the mean, this small difference in uncertainty parameters should have very little impact on the overall estimate of flood damage.

Table 12. Coyote Creek Tide Gage 2017 5, 50, 95 ACE Water Levels

	Coyote Creek Tide Gage (9414575)		
	2017 (5%)	**2017 (50%)**	**2017(95%)**
FREQ (%)	**[ft NAVD88]**	**[ft NAVD88]**	**[ft NAVD88]**
99.99	8.14	8.42	8.54
50	8.97	9.25	9.37
20	9.43	9.71	9.83
10	9.71	9.99	10.11
4	10.04	10.32	10.44
2	10.27	10.55	10.67
1	10.48	10.76	10.88
0.4	10.74	11.02	11.14
0.2	10.93	11.21	11.33

The El Niño-Southern Oscillation (ENSO) is a quasi-periodic climate pattern that occurs across the tropical Pacific Ocean about every two to seven years. It is characterized by variations in the sea-surface temperature of the tropical eastern Pacific Ocean (NRC, 2012). ENSO is the dominant cause of sea-level variability in the northeast Pacific Ocean on interannual timescales (Zervas, 2009). Sea level rises off the west coast of the United States during El Niño events and falls during La Niña events. The highest sea levels recorded along the west coast and at the San Francisco tide gage were associated with El Niño events. On January 27, 1983, during one of the largest El Niños in half a century, seven tide gages along the west coast recorded their highest water levels. This event produced a water level 2.82 feet above MHHW at the San Francisco gage. Figure 6 (San Francisco Tide Gage Record Showing Relative Sea Level Rise Increases during Major El Niño Events [From (NRC, 2012)]) and Figure 7 (Detrended San Francisco Tide Gage MEHW, Moving Average Showing Range Interannual Variability Due to ENSO) show the impact of ENSO on relative sea levels (NRC, 2012).

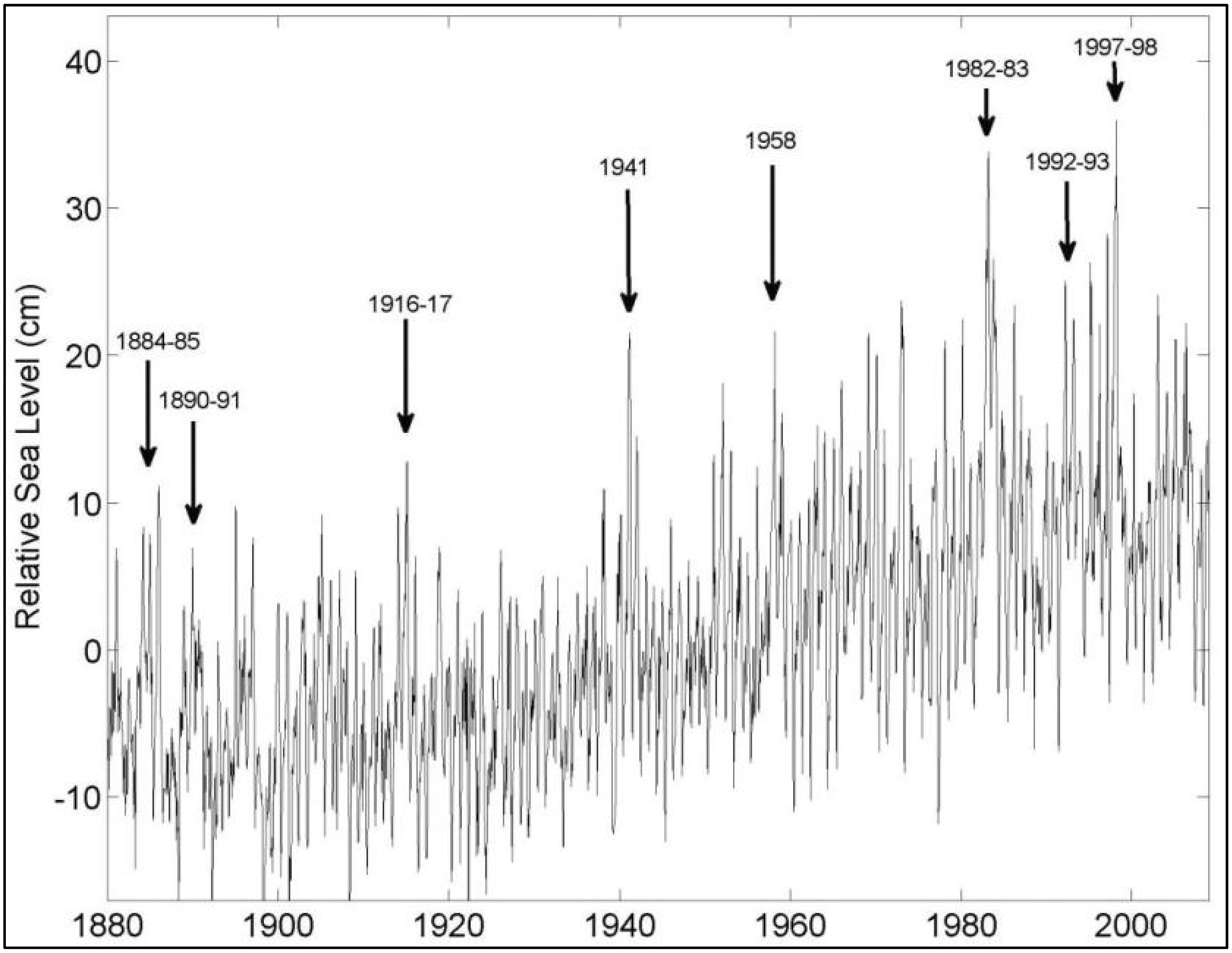

Figure 6. San Francisco Tide Gage Record Showing Relative Sea Level Rise Increases during Major El Niño Events [From (NRC, 2012)]

Most recent work on the impact of ENSO on west coast sea levels estimate the variability due to ENSO to be in the range of 0.3 to 1.0 feet (10 to 30 cm), with 0.7 feet (20 cm) the consensus. This estimate is visible by examination of Figure 7 (Detrended San Francisco Tide Gage MEHW, Moving Average Showing Range Interannual Variability Due to ENSO), which shows variability of the ENSO pattern imposed on the Monthly Extreme High Water (MEHW) level by a seven-month moving average shown in red.

Decadal and longer variability in sea level off the United States West Coast often corresponds to forcing by regional and basin scale winds associated with climate patterns such as the Pacific Decadal Oscillation (PDO) (NRC, 2012).

The daily, monthly and annual tidal cycles account for some of the natural variability in water levels and may contribute to an extreme water level when combined with other contributing factors. The Earth-Moon-Sun orbital geometry results in heightened high tides twice monthly (spring tides, near the times of the full and new moon) and every 4.4 years and 18.6 years (NRC, 2012). The largest tidal amplitudes of the year impacting San Francisco Bay occur in the winter and in summer are often more than 0.7 feet (20 cm) higher than tides in the spring and fall months. The peaks in the 4.4-year and 18.6-year cycles produce monthly high tides that are about

0.49 and 0.26 feet (15 cm and 8 cm) respectively, higher than they are in the intervening years (Flick, 2000) Table 13 (Summary of Extreme Water Level Natural Variability) summaries the various factors impacting extreme water levels.

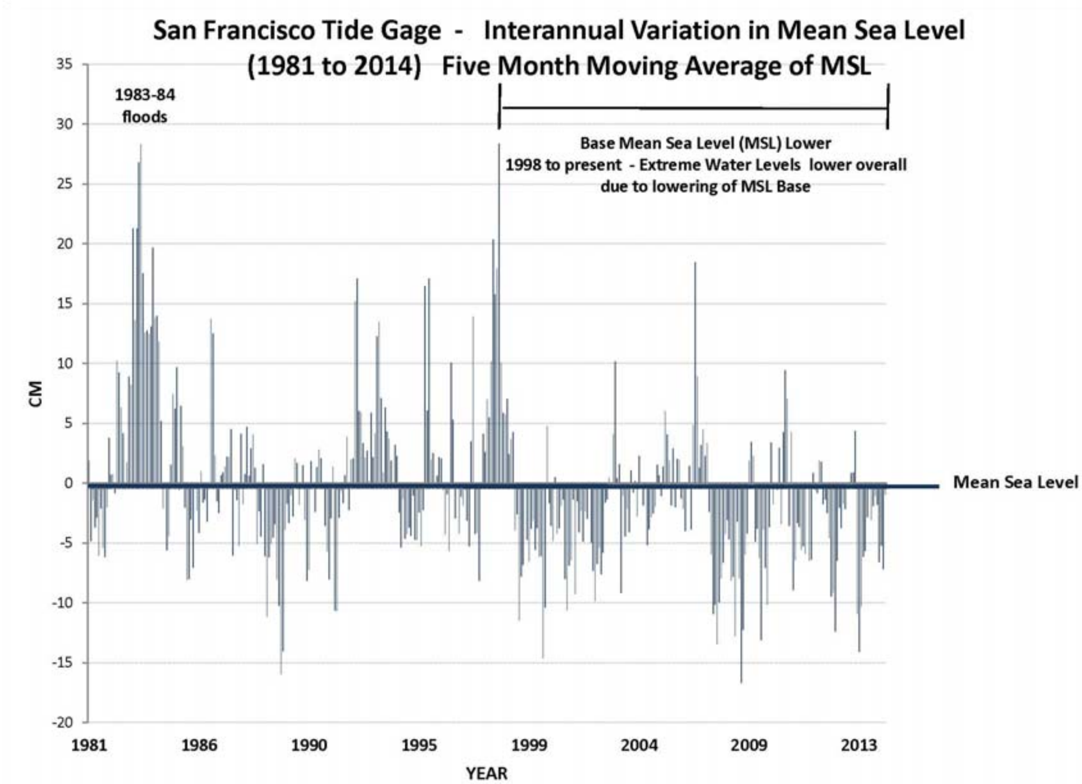

Figure 7. Detrended San Francisco Tide Gage MEHW, Moving Average Showing Range Interannual Variability Due to ENSO

Table 13. Summary of Extreme Water Level Natural Variability

Variability due to Single Event and Seasonal Climate Trends			Variability due to Tidal Cycles (added to peak)		
	Storm Surge	**ENSO**	**Seasonal**	**1 in 4.4 years**	**1 in 18.6 years**
feet	0.55 – 1.55	0.32 – 0.98	0.66	0.49	0.26
cm	17 – 47	10 – 30	20	15	8
Mean (feet)	0.85	0.66	0.66	0.49	0.26
S (feet)	0.54	0.33			

The water level component variability discussed in this section and summarized in Table 13 is reflected in the overall statistics developed for the San Francisco tide gage and DTM function for Coyote Creek. Uncertainty in the ACE for the Coyote Creek tide gage is estimated by a simple uncertainty model created through estimates of two of the major factors identified in Table 13. The total uncertainty in extreme water levels for the Coyote Creek tide gage is developed using Equation 1-4, adapted from EM 1110-2-1619 [(USACE, 1996), (Risk-Based Analysis for Flood Damage Reduction Studies)]:

$$S_{Z,total} = \sqrt{S^2_{Z,natural} + S^2_{Z,\mathrm{model}} + S^2_{Z,datum}}$$ Equation 1.4

where

$S_{Z,\,total}$ = total standard deviation of error representing uncertainty in extreme water levels

$S_{Z,\,natural}$ = the standard deviation associated with uncertainty in extreme water levels due to natural variability

$S_{Z,\,model}$ = the standard deviation associated with uncertainty in extreme water levels due to application and assumptions in the Direct Transfer Function (DTM)

$S_{Z,\,datum}$ = the standard deviation associated with uncertainty in extreme water levels due to tidal datum to geodetic datum gage conversion

The factors comprising the total uncertainty [see Table 14 (Uncertainty Estimate for the Confidence Intervals for the Coyote Creek Gage ACE)] are assumed to occur independently of each other, and determine the confidence interval applied to the ACE water surface elevations for Coyote Creek tide gage. The ACE elevations and associated confidence interval represent the coastal elevation-probability function which describes exposure in the economics model, HEC-FDA. The approximate confidence interval estimated by equation 1-4, 0.76 feet, is input as an “equivalent gage record” value in HEC-FDA. The equivalent gage record was estimated by a sensitivity analysis using HEC-SSP software in which gage record lengths in years were input into a graphical frequency analysis model created with the San Francisco tide gage Annual Extreme High Water (AEHW) level values and run to produce confidence intervals roughly equivalent to the value developed by equation 1.4 (Deering, 2014), in effect “backing into an equivalent gage value” which approximates the uncertainty estimate developed by equation 1.4. The HEC-SSP sensitivity analysis yielded an equivalent gage value of approximately 35 to 40 years.

Table 14. Uncertainty Estimate for the Confidence Intervals for the Coyote Creek Gage ACE Values

	Source/Type of Uncertainty				
	Natural		**Model**	**Datum**	**Total**
	Storm Surge	**ENSO**	**DTM function**		
S (feet)	0.54	0.33	0.33	0.25	
S^2 (feet)^2	0.29	0.11	0.11	0.06	0.57
S (feet)					0.76

2.5 SEDIMENT DYNAMICS

The general circulation pattern of sediment within San Francisco Bay has been well described by several researchers [e.g., (OBA, 1992)]. Quantification of these various transport mechanisms is very problematic, but a qualitative description of the dominant processes can be given for general guidance. San Francisco Bay can be geomorphologically divided into three bays: North Bay (e.g. San Pablo Bay), Central Bay, and South Bay. We now further divide the South Bay into South Bay (from roughly the Bay Bridge to the Dumbarton Bridge) and Far South Bay (the portion of the bay located south of Dumbarton Bridge). The hydrologic study area is located within and adjacent to Far South Bay.

Sediment supplied to San Francisco Bay via the Sacramento/ San Joaquin Delta tends to settle in the upper bays. Some large flow events can carry suspended sediment all the way to Central and South Bay, but most of the annual sediment load is deposited further upstream. Most of this sediment inflow occurs during the winter and spring. In the summer, daily winds tend to re-suspend the sediment in the shallows via wind-wave action. The sediment is then slowly transported though the bay system to Central Bay. When the sediment reaches Central Bay, it either resettles in Central Bay, travels through the Golden Gate and out of the system, or is transported into South Bay. Once in South Bay, the sediment is either deposited within the bay, or passes through Dumbarton Bridge into Far South Bay.

In addition, wave heights in Far South Bay are mitigated by their passage though the gap at Dumbarton Bridge (Smith, 2009), the dog-leg in the tidal channel and the sheltering effect provided by the pond-dike system (Annex 4 of this report). This can create a suspended sediment concentration gradient across the Dumbarton Bridge opening, and drive a net tidal dispersive transport towards Far South Bay. Sediment deposits in Far South Bay until an equilibrium is achieved between sediment supply and hydraulic erosion (tidal and wind wave erosion). The excess sediment is then transported towards Central Bay via the main tidal channel, and recirculates through the system. Also, locally derived sediment from tributaries is a significant fraction of the total available sediment in the system. These sediments are transported together with the sediments derived from the Sacramento/ San Joaquin Delta.

Suspended solids concentration (SSC) in South Bay exhibits highly dynamic short-term variability, primarily in response to sediment input from tributaries and sloughs and to tidally driven and wind-driven resuspension [(Cloern, et al., 1989); (Powell, et al., 1989); and (Schoellhamer, 1996)]. SSCs are temporally variable on tidal and seasonal scales and exhibit strong diurnal and spring-neap variability, with the highest SSCs occurring on spring tides. On a seasonal time scale, SSCs are higher in the summer months when average wind speeds and wind-wave action are greatest. Greater wind-wave action increases resuspension and reworking of the sediment deposited during the previous winter months. Wind is the most dynamic factor affecting temporal and spatial variability in SSCs (May, et al., 2003). In general, increases in fetch and wind speed will result in larger wind waves, and, in the South Bay's broad shoals, these wind waves re suspend sediments, creating more turbid conditions. Lateral exchange is also an important mechanism for sediment transport [(Jassby, et al., 1996); (Schoellhamer, 1996)]. Lateral surface flows (between the channel and shoal) result from differing velocities in the channel relative to the shoals and the interaction of tidal flow with channel-shoal bathymetry. These lateral flows can transport a significant amount of sediment to the channel (Jassby, et al., 1996), which can in turn lead to an export of sediment to Central Bay.

2.5.1 SEDIMENT TRANSPORT

The existing conditions sediment transport was modeled using the ADH hydrodynamic model coupled with the (Teeter, et al., 2001) sediment transport method (Brown, 2010). Modeling results indicate that Far South Bay currently receives surplus sediment, which is either stored as net deposition, or exported from Far South Bay via ebb currents in the main tidal channel. The numerical modeling analysis shows that, for the limited increase in sediment demand due to the proposed pond-breaching projects associated with the Year 0/baseline (2017) conditions, the sediment needed to supply these ponds will likely be derived from outside the far South Bay system. Therefore the equilibrium between the sediment supply and the hydrodynamic conditions should be maintained at Year 0, and, furthermore, the projected sediment supply through Year 50 should keep up with sea level rise for USACE Intermediate SLC scenario. Far South Bay (south of Dumbarton Bridge) currently receives surplus sediment, which is either stored as net deposition or exported from Far South Bay via ebb currents in the main tidal channel. The crucial threshold for disruption of the recent historical morphologic trend toward net deposition in Far South Bay is the threshold sediment demand, where the system switches from a sediment-rich system to a sediment-starved system.

2.5.2 SEDIMENT BUDGET

The sediment budget for South Bay—which is an accounting of all sediment delivery, export, and storage—includes mostly waterborne sediments in tributary inflows, outflows to Central Bay, dredging and deposition within open water areas, existing marshes, and restored ponds. Published sediment budgets for San Francisco Bay covering the period of 1955 through 1990 [(Krone, 1979); (Krone, 1996); (OBA, 1992); (Schoellhamer, 2011)] were reviewed and used in this study. These budgets include estimates of fluvial sediment inputs from the Sacramento/ San Joaquin Delta and local watersheds, bathymetric change, upland disposal of dredge material, and loss of sediment under Golden Gate Bridge. Recent research by (Foxgrover, et al., 2004) proposes significant revisions to earlier sediment budgets with important implications for the hydrologic study area and suggest that South Bay has undergone net erosion from 1956 through 1983, rather than deposition. The most recent review (Zoulas, 2013) and research (Barnard, et al., 2013) were not used in this study. These references should be consulted during the PED phase of the project to determine if design changes are needed at that time.

As part of this study, (Scott, 2009) developed a new analysis of these local tributary inflows using the same data source, as well as one-dimensional Hydrologic Engineering Center (HEC)-6 numerical modeling results. The analysis indicates a significantly lower sediment yield to South Bay than is predicted by the previous methods, especially with respect to tributary inflows to Far South Bay. This is likely because the previous analyses assume that a large fraction of sediment load in the river reaches South Bay. Scott's analysis accounts for the fact that most coarse-grained sediments are not transported to South Bay because of the sharp decrease in hydraulic gradient in the tributaries as they approach South Bay. These coarse-grained sediments settle in the channel and riparian floodplain, and they either remain in situ (in place) or are dredged or mined. Therefore, Scott's analysis accounts for only the fraction of sediment that reaches South Bay, which yields a smaller estimate of these tributary inflows. (Scott, 2009) provided local tributary sediment inflow estimates that total 109 thousand tons per year (Ktons/yr), with 80 [Ktons/yr] flowing into South Bay and another 29 [Ktons/yr] flowing into Far South Bay.

(Brown, 2010) developed a sediment budget for Far South Bay using the tributary sediment inflow data of (Scott, 2009) and the bathymetric change calculations given in (OBA, 1992). The sediment budget was developed for historical (1956-1990) and baseline (2017) conditions; the results are shown in Table 15 (Sediment Budgets for Historical and Baseline Conditions for the South Bay and Far South Bay).

Table 15. Sediment Budgets for Historical and Baseline Conditions for South Bay and Far South Bay

	Sediment Budget (Rate) [Thousand Tons per Year]*		
Sediment Source/Sink Term	**South Bay**	**Far South Bay**	**Total**
Historical Condition (1956 – 1990)			
Tributary Sediment Inflow	80	29	109
Net erosion/deposition of bed sediments (erosion is positive)	174	-579 (-132)	-405 (42)
Sediment exchange from Central Bay (Flux from Central Bay to South Bay is positive)	N/A	N/A	297 (-67)
Baseline Condition (2017)			
Tributary sediment inflow	80	29	109
Net erosion/deposition of bed sediments (erosion is positive)	174 (0)	0	174 (0)
Net deposition associated with restored ponds: A6, A8, A19, A20, and A21	0	–69	–69
Additional deposition due to accelerated sea level rise (0.12 inches per year)	0	–58	–58
Sediment exchange from Central Bay (flux from Central Bay to South Bay is positive)	N/A	N/A	-155 (19)

*Values in parenthesis are calculations assuming no subsidence in Far South Bay.

2.6 WATER WAVES

The waves commonly observed along the Pacific Coast and in San Francisco Bay are technically referred to as water (media of propagation) wind-driven (primary disturbing force) gravity (primary restoring force) waves, water gravity waves, wind waves, or water waves. The period of these water waves (the time duration between successive wave crests occurring) range from 1 second to 30 seconds. These waves are commonly divided into either locally generated wind waves called “seas”, or waves that have propagated long distances from their disturbing force called “swell”. Seas tend to have shorter wave periods than swell and typically look less organized. In addition to seas and swell for the hydrologic study area, seismic sea waves, also called tsunamis, may be important. For a more complete list of water wave types, see Figure 1 of (Oltman-Shay & Hathaway, 1989).

2.6.1 SEAS (WIND WAVES)

Due to the sheltering effect provided by the neighboring salt ponds and levees, seas (wind-generated short-period waves) within the hydrologic study area are minimal. Simplified wave growth formulas that predict wave growth based on restricted fetches and duration-limited criteria (Leenknecht, et al., 1992) were applied to estimate the magnitude of seas approaching the outboard dikes in accordance with respective restricted fetches and duration. The forcing wind conditions, including wind speed and direction, to estimate wave heights are identical to those used in Annex 3 of this report (South San Francisco Bay Long Wave Modeling Report). The results from the analysis are provided in a wave height lookup table (see Table 16 (Wind Waves (Seas) Look-up Table for Point 7 of the Numerical Model)). The increased water level due to seas is included in Table 10 (Water Level Frequency at Point 7 from Numerical Modeling); comparison with Table 11 (Comparison of 1% ACE Water Level with Prior Studies)shows that wind generated waves have a minimal effect on the total water elevation at the hydrologic study area.

Table 16. Wind Waves (Seas) Look-up Table for Point 7 of the Numerical Model

Wind Speed [mph]	Effective Depth [feet]					
	8.0		10.0		12.0	
	Wind Direction [Degrees]					
	292.5	315.0	292.5	315.0	292.5	315.0
Significant Wave Height [feet]						
10	0.2	0.2	0.2	0.2	0.2	0.2
20	0.6	0.6	0.6	0.6	0.6	0.6
30	1.0	1.0	1.0	1.0	1.0	1.0
40	1.4	1.4	1.5	1.4	1.5	1.4
Wave Period [seconds]						
10	0.9	0.9	0.9	0.9	0.9	0.9
20	1.5	1.4	1.5	1.5	1.5	1.5
30	1.9	1.8	1.9	1.8	1.9	1.9
40	2.2	2.1	2.2	2.2	2.2	2.2

2.6.2 SWELL

Swell is not a significant factor in determining total water level in South San Francisco Bay, due to a number of landscape constrictions within the bay. Swell must first pass through the Golden Gate, which blocks a significant portion of the swell wave energy. The swell then radiates out eastward and southward, where swell wave energy is further reduced by the land constriction near the Bay Bridge. The southward propagating swell's energy is further reduced by the land constriction by Dumbarton Bridge. What little swell energy remaining must then propagate through the dog-leg of the channel before reaching the hydrologic study area. (DHI, 2010) estimates the 1% ACE and 0.2% ACE swell to be 0.01 foot. Swell was therefore not used in determining total water level for tidal flood inundation statistics.

2.6.3 TSUNAMI

Tsunami is a Japanese word meaning "harbor wave". Tsunamis are a series of water waves generated by a large displacement of water, usually caused by a submarine earthquake; but can also be caused by volcanic eruptions, underwater explosions, landslides, ice sheets breaking apart, or meteorite impacts, above or below the water surface. The risk of inundation from a tsunami at the hydrologic study area is very low. The tsunami inundation map for the hydrologic study area only shows the potential for tsunami inundation at the outboard side of the ponds (CEMA, 2009), with the community of Alviso not at risk from tsunami inundation.

2.7 WATER SURFACE ELEVATION DEFINED HABITATS

Water surface elevations based on tidal datums and sedimentation rates was provided to delineate aquatic habitats in order to determine movement of those habitat boundaries with time. The tidal datums have been previously given in Table 6 (Comparison of Vertical Datum Information between the San Francisco and Coyote Creek Gages) of Section 2.4.1 (San Francisco Bay Tide Data). The habitat type and boundaries are given in Table 17 (Habitat Delineations based on Tidal Datums). It should also be noted that the tidal datums used for habitat delineation were not the same as those given in Table 6 [see Table 7 of (ESA PWA, 2012)], and these differences are also shown in Table 17. The differences between the two elevation ranges are less than two inches and are considered insignificant in determining habitat boundaries.

Table 17. Habitat Delineations based on Tidal Datums

Habitat*	Elevation* [ft NAVD88]	2017 Elevation* [ft NAVD88]	Difference from Table 6 [ft NAVD88]
Deep Subtidal	Deeper than 6m below MLLW	< -21.16	< -21.03
Shallow Subtidal A	2 to 6 m below MLLW	-21.16 to -8.04	-21.03 to -7.91
Shallow Subtidal B	2 m below MLLW to MLLW	-8.04 to -1.48	-7.91 to -1.52
Intertidal Mudflat	MLLW to MTL + 0.3 m	-1.48 to 4.33	-1.52 to 4.46
Cordgrass Dominated	MTL + 0.3 m to MHW	4.33 to 6.96	4.46 to 6.99
Pickleweed Dominated	MHW to MHHW	6.96 to 7.51	6.99 to 7.64
Upland	Above MHHW	> 7.51	>7.64

*From Table 7 of (ESA PWA, 2012)

The sediment historically deposited within the Alviso pond complex is a mix of sand, silt, and clay. The USGS collected sediment data between April and June 2003 indicating that the sediments on the pond bottoms within the Alviso pond complex are composed of 38 percent sand, 36 percent silt, and 26 percent clay (USGS, 2005). Grain size distributions show a marked difference from those of area sloughs, where channels are composed of 13 percent sand, 54 percent silt, and 33 percent clay (USGS, 2005).

The rate of sedimentation in natural and restored marshes depends on sediment supply in the water column, settling velocities, and the period of marsh inundation. Rates of sedimentation decrease over time as mudflats and marsh plains accrete and the period of tidal inundation decreases. Sedimentation rates near the Alviso pond complex are generally higher at present than those near the Eden Landing and Ravenswood pond complexes because of higher suspended sediment concentrations (sediment availability) and higher average sedimentation rates; historically, this was due to subsidence. Subsidence of land relative to water levels in the South Bay moderates sedimentation deceleration by maintaining low land elevations (relative to tidal water levels). This subsequently results in higher average sedimentation rates over specific periods of time. The sedimentation within the former salt ponds has not kept pace with past subsidence due to the reduced sediment supply to the ponds by the management operations. Consequently, the average elevation within the former salt ponds is several feet lower than the elevations of the adjacent wetlands just outside of the outboard levees.

2.8 FLOOD RISK

Flood risk is the combination of the likelihood of a flood hazard event and the consequences should that event happen. More detailed quantitative and qualitative description of the flood risk for the hydrologic study area is given in the Economics Appendix of the Integrated Document (Appendix D). USACE regulation ER 1105-2-101(USACE, 2006) requires a qualitative description of the flood risk, suitable for the public. The qualitative descriptions of flood risk for the historical and existing conditions are presented herein. Sections 3.8 (Flood Risk) and 4.8 (Flood Risk) describe the flood risk for future without project and future with-project conditions, and the residual flood risk that remains once the project is built.

2.8.1 HISTORICAL FLOOD RISK

The community of Alviso has been subjected to high rates of subsidence from groundwater withdrawal for agriculture for the first half of last century, causing lands to sink by four to six feet. Beginning in 1971, surface water importation from the San Francisco Regional Water System and State Water Project virtually halted further subsidence in the region by offsetting the need for groundwater pumping. While the subsidence has stopped, large portions of Alviso remain below sea level (as there is no mechanism to raise the land once it has subsided), making Alviso very susceptible to flooding.

Alviso is bordered by two watercourses, Coyote Creek to the east and Guadalupe River to the west, making Alviso vulnerable to riverine flooding. Alviso has experienced riverine flooding many times in the past, the most notable recent event being the flood from Guadalupe River in 22 – 30 January1983.

The community of Alviso has not historically suffered from a bayside (tidal) flood event. While there has been no recorded tidal flood event at Alviso, the 22 – 30 January 1983 Guadalupe River flood event also corresponded with coastal storms and extreme high tides (including the largest recorded elevation in the 105-year record of the San Francisco Gage on 27 January 1983). The Sunnyvale West Channel flood was attributed to tidal flooding on 27 January 1983 (SCVWD, 1983), and it is possible that the Guadalupe River flood event occurring at the same time could have masked any tidal flooding at Alviso; or the high tides may not have directly caused any flooding, but exacerbated the riverine flooding from Guadalupe River.

2.8.2 EXISTING FLOOD RISK

Flood risk management projects on lower Coyote Creek and Guadalupe River have significantly lowered the risk of riverine flooding for the community of Alviso. The largest remaining flood risk for Alviso comes from tidal flooding. The community of Alviso has a population at risk of tidal flooding of approximately 6,000 people; this number includes residents of Alviso as well as people who work in Alviso, but does not include people commuting through Alviso. There are also over 1,100 structures at risk from tidal flooding; made up of over 1,000 residential structures, along with other commercial, industrial, and public structures. In addition the San José-Santa Clara Regional Wastewater Facility (Wastewater Facility) is at risk from tidal flooding. The Wastewater Facility serves 1.4 million people and approximately 16,000 businesses, and has a capacity of approximately 170 million gallons per day. The Wastewater Facility has a total estimated replacement value of approximately $2.8 billion.

Based on the analyses given in Appendices D (Economics) and F (Tidal Flood Risk Analysis Summary Report) of the Integrated Document, there is an approximately one in three chance of Alviso experiencing a tidal flood event under the existing condition in any given year. It is almost certain (much greater than a 99.99% chance) that tidal flooding will occur over a 30-year mortgage period under existing conditions. Without flood risk management actions, it is almost certain that Alviso will eventually experience a tidal flood event under the existing condition. The consequences of a tidal flood at Alviso would be similar to the consequences of the riverine flood of the Guadalupe River in January 1983, resulting in substantial damages to residential and other structures and the potential for loss of life.

In addition to the tidal flood risk, there is still a residual risk of flooding from the Guadalupe River (see Section 4.8.2 for a discussion of residual risk). However this flood risk is much lower than the tidal flood risk, because of the Lower Guadalupe River flood risk management project. Similarly, there is a residual risk of fluvial flooding from Coyote Creek, but the flood waters break out above the hydrologic study area (see Plate 50 from Annex 1 of this report) and do not inundate the hydrologic study area. There is also the possibility of nuisance flooding from the existing storm drain network in the hydrologic study area. The network was originally designed to contain a 33% ACE (3-year return period) flood event and may be assumed to be currently under capacity (Schaaf & Wheeler, 2010).

3 FUTURE WITHOUT-PROJECT CONDITION

3.1 WATERSHED

The Coyote watershed within the hydrologic study area under the future without-project condition is expected to remain relatively the same as under the existing conditions without considering climate change effects. The City of San Jose's growth projections for 2012-2016 show minimal commercial development in the Alviso community, and therefore the hydrologic study area is not expected to see a significant increase in surface runoff. The upstream portions of the watershed could show significant increase in urbanization in the future. However, any increases in surface runoff from the upstream portions of the watershed are expected to be mitigated before reaching the hydrologic study area.

Climate change effects are expected to have a significant effect on the Coyote watershed. The hydrologic study area, within the downstream portion of the watershed, will be inundated from accelerated sea level rise during the fifty-year study horizon (2017 – 2067). Storm events are also expected to become more intense and of shorter durations. There is not yet enough research done to quantify the future climate statistics and they have therefore not been incorporated into the hydraulic modeling.

3.2 HYDROLOGY

Hydrology for the future without-project condition was not assumed to change significantly between Year 0 (2017) and Year 50 (2067). The San Francisquito Creek is also located in South San Francisco Bay and would experience similar hydrology changes as the hydrologic study area. According to the San Francisquito Creek Hydrology Study (SCVWD, 2007), the changes in future flows for the 1% ACE event only increase by approximately 1-2%, which is considered insignificant. This is mainly due to the limited capacity of the storm drain system, which is typical of the South San Francisco Bay Area. Therefore, no changes were made to the hydrology for Year 50.

3.3 FLUVIAL HYDRAULICS

There has not yet been enough research conducted on regional to local scale climate change effects for the hydrologic study area to quantify the future climate statistics, and they have therefore not been incorporated into the hydraulic modeling. The results of the Year 50 (2067) HEC-RAS analyses found that the water surface elevations did not change significantly from Year 0 (2017) to Year 50 (2067). From the coincident frequency analysis it was found that the Year 50 sea level change of +0.73 feet (Modified NRC Curve I) has little effect on the downstream boundary conditions, such that there is little change between Year 0 and Year 50 water surface elevations. Therefore, there is little to no change in the volume of water leaving the streams and entering the floodplains from Year 0 to Year 50. As a result there is no change in the fluvial flood inundation maps for Year 0 and Year 50 riverine floodplains for Coyote Creek and Guadalupe River (Alviso Slough).

3.3.1 COYOTE CREEK

The future without-project hydraulics for Coyote Creek are expected to remain the same as under the existing condition, which are given in Section 2.3.1 (Coyote Creek) of this report.

3.3.2 GUADALUPE RIVER (ALVISO SLOUGH)

The future without-project hydraulics for Guadalupe River are expected to remain the same as existing conditions, which are given in Section 2.3.2 (Guadalupe River (Alviso Slough)) of this report.

3.4 TIDAL HYDRAULICS

The future condition in the hydrologic study area is impacted by sea level change (rise), which in turn further reduces the performance and reliability of the existing west and east dike pond systems currently preventing tidal flooding in the hydrologic study area. Under the three USACE sea level change (SLC) scenarios, the assumption is that the tidal ranges in San Francisco Bay remain unchanged, but shift to higher levels and inland. The water level statistics are projected forward under the three USACE SLC rates. The ability of the existing dike-pond systems to prevent tidal flooding declines significantly and rapidly under the USACE High SLC scenario. Figure 8 (Alviso and the Coyote Creek Gage Exterior-Interior Relationship for Outboard Dike Breaching) illustrates the transfer in volume under an assumed failure of the dike-pond system that defines the exterior-interior relationship between Coyote Creek and Alviso in the base year of 2017.

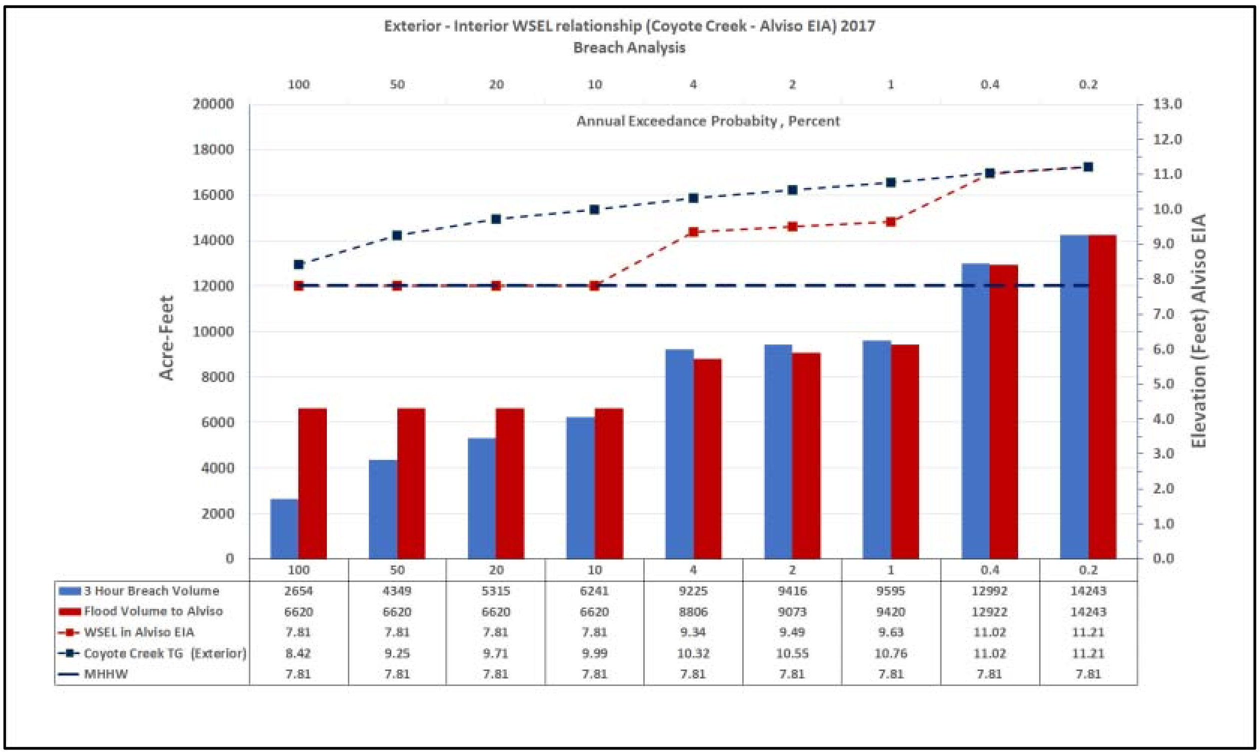

Figure 8. Alviso and the Coyote Creek Gage Exterior-Interior Relationship For Outboard Dike Breaching

The impact of SLC on the performance of the dike-pond system and the change in exterior-interior water surface elevation relationship can be seen in Figure 9 (Water Levels for Coyote Creek and Alviso for 2016 and 2067 under the USACE High SLC Scenario). The change in mean sea level, potentially several feet higher under the USACE High SLC scenario effectively eliminates any flood risk reduction benefit by the dike-pond system through storage. Water would only need to rise by 1 to 1.5 feet for the inboard dikes to be overtopped and fail. The transition to a completely open system now occurs at the 50% ACE, and the exterior-interior relationship is no longer in effect. Water surface elevations are developed in 10-year increments for the base year 2017 through 2067 using the web tool at https://corpsclimate.us/ccaceslcurves.cfm. The low rate is used for all 2017 scenarios since the base year of 2017 is so close to the current year.

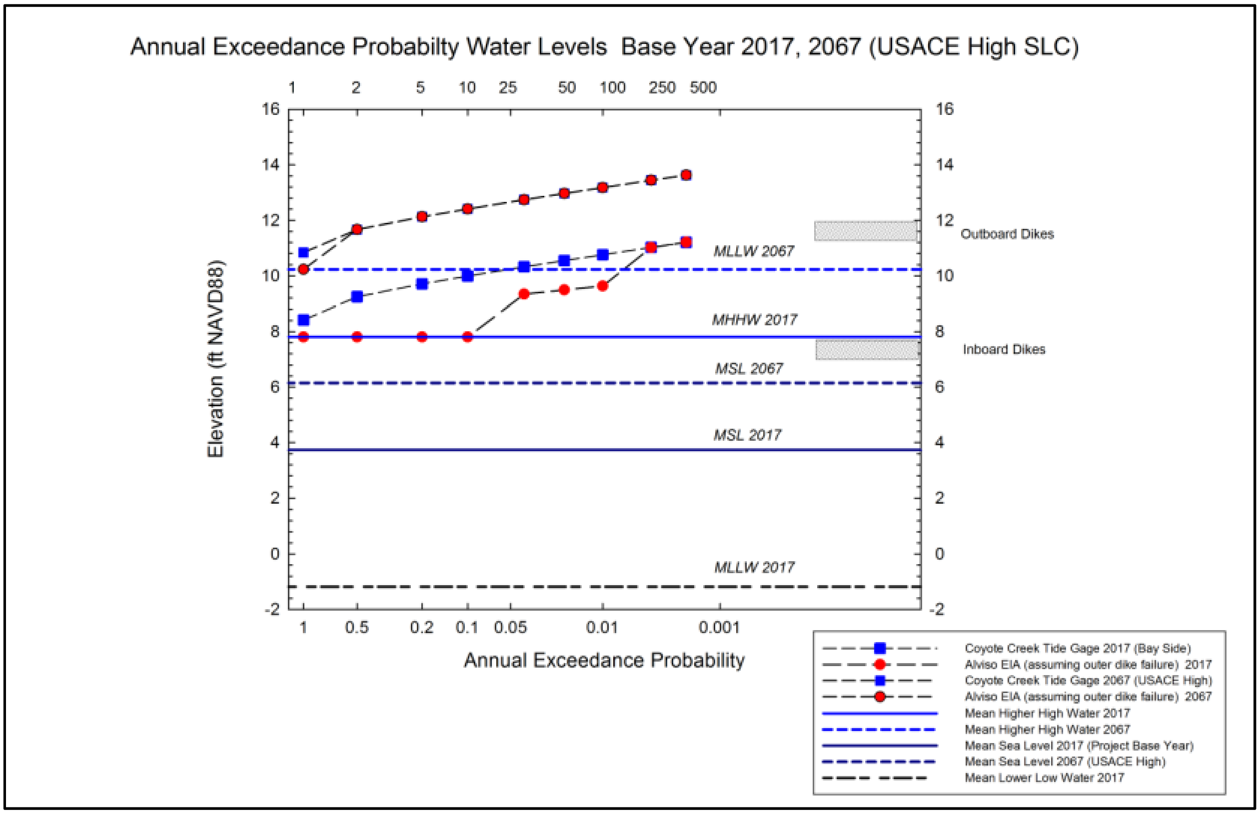

Figure 9. Water Levels for Coyote Creek and Alviso for 2016 and 2067 under the USACE High SLC Scenario

Exterior-interior relationships between the Coyote Creek tide gage and Alviso based on breach analysis developed for the existing without-project condition are estimated for the future SLC scenarios, accounting for changes impacting performance. Table 18, Table 19, and Table 20 contain ACE water levels for the three SLC scenarios, USACE Low, Intermediate, and High.

Table 18. USACE Low SLC Scenario - ACE Water Levels, Ext - Coyote Creek Gage, Int - Alviso

	2017		2027		2037		2047		2057		2067	
ACE (%)	Ext (ft.)	Int (ft.)	Ext (ft.)	Int (ft.)	Ext (ft.)	Int (ft.)	Ext (ft.)	Int (ft.)	Ext (ft.)	Int (ft.)	Ext (ft.)	Int (ft.)
99.99	8.42	7.81[1]	8.49	7.88[1]	8.55	7.94[1]	8.62	8.01[1]	8.69	8.08[1]	8.76	8.15[1]
50	9.25	7.81[1]	9.32	7.88[1]	9.38	7.94[1]	9.45	8.01[1]	9.52	8.08[1]	9.59	8.15[1]
20	9.71	7.81[1]	9.78	7.88[1]	9.84	8.50	9.91	8.45	9.98	8.65	10.05	9.20
10	9.99	7.81[1]	10.06	8.30	10.12	8.70	10.19	8.90	10.26	9.15	10.33	9.45
4	10.32	9.34	10.39	9.36	10.45	9.65	10.52	9.80	10.59	9.99	10.66	10.20
2	10.55	9.49	10.62	9.57	10.68	9.75	10.75	9.92	10.82	10.70	10.89	10.80
1	10.76	9.63	10.83	9.75	10.89	9.85	10.96	10.80	11.03	11.03	11.10	11.10
0.4	11.02	11.02	11.09	11.09	11.15	11.15	11.22	11.22	11.29	11.66	11.36	11.36
0.2	11.21	11.21	11.28	11.28	11.34	11.37	11.41	11.41	11.48	11.85	11.85	11.85

Table 19. USACE Intermediate SLC Scenario - ACE Water Levels, Ext - Coyote Creek Gage, Int - Alviso

	2017		2027		2037		2047		2057		2067	
ACE (%)	Ext (ft.)	Int (ft.)	Ext (ft.)	Int (ft.)	Ext (ft.)	Int (ft.)	Ext (ft.)	Int (ft.)	Ext (ft.)	Int (ft.)	Ext (ft.)	Int (ft.)
99.99	8.42	7.81[1]	8.60	7.99[1]	8.73	8.12[1]	8.89	8.28[1]	9.06	8.45[1]	9.26	8.65[1]
50	9.25	7.81[1]	9.43	7.99[1]	9.56	8.12[1]	9.72	8.28[1]	9.89	8.45[1]	10.09	8.65[1]
20	9.71	7.81[1]	9.89	7.99[1]	10.02	8.50	10.18	9.45	10.35	9.78	10.55	10.55
10	9.99	7.81[1]	10.17	8.50	10.30	9.50	10.46	9.65	10.63	10.49	10.83	10.83
4	10.32	9.34	10.50	9.40	10.63	9.80	10.79	10.40	10.96	10.96	11.16	11.16
2	10.55	9.49	10.73	9.68	10.86	10.60	11.02	11.02	11.19	11.19	11.39	11.39
1	10.76	9.63	10.94	10.55	11.07	11.07	11.23	11.23	11.40	11.40	11.60	11.60
0.4	11.02	11.02	11.20	11.20	11.33	11.33	11.49	11.49	11.66	11.66	11.86	11.86
0.2	11.21	11.21	11.39	11.39	11.52	11.52	11.68	11.68	11.85	11.85	12.05	12.05

Table 20. USACE High SLC Scenario - ACE Water Levels, Ext - Coyote Creek Gage, Int - Alviso

	2017		2027		2037		2047		2057		2067	
ACE (%)	Ext (ft.)	Int (ft.)	Ext (ft.)	Int (ft.)	Ext (ft.)	Int (ft.)	Ext (ft.)	Int (ft.)	Ext (ft.)	Int (ft.)	Ext (ft.)	Int (ft.)
99.99	8.42	7.81[1]	8.94	8.33[1]	9.30	8.69[1]	9.74	9.13[1]	10.26	9.65[1]	10.84	10.23[1]
50	9.25	7.81[1]	9.77	8.33[1]	10.13	8.69[1]	10.57	9.85	11.09	11.09	11.67	11.67
20	9.71	7.81[1]	10.23	8.75	10.59	9.70	11.03	11.03	11.55	11.55	12.13	12.13
10	9.99	7.81[1]	10.51	9.50	10.87	10.10	11.31	11.31	11.83	11.83	12.41	12.41
4	10.32	9.34	10.84	9.80	11.20	11.20	11.64	11.64	12.16	12.16	12.74	12.74
2	10.55	9.49	11.07	11.07	11.43	11.43	11.87	11.87	12.39	12.39	12.97	12.97
1	10.76	9.63	11.28	11.28	11.64	11.64	12.08	12.08	12.60	12.60	13.18	13.18
0.4	11.02	11.02	11.54	11.54	11.90	11.90	12.34	12.34	12.86	12.86	13.44	13.44
0.2	11.21	11.21	11.73	11.73	12.09	12.90	12.53	12.53	13.05	13.05	13.63	13.63

3.5 SEDIMENT DYNAMICS

3.5.1 SEDIMENT TRANSPORT

The predicted morphology of Far South Bay for the Year 50 condition is largely dependent on the rate of sea level rise. At lower rates of sea level rise, the sediment supply to Far South Bay exceeds the demand imposed by the rate of rise, and the morphology maintains an equilibrium planform relative to the water surface. As sea level rise accelerates, at some point a threshold is reached where the sediment supply to Far South Bay can no longer keep pace with the rate of rise, and Far South Bay becomes sediment starved. At that point, it is expected that the significant changes in the mudflat planform will occur, the mudflats begin to erode, and sediment redistributed to the most efficient sinks within the system.

Figure 10 (Year 50 (2067) Bathymetry for the USACE Intermediate SLC Scenario) is a color contour plot of the expected Year 50 bathymetry for the NRC I curve rate of sea level rise. The overall platform elevation has increased by 0.72 feet (0.22 m) over the Year 0 planform elevation, to account for the total sea level rise over the project life. This maintains the same average depth in Far South Bay, indicating that the planform is in equilibrium. Pond A6 is filled completely, and Pond A8 is partially filled.

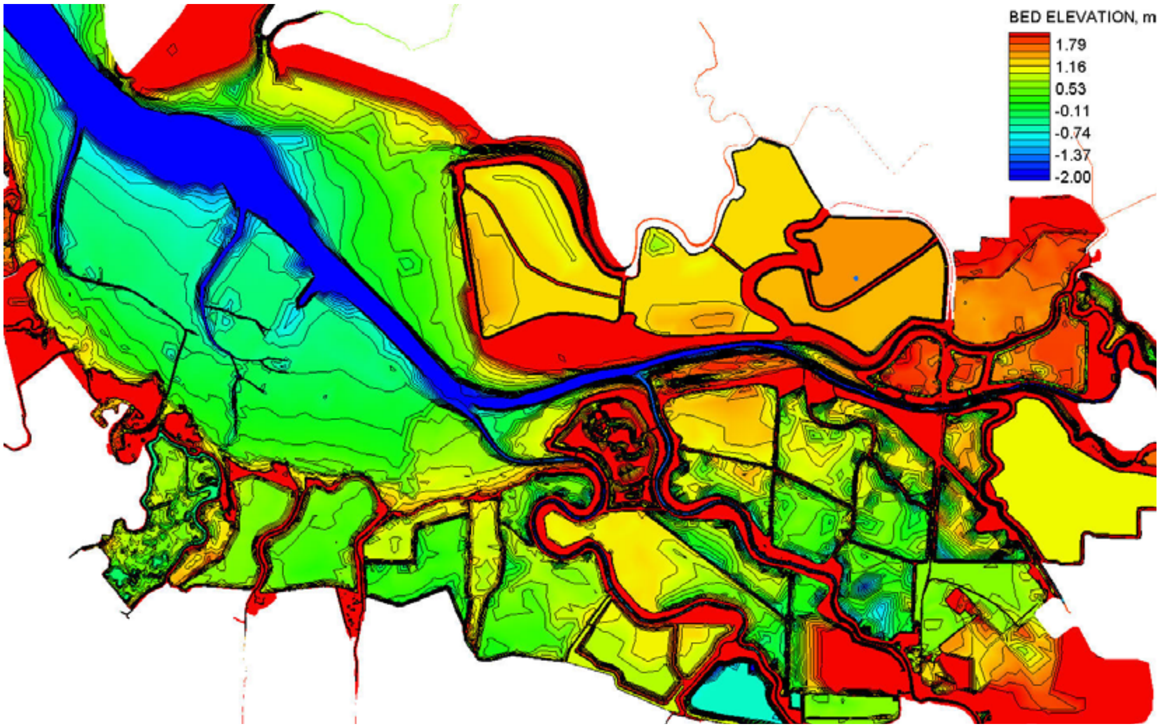

Figure 10. Year 50 (2067) Bathymetry for the USACE Intermediate SLC Scenario

3.5.2 SEDIMENT BUDGET 2067

Similarly to the historic and baseline conditions [see Table 15 (Sediment Budgets for Historical and Baseline Conditions for South Bay and Far South Bay)], a sediment budget was developed for the South Bay and Far South Bay, which used the NRC I curve to incorporate sea level change, and is shown in Table 21 (Sediment Budgets for 2067 Without Project Condition for South Bay and Far South Bay) [from (Brown, 2010)].

Table 21. Sediment Budgets for 2067 Without Project Condition for South Bay and Far South Bay

	Sediment Budget (Rate) [Thousand Tons per Year]*		
Sediment Source/Sink Term	**South Bay**	**Far South Bay**	**Total**
Tributary Sediment Inflow	80	29	109
Net erosion/deposition of bed sediments (erosion is positive)	174 (0)	0	174 (0)
Net deposition associated with restored ponds: A6, A8, and the Island Ponds	0	-23	-23
Sea Level Rise (0.00572 m/yr)	0	-150	-150
Sediment exchange from Central Bay (flux from Central Bay to South Bay is positive)	N/A	N/A	-110 (64)

*Values in parenthesis are calculations assuming no subsidence in Far South Bay.

3.6 WATER WAVES

3.6.1 SEAS (WIND WAVES)

There has not yet been enough research conducted on a regional scale to determine climate change effects for the hydrologic study area, and the seas statistics for the hydrologic study area are assumed to be the same as under the existing condition.

3.6.2 SWELL

There has not yet been enough research conducted on a regional scale to determine climate change effects for the hydrologic study area, and the swell statistics for the hydrologic study area are assumed to be the same as under the existing condition given in Section 2.6.2 (Swell); and therefore was not used in determining total water level for tidal flood inundation statistics.

3.6.3 TSUNAMI

The future without-project condition for tsunami inundation of the hydrologic study area is not expected to change from the existing condition; see Section 2.6.3 (Tsunami) for the expected condition.

3.7 WATER SURFACE ELEVATION DEFINED HABITATS

Similarly to the historic and baseline conditions (see Table 15 (Sediment Budgets for Historical and Baseline Conditions for South Bay and Far South Bay)), a sediment budget was developed for the South Bay and Far South Bay, which used the NRC I curve to incorporate sea level change, and is shown in Table 21 (Sediment Budgets for 2067 Without Project Condition for South Bay and Far South Bay). All ponds within the hydrologic study area are expected to be managed similarly to the existing condition, without a significant change in habitat. However, neighboring ponds that have been or will be breached as part of the South Bay Salt Ponds Restoration Project (such as Ponds A6 and A8) will initially increase the tidal prism, thereby scouring the channels deeper and then eventually fill in, thereby reducing the sediment supply to the hydrologic study area and limiting marsh development. Therefore, there will be a shift in habitat types towards more acreage of subtidal habitat under the future without-project condition.

3.8 FLOOD RISK

Future tidal flood risk was evaluated under the three required sea level change (SLC) scenarios: USACE Low SLC scenario, USACE Intermediate SLC scenario, and USACE High SLC scenario. There is an approximately 1 in 2 chance of Alviso experiencing a tidal flood event under the USACE Intermediate SLC scenario in any given year by 2067. It is almost certain (much greater than a 99.99% chance) that tidal flooding will occur over a 30-year mortgage period under all three scenarios. It is almost certain that Alviso will eventually experience a tidal flood event under all future without-project condition SLC scenarios. The consequences of a tidal flood at Alviso would be similar to consequences of the riverine flood of Guadalupe River in January 1983, resulting in substantial damages to residential and other structures and the potential for loss of life.

Since the hydrology for future conditions is assumed to not change significantly from existing conditions, the residual fluvial flood risk is expected to remain the same as existing conditions. Nuisance flooding of the storm drain network is expected to increase with time due to SLC. Recent work by (NOAA, 2014) shows a national trend of increased nuisance flood days, as well as the regional trend (from the San Francisco tide gage 9414290) showing similar results. Conditions at the hydrologic study area are expected to be similar. However, this increase in nuisance flooding may be mitigated, as the City of San Jose plans to upgrade the storm drain network in the future.

4 FUTURE WITH-PROJECT CONDITION

4.1 WATERSHED

Ignoring climate change effects, the with-project features (levees and ecotones) will not have any significant effect on the drainage of the watershed and therefore the future with-project condition for the Coyote watershed is expected to remain the same as under the future without-project condition given in Section 3.1 (Watershed) of this report. However, the future with-project condition will show a significant improvement over the future without-project condition when climate change effects are considered. The with-project levee features will prevent the coastal flood inundation of the downstream portion of the Coyote watershed (i.e. the hydrologic study area).

4.2 HYDROLOGY

Construction activities for the future with-project condition are expected to cause temporary disruptions to drainage paths of minor significance. These effects will be short-term and therefore the future long-term hydrology of the with-project condition is assumed to be the same as for the future without-project condition given in Section 3.2 (Hydrology) of this report, with the exception of pond breaching. Pond breaching will have a significant effect on the existing storage capacity between the outboard pond-dike and the newly constructed levee system and will alter the habitat distribution in that area. However, inboard of the levee system the hydrology is expected to remain the same.

4.3 FLUVIAL HYDRAULICS

The proposed levees will tie into the existing riverine levees on Guadalupe River/Alviso Slough and Coyote Creek. The proposed geometry would not reduce the available flow area or constrict the flow in the channel; therefore, it will not have an effect on water surface elevations in Guadalupe River/Alviso Slough or Coyote Creek. HEC-RAS models of Coyote Creek and Guadalupe River/Alviso Slough used in the without-project analysis were modified per the proposed levee design. Also, maximum tidewater elevations were increased in the with-project models to 15 feet NAVD88 to account for storm surge effects (that were not accounted for in the without project conditions). Minimum tidewater elevation under both without and with-project conditions was 2.83 ft NAVD88. Flow hydrographs representing the 1%, 0.4% and 0.2% ACE flood events were used for the with-project analyses for both watercourses. Federally constructed riverine levees on both Coyote Creek and Guadalupe River were designed to safely contain the 1% ACE flood event. Flows of magnitude equal to or less than the 1% ACE flood event will be contained in the channels within the hydrologic study area. Modeling results indicate that neither modification of the cross-section geometries (to account for the coastal levee) nor increasing the tidewater elevation to a maximum value of 15 feet NAVD88 had a significant effect on predicted backwater profiles or breakout flow rates (all changes were less than 2% -- see Tables 19.1 and 19.2 in Annex 1 (Riverine Hydraulics) of this report).

4.3.1 COYOTE CREEK

The future with-project hydraulics for Coyote Creek are expected to remain essentially the same as under the existing condition, which is given in Section 2.3.1 (Coyote Creek) of this report.

4.3.2 GUADALUPE RIVER (ALVISO SLOUGH)

The future with-project hydraulics for Guadalupe River are expected to remain essentially the same as under the existing condition, which are given in Section 2.3.2 (Guadalupe River (Alviso Slough)) of this report.

4.4 TIDAL HYDRAULICS

The with-project tidal hydraulics are significantly changed from the without-project condition. The with-project condition will have a levee of either 13.5 feet NAVD88 or 15.2 feet NAVD88 elevation in height, with the height of the levee depending on the alternative selected for the project. As shown in Table 20 (USACE High SLC Scenario - ACE Water Levels, Ext - Coyote Creek Gage, Int – Alviso), even under the USACE High SLC rate, the residual tidal flood risk has been significantly reduced, below the 0.2% ACE (500-year return period) tidal flood event up to 2057, and the 15.2 feet NAVD88 levee past 2067.

4.5 SEDIMENT DYNAMICS

The UnTRIM-SediMorph Bay-Delta modeling system was used to model bathymetry for the Year 50 (2067) with-project condition (see Annex 3 of this report (South San Francisco Bay Long Wave Modeling Report)). The model simulations incorporate both the expected accretion within the project ponds, which has been estimated as part of the ecosystem design (ESA PWA, 2012), as well as estimated channel evolution in the vicinity of the project area. It is expected that the channel and mudflat bathymetry in the project area may evolve in response to both sea level rise and due to channel adjustment, which will occur following the opening of the salt ponds to tidal action. The analysis makes use of three different methods of evaluation which use a combination of modeling and historical data analysis to estimate channel evolution in the vicinity of the project area for Year 50 condition.

First, a comparison between bathymetric and LiDAR data collected in 2004 and 2010 allowed for an assessment of the channel evolution that has occurred in the Coyote Creek region following the breaching of the three island ponds (Ponds A19, A20, and A21) in March 2006 under the South Bay Salt Ponds Restoration Project. This analysis considered the channel evolution in the project area for subtidal, intertidal and marsh areas. Second, sediment deposition patterns in mudflat and marsh areas in the Coyote region were evaluated through a short sediment transport simulation during a period when a strong net sediment flux into the Far South Bay was observed at Dumbarton Bridge. Third, the expected channel scour resulting from the restoration of Ponds A9 through A15 and Pond A18 to tidal action were investigated through simulations of channel shear stress and velocity under existing conditions and under future conditions with SLC and projected Year 50 pond bathymetry. Finally, the results of the three separate analyses were combined into a single estimate of bathymetric change in the project area to establish Year 50 (2067) conditions which included 2.13 feet (0.649 m) of sea level rise based on Modified NRC Curve III and the planned restoration of Ponds A9 through A15 and Pond A18 [see Figure 11 (Predicted Bathymetric Change for With-Project Conditions for Year 50 (2067)].

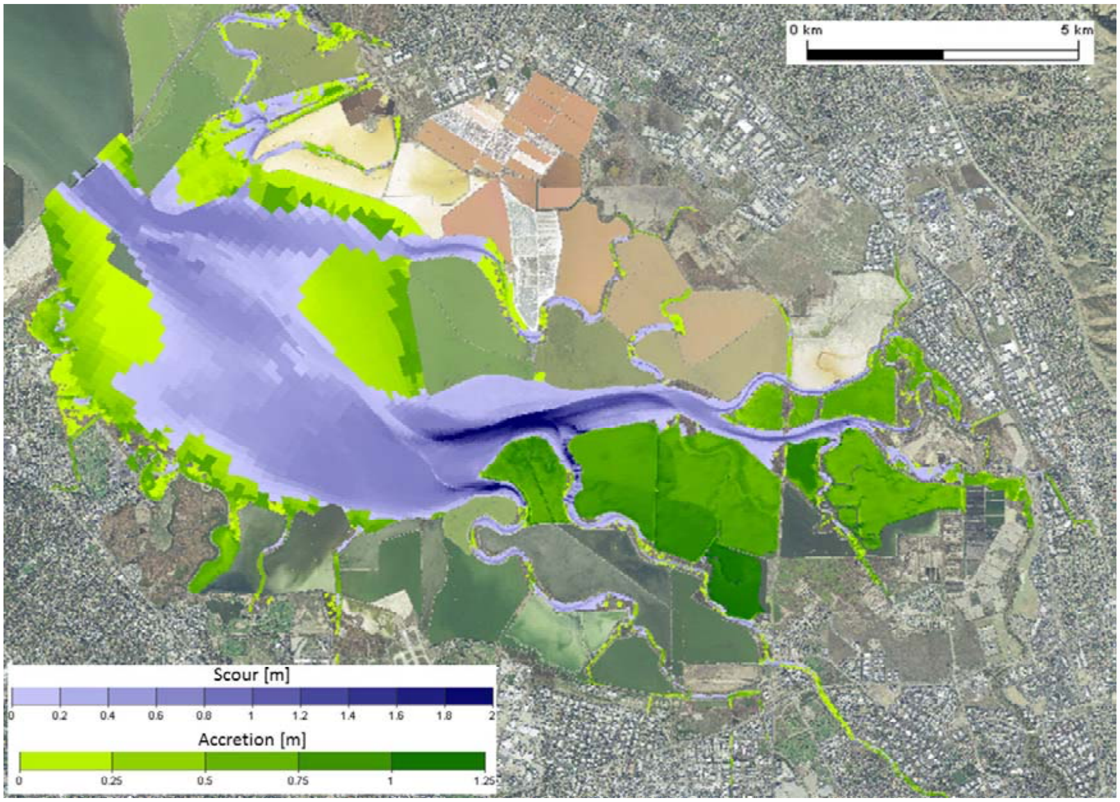

Figure 11. Predicted Bathymetric Change for With-Project Conditions for Year 50 (2067)

4.6 WATER WAVES

4.6.1 SEAS (WIND WAVES)

There has not yet been enough research conducted on a regional scale to determine climate change effects for the hydrologic study area, and the seas statistics for the hydrologic study area are assumed to be the same as under the existing condition given in Section 2.6.1 (Seas (Wind Waves)). While significant wave heights can reach up to 1.5 feet (see Table 16 (Wind Waves (Seas) Look-up Table for Point 7 of the Numerical Model)), the occurrence of large waves is associated with a very low probability (as can be inferred from Table 11 (Comparison of 1% ACE Water Level with Prior Studies)) and did not affect the design crest elevation of the with-project levee.

4.6.2 SWELL

As mentioned in Section 2.6.2 (Swell), swell will have an insignificant effect on the total water elevation for the South San Francisco Bay adjoining the hydrologic study area. The uncertainty in Coyote Creek extreme water level statistics, given in Section 2.4.4 (Variability in Extreme Water Level Statistics), are much larger than the swell; and therefore the with-project levee design is still considered conservative, even without accounting for swell.

4.6.3 TSUNAMI

The future with-project condition for tsunami inundation for the hydrologic study area may change from the existing and future without project conditions. The red area for tsunami inundation shown in (CEMA, 2009) may move shoreward towards Alviso. However, the community of Alviso is still not at risk from tsunami inundation; the with-project levee system will provide sufficient protection from tsunami inundation for the community.

4.7 WATER SURFACE ELEVATION DEFINED HABITATS

As described in Section 4.5 (Sediment Dynamics), the UnTRIM-SediMorph Bay-Delta modeling system was used to model the bathymetric changes in Year 50 (2067) future with-project condition, with the results shown in Figure 11 (Predicted Bathymetric Change for With-Project Conditions for Year 50 (2067)). The results for the hydrologic study area suggest that the majority of the sediment accretion will occur in marsh areas, that relatively little deposition will occur in mudflat areas, and that channel areas are likely to scour downstream of pond areas that are restored to tidal action. Further details are given in Annex 3 of this report (South San Francisco Bay Long Wave Modeling Report).

4.8 FLOOD RISK

4.8.1 WITH-PROJECT FLOOD RISK

Building the National Economic Development (NED) flood risk management structure (the 13.5 feet NAVD88 levee) will significantly reduce the tidal flood risk to the Alviso community. The risk of tidal flooding at Alviso ranges from an approximately 1 in 50 chance to a 1 in 2 chance at Year 2067, depending on the chosen SLC scenario. There is an approximately 1 in 50 chance of Alviso suffering a tidal flood event under the USACE Intermediate SLC scenario in any given year. The risk of tidal flooding over a 30-year mortgage period for the three SLC scenarios varies from less than a 1 in 100 chance to a 1 in 7 chance.

Building the recommended locally preferred plan (LPP) flood risk management structure (the 15.2 feet NAVD88 levee) will nearly eliminate the tidal flood risk to the Alviso community for the foreseeable future. The additional 1.7 feet of height over the NED structure further reduces the tidal flood risk to contain events much greater than those mapped by the FEMA or the USACE in 2017, and still greater than the potential FEMA base flood event by 2067.

The consequences of a tidal flood at Alviso would be similar to the consequences of the riverine flood of the Guadalupe River in January 1983, resulting in substantial damages to residential and other structures and the potential for loss of life. Building either the NED or LPP levee will provide tidal flood risk reduction sufficient to contain an event of similar magnitude to the Guadalupe River flood event of January 1983.

4.8.2 RESIDUAL FLOOD RISK

It is impossible to design and build a flood risk management structure that will provide a 100% guarantee against flooding; there will always be some remaining risk of flooding. Residual flood risk is the risk that remains after all flood risk management actions have been taken (including the building of structures, and non-structural solutions such as flood warning systems, floodplain management plans, emergency action and evacuation plans, flood related building codes, etc.). The 0.2% ACE, or 500-year return period, flood event is typically used to quantify and estimate the residual risk of a project. Expected annual damages (EAD) are also used to estimate and quantify residual risk. The residual tidal flood risk at 2017 building either the NED levee or LPP levee is so small that it could not be mapped and its EAD is negligible (nearly $0). By 2067 the EAD is still very low ($1M) for the NED levee and much less for the LPP levee, with still very little area mapped for the 0.2% ACE event.

Once the tidal flood risk management project is built, the largest residual flood risk in the hydrologic study area will come from fluvial flooding from the Guadalupe River. The residual flood risk from the Guadalupe River is shown in Figure 12. Nuisance flooding from the storm drain network is expected to remain the same as described in Section 3.8.

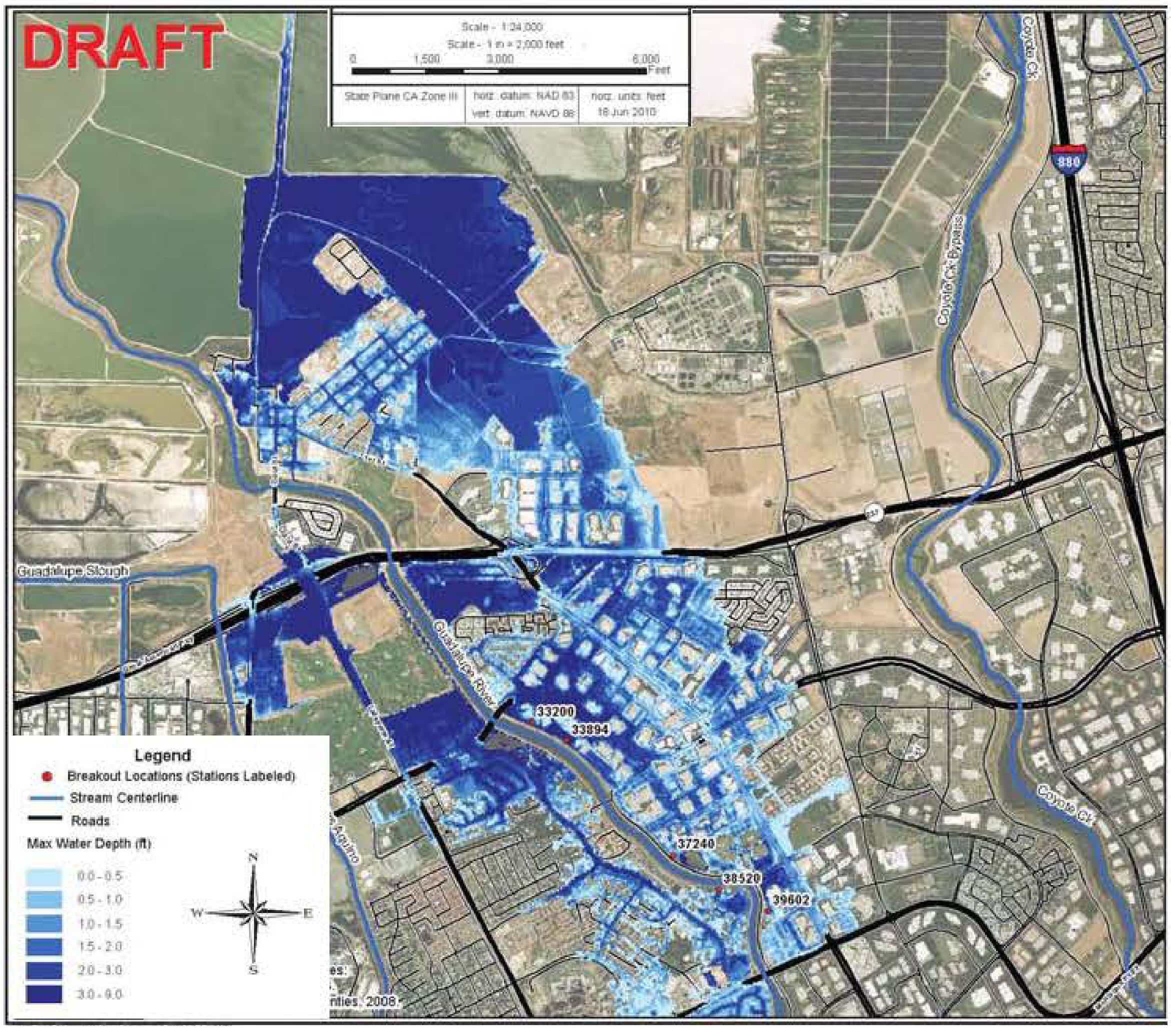

Figure 12. Residual Flood Risk from the Guadalupe River [from Plate 55 of Annex1]

5 CONCLUDING REMARKS

5.1 SUMMARY

Water resources engineering technical work for the South San Francisco Bay Shoreline Study Phase 1, Alviso Economic Impact Area, spans a decade of effort and supports the planning and Federal interest determination for the study. This report is not intended to be inclusive of all the technical work that has been performed for the study, but rather a summary of relevant technical analyses used in the study to support the planning and Federal interest decision processes. This report summarized relevant analyses, data, results, and other information on the watershed, hydrology, fluvial hydraulics, tidal hydraulics, sediment dynamics, water waves, and flood risk for the hydrologic study area. Of particular importance was the tidal hydraulics and the transferring of tide data from the long record at the San Francisco tide gage to the hydrologic study area (the Coyote Creek tide gage), which is described in more detail in Appendix F of the Integrated Document (Tidal Flood Risk Analysis Summary Report). The technical work described in this report has been reviewed following accepted USACE practice and is complete and sufficient for planning purposes, Federal interest determination, and selection of a recommended plan. No further water resources engineering work is required until the PED phase of the project.

5.2 HYDROLOGIC STUDY AREA TIDAL FLOOD RISK

Flood risk management projects on lower Coyote Creek and Guadalupe River have substantially lowered the risk of riverine flooding for the community of Alviso. The largest remaining flood risk for Alviso comes from tidal flooding. The community of Alviso is at significant risk from tidal flooding, with an approximately one in three chance of Alviso suffering a tidal flood event under in any given year. Under the existing condition, it is almost certain that tidal flooding will occur in Alviso within the next 30 years. Should flooding occur, damages similar to those experienced during the riverine flood of the Guadalupe River in January 1983 are expected.

Future sea level rise over the next fifty years will make it almost a certainty that tidal flooding will occur in Alviso in the absence of a flood risk management project. Building the 13.5 feet NAVD88 levee will significantly reduce the tidal flood risk to the Alviso community with the chance of tidal flooding in 2067 ranging from 1 in 2 to 1 in 50, depending on how fast sea level rises. For the next ten years after building the levee the chances of tidal flooding are significantly less than this range. Building the 15.2 feet NAVD88 levee will nearly eliminate the tidal flood risk to the Alviso community for the foreseeable future.

The residual tidal flood risk at 2017 after building either levee is so small that it could not be mapped on the 500-year floodplain and its expected damages are negligible (nearly $0). By 2067 the damages are still very low ($1M or smaller), with still very little area to be mapped. Riverine flooding and storm water flooding will become the largest sources of flood risk once the 13.5 or 15.2 feet NAVD88 levee is built.

5.3 FUTURE CONSIDERATIONS

No further water resources engineering work is required during the Feasibility phase of this project. Water resources engineering technical work will however be required during the Preconstruction Engineering and Design (PED) phase of the project. As is typical during the PED phase, USACE water resources staff will either be the lead engineer or support staff for the development of the Design Documentation Report (DDR). Typical DDR tasks required include refinements to project hydrology, storm statistics, and wave statistics, and determination of pertinent hydraulic design features. In addition, water resources staff will review the plans and specifications, conduct site visits, participate in value engineering (VE) studies, participate in contract negotiations, and other tasks as appropriate for the project.

Based on the technical work conducted during the Feasibility phase, the following items are recommended to be considered during the PED phase:

- Review of actual sea level change since this report and whether adaptive management or post-authorization actions are required;

- Review of changes to hydrology, and storm and wave statistics, since this report and whether these changes significantly affect the design of the project;

- Establishment of a long-term tide gage at Coyote Creek, and ensuring the survey of the gage meets the USACE's Comprehensive Evaluation of Project Datums (CEPD) criteria;

- Development of flood inundation maps based on project hydrodynamics, to aid in the communication of flood risk to the community of Alviso.

6 REFERENCES

Barnard, P. L. et al., 2013. Integration of bed characteristics, geochemical tracers, current measurements, and numerical modeling for assessing the provenance of beach sand in the San Francisco Bay Coastal System. *Marine Geology,* Volume 336, pp. 120-145.

Brown, G. L., 2010. *Sediment Analysis and Modeling for the South San Francisco Bay Shoreline Study, draft,* Vicksburg, MS: Coastal and Hydraulics Laboratory, ERDC, USACE.

CEMA, 2009. *Tsunami inundation map for emergency planning, Milpitas quadrangle.* Sacramento, CA: California Emergency Management Agency.

Cloern, J., Powell, T. & Huzzey, L., 1989. Spatial and temporal variability in South San Francisco Bay (USA), 2. Temporal changes in salinity, suspended sediments, and phytoplankton biomass and productivity over tidal time scales. *Estuarine, Coastal, and Shelf Science,* 28(6), pp. 599-613.

Deering, 2014. *Personal communication.* s.l.:s.n.

DHI, 2010. *Regional coastal hazard modleing study for North and Central San Francsico Bay, Final Draft ,* Solana Beach, CA: DHI Water and Envrionement Inc..

ESA PWA, 2012. *Shoreline Study Preliminary Alternatives and Landscape Evolution,* San Francisco, CA: ESA PWA.

Flick, R. E., 2000. Time-of-day of peak tides in a mixed-tide regime. *Shore & Beach,* pp. 15-17.

Foxgrover, A. C. et al., 2004. *Deposition, erosion, and bathymetric change in south San Francisco Bay: 1858 - 1983,* Santa Cruz, CA: U. S. Geological Survey, Pacific Coastal and Marine Science Center.

Jassby, A., Koseff, J. & Monismith, S. G., 1996. Processess underlying phtoplankton variability in San Francisco Bay. In: J. T. Hollibaugh, ed. *San Francisco Bay: The Ecosystem.* San Francisco, CA: American Association for the Advancement of Science , pp. 325-349.

Knuuti, K., 1995. *Extreme tide prediction for San Francisco Bay,* Berkeley, CA: University of California.

Krone, R. B., 1979. Sedimentation in the San Francisco Bay System. In: T. J. Conomos, ed. *San Francisco Bay: The Urbanized Estuary.* San Francisco, CA: American Association for the Advancement of Science, Pacific Division .

Krone, R. B., 1996. Recent sedimentation in the San Francisco Bay System. In: J. T. Hollibaugh, ed. *San Francisco Bay: The Ecosystem.* San Francisco, CA: American Association for the Advancement of Science .

Leenknecht, D. A., Szuwalski, A. & Sherlock, A. R., 1992. *Automated Coastal Engineering System, users guide and technical reference,* Vicksburg, MS: Waterways Experiment Station, USACE.

May, C. et al., 2003. Effects of spatial and temporal variability of turbidity on phytoplankton blooms. *Marine Ecology - Progress Series,* Volume 254, pp. 111-128.

NHC, 2006. *Berryessa Creek Watershed Hydrology Report,* West Sacramento, CA: Northwest Hydraulic Consultants.

NOAA, 2014. *Sea Level Rise and Nuisance Flood Frequency Changes around the United States, Technical Report NOS CO-OPS 073,* Silver Spring, MD: National Oceanic and Atmospheric Administration, Center for Operational Oceanographic Products and Services.

NRC, 1987. *Responding to Changes in Sea Level: Engineering Implications,* Washnington, DC: National Research Council, The National Acadamies Press.

NRC, 2012. *Sea-Level Rise for the Coasts of California, Oregon, and Washington: Past, Present, and Future,* Washington, DC: National Research Council, The National Acadamies Press.

OBA, 1992. *Sediment Budget Study for San Francisco Bay,* Portland, OR: Ogden Beeman & Associates and Ray B. Krone & Assoicates.

Oltman-Shay, J. & Hathaway, K., 1989. *Infragravity energy and its implications in nearshore sediment transport and sandbar dynamics,* Vicksburg, MS: Coastal Engineering Research Center, USACE.

Powell, T., Cloern, J. & Huzzey, L., 1989. Spatial and temporal variability in South San Francisco Bay (USA), 1. Horizontal distributions of salinity, suspended sediments, and phytoplankton biomass and productivity. *Estuarine, Coastal, and Shelf Science,* 28(6), pp. 583-597.

PWA, 2007. *South Bay Salt Pond Restoration Project Flood Analyses Report,* San Francisco, CA: Phillip Williams and Associates.

Schaaf & Wheeler, 2010. *Hydrology and Water Quality for San Jose, California, Envision San Jose 20240,* Santa Clara, CA: Scahaaf & wheeler Consulting Engineers.

Schoellhamer, D., 1996. Factors affecting suspended-solids concentrations in South San Francisco Bay, California. *Journal of Geophysical Research - Oceans,* 101(C5), pp. 12087-12095.

Schoellhamer, D., 2011. Sudden clearing of estuarine waters upon crossing the threshold from transport to supply regulation of sediment transport as an erodible sediment pool is depleted: San Francisco Bay, 1999. *Estuaries and Coasts,* 34(5), pp. 885-899.

Scott, S. H., 2009. *South San Francisco Bay Shoreline Study, Sediment Transport and Fate from South Bay Streams,* Vicksburg, MS: Coastal and Hydraulics Laboratory, ERDC, USACE.

SCVWD, 1983. *Report on flooding and flood related damages, Santa Clara County, January 1 to April 30, 1983,* San Jose, CA: Santa Clara Valley Water District.

SCVWD, 2007. *San Francisquito Creek Hydrology Study,* San Jose, CA: Santa Clara Valley Water District.

Smith, J. M., 2009. *Short-Wave modeling for South San Francisco Bay SHoreline Study, draft,* Vicksburg, MS: Coastal and Hydraulics Laboratory, ERDC, USACE.

Teeter, A. M. et al., 2001. Hydrodynamic and sediment transport modeling with emphasis on shallow-water vegetated areas (lakes, reservoirs, estuaries and lagoons). *Hydroniologia,* Volume 444, pp. 1-23.

USACE, 1977. *Hydrologic Engineering Office Report, Guadalupe River and Coyote Creek, Santa Clara County, California,* San Francisco District, CA: San Francisco District.

USACE, 1984. *Tidal Stage versus Frequency Study,* San Francisco, CA: San Francisco District.

USACE, 1988. *Office Report, Southern Alamenda and Santa Clara Counties, Interim San Francisco Bay Shoreline Study,* San Francisco, CA: San Francisco District.

USACE, 1991. *Guadalupe River, General Deisgn Memorandum, Volume 1 of 2*, San Francisco, CA: San Francisco District.

USACE, 1996. *Risk-Based Analysis for Flood Damage Reduction Studies, EM 1110-2-1619,* Washington, DC: Headquarters.

USACE, 2001. *Coyote Creek at Rock Springs Road, Review of Existing Hydrology,* San Francisco, CA: San Francisco District.

USACE, 2004. *South San Francisco Bay Shoreline Project, Section 905(b) (WRDA 86) Analysis,* San Francisco, CA: San Francisco District.

USACE, 2006. *Risk analysis for flood damage reduction studies, ER 1005-2-101*, Washington, DC: Headquarters.

USACE, 2009. *Guadalupe Watershed Hydrologic Assessment,* San Francisco, CA: San Francisco District.

USACE, 2010. *Standards and Procedures for Referencing Project Evaluation Grades to Nationwide Vertical Datums, EM 1110-2-6056,* Washington, DC: Headquarters.

USACE, 2011a. *Memorandum for Commander, South Pacific Division (CESPD-PD), Subject: Issue Resolution Plan for the South San Francisco Bay Shoreline Study, California.* Washington, DC: Headquarters.

USACE, 2011b. *Sea-Level Change Considerations for Civil Works Programs, EC 1165-2-212,* Washington, DC: Headquarters.

USACE, 2013. *Incorporating Sea Level Change in Civil works Programs, ER 1100-2-8162*, Washington, DC: Headquarters.

USGS, 2005. *South Bay Salt Pond Restoration project short-term data needs, 2003 - 2005,* Vallejo, CA: U. S. Geological Survey.

Walters, R. A., Cheng, R. T. & Conomos, T. J., 1985. Time scales of circulation and mixing processes of San Francisco Bay waters. *Hydrobiologia,* pp. 13-36.

Zervas, C., 2009. *Sea Level Variations of the United States 1854–2006, NOAA Technical Report NOS CO-OPS 053,* Silver Spring, MD: NOAA.

Zoulas, J., 2013. *A sediment budget for the San Francisco Bay, and implications for regional sediment management,* San Francisco, CA: USACE, San Francisco District.

ANNEX 1: RIVERINE HYDRAULICS

South San Francisco Bay Shoreline Study
Santa Clara County & Alameda County, California

RIVERINE HYDRAULICS

U.S. Army Engineer District, San Francisco
Corps of Engineers
San Francisco, California
May 2013

Due to its large size, Annex 1 of Appendix E of the South San Francisco Bay Shoreline Study, Phase 1, Alviso Economic Impact Area report, will be provided under its own separate cover.

ANNEX 2: DOCUMENTATION OF STORM DATA ANALYSIS

14 January 2008

CESPN-ET-EW

Memorandum for Record

Subject: South San Francisco Bay Shoreline Study, Documentation of Data Analysis

Introduction

The purpose of this memo is to document coastal data analysis related to the risk-based statistical and uncertainty analyses of coastal flood stages. Most of the analyses summarized below address tasks D2, D3, and A5 of the "South San Francisco Bay Shoreline Study Scope of Work & Related Documents" (McAdory, 2006) and the recommendations of "South San Francisco Bay Shoreline Study Review of Proposed Technical Approach" (Collins, Dean, and Divoky, 2006). This memo includes background information on coastal flood forcing parameters, discussion of the statistical analysis of tide and wind data, and discussion of the application of different statistical approaches for flood stage frequency analysis.

Background information in Section 1.0 provides a general sense (order of magnitude) of the contributions of each forcing parameter to coastal flood elevation. Section 2.0 summarizes the collection of tide and wind data and the derivation of their related recurrent frequency curves using different statistical approaches. These curves were compared against each other to determine appropriate criteria for the selection of extreme events to be used for stage frequency analysis. Statistical approaches using historical data alone and using synthesized data were applied to estimate flood stage frequencies at a tide gage in San Francisco. Both annual peak and conditional sampling methods were adopted to select extreme events for stage frequency analysis at this tide gage.

Section 3.0 summarizes the development of flood stage frequency curves for a tide gage near the Dumbarton Bridge—the closest gage to the project site with a sufficient length of tide data records—using two different statistical approaches. In the first approach, selected San Francisco gage historical data was transferred to Dumbarton Bridge based on assumptions supported by the tide data and by hydrodynamics for the establishment of preliminary flood stage frequencies. The other statistical approach, using synthesized data and employing the Joint Probability Method, was fully developed for this study and the computational procedures were exercised to combine predicted tide and residual tide (tide parameters that are defined in Section 1.0) for stage frequency analysis at Dumbarton Bridge. The results developed from both statistical approaches are in good agreement and will be useful in future computation plan development. Further analysis and integration of a complete set of coastal flood forcing parameters, including in-bay wind set-up and wave set-up, will be carried out at a later stage of this study.

1.0 Background Information

(A) High predicted (or astronomical) tide, tidal residual, and wind have been identified as primary contributors to coastal floods in South San Francisco Bay. A linear process was assumed to decouple the measured (verified) tide into two components, predicted tide and residual. The residual is primarily generated by offshore storm systems due to its central and peripheral barometric pressure difference. Additional El Niño effects due to ocean water expansion could also contribute to the residual.

(B) The predicted tide at the project site in South Bay is approximated by amplifying flood tide stage at the San Francisco (Presidio) tide gage by a factor of 1.31 to 1.59, values derived using data available at NOAA's Tides and Currents website. This gives the project site a tide range of about 7.6 to 9.3 feet between Mean Higher High Water (MHHW) and Mean Lower Low Water (MLLW). The amplification can be attributed to water depth and geometry effects of the South Bay. The residual is a long wave with durations ranging from 2 to 8 days and peak heights ranging from 0.8 to 3.7 feet at the Presidio. The effect of El Niño on the total residual is about 0.5 to 1.0 foot at the Presidio. The range of peak heights of the residual at the project site is expected to be the same as or slightly reduced from the range at the Presidio. Two other variables at the project site, the storm duration (or residual duration) and the residual's phase relationship with predicted tide, are also expected to either remain unchanged or have slight changes from what is observed at San Francisco. A 0.4-foot wind-induced setup at Alviso, calculated by a FEMA-recommended 1-D wind setup model under a 40 mile-per-hour (mph) uniform northwest (NW) wind, has been reported.

(C) A significant event has been characterized as the combination of high predicted tide (heights exceeding neap tide, or about 5.4 feet MLLW), large residual (heights exceeding 1.5 feet), and strong bay winds (larger than 20 mph). It is estimated that the ranges of contributions of predicted tide, residual, and wind setup to the total surge at the project site are about 3 to 4 feet, 1.5 to 3 feet, and 0.5 to 1 foot, respectively, above Mean Tide Level (MTL). The corresponding wave height is about 3 to 4 feet and wave period is about 6 to 7 seconds. The wave induced setup could be on the order of 1 foot or smaller.

(D) Once the response functions at the project site are generated, either by numerical simulation or by analysis of measured data, one can apply joint probability method (JPM), Monte Carlo simulation (MCS), and empirical simulation technique (EST) to estimate coastal flood statistics. Fluvial flood statistics will be estimated through hydrologic and hydraulic analysis and modeling. The combined flood statistics in the area affected by fluvial and coastal flood events will also be estimated through statistical analysis or computer modeling approaches.

2.0 Statistical Analysis of Tide and Wind Data

Analysis of Tide Data at San Francisco (Presidio) Gage

Statistical analysis was performed on tide data collected at the San Francisco gage (Station

9414290). Two sets of data were available at NOAA's Tides and Currents webpage: verified (or measured) data and predicted data. A third set of data, residual data, was calculated by subtracting, at a given time, the predicted data from the verified data. Data from 1901 to 2005 (a span of 105 years) was collected. The annual peak values of all 105 years are shown in Plate 2-1.

Plate 2-1 shows that a sizable number of the annual peak verified data values fall below the annual peak predicted data values for their respective years, with some numbers significantly lower than the predicted data value. Plotting the annual mean values for hourly verified, predicted, and residual data (Plate 2-2) shows that a trend exists in both the verified and residual data but not in the predicted data. This trend corresponds to the rise in sea level at the San Francisco gage.

In order to achieve more reliable statistical analysis, the water level trend was removed from both the annual mean verified data and the annual mean residual data, in a manner similar to the mean sea level trend adjustment done by Knutti (1995). The predicted data was left unchanged. The year 2005 was assumed as the year not needing trend adjustment. Plate 2-3 shows the results of this treatment. The new annual mean verified and annual mean residual data have trend lines that are a constant height above the datum used (MLLW, 1983-2001 Tidal Datum Epoch).

The adjustments in mean verified and mean residual values for each year were then applied to all tide data used in this statistical analysis. Plate 2-4 shows adjusted annual peak values. Table 2-1 shows the unadjusted annual peak tide values selected, the adjustment increment applied to each year's tide values, and the adjusted annual peak values, with water level trend removed (it was not necessary to adjust predicted tide data).

The following statistical analyses were performed on the tide data:

(A) A return period curve based on annual peak verified data was produced. Annual peak verified values with the water level trend removed were used to produce Normal, Weibull, and Gumbel cumulative distribution functions (CDFs), which were converted into the return period curves shown in Plate 2-5.

(B) The annual peak sampling method may create error and uncertainty for extreme probabilistic analysis in that it may fail to capture multiple significant events occurring in a given year (i.e. only the greatest event in a year is sampled). If an event were to produce tide levels that are not the peak of the year, but exceed the peaks of other years, it would not be sampled by the annual peak method. This is especially problematic during El Niño years, which occur every 7 to 14 years along the west coast of the United States and have historically shown the tendency to produce multiple significant events within a given year, as observed in the tide data at the San Francisco gage. The conditional sampling method can address the deficiencies of annual peak sampling and improve the accuracy of statistical analysis in the lower recurrent frequency range (larger return period) by capturing the most significant events regardless of calendar year.

The conditional sampling method was used to select significant events for coastal flood stage analysis. In general, high predicted tide, residual, wind set-up, wave set-up and run-up, and river discharge are the forcing parameters contributing to coastal floods at the project site (wind speed is not considered a parameter because its generated wind set-up is negligible in the deep water area). High predicted tide and residual are generated offshore and propagate into the project site, while wind set-up and wave run-up are generated inside the South Bay and contribute to flood levels in the shallow water area. River discharge has been tested by computer simulation and concluded to be negligible in the coastal area. Therefore, high predicted tide and residual at the San Francisco gage were the two parameters considered for the selection of significant events.

Conditional sampling was done on the 105 years of tide data at San Francisco to select extreme events for statistical analysis. In order to focus on more extreme tide events, two conditions—predicted data exceeding 4.5 feet MLLW and residual data exceeding 1.5 feet MLLW—were used to capture tide data where high residual events coincided with high tides. Selected tide data occurring at adjacent times were grouped together, and 11-day tide time series of predicted and residual tide data were plotted across these groupings, producing 37 time series graphs (Plates 2-6 to 2-15). From examination of these 37 graphs, 47 high residual events (pulses along the residual time series) were identified, and 3-day time series were plotted across them. Maximum verified, predicted, and residual values were collected within each of these 47 3-day time series (Table 2-2), and three return period curves based on the 47 maximum verified values (Plate 2-16) were produced for comparison.

(C) An additional condition was added to the conditional sampling analysis performed in (B) to ensure that, for each event, the sum of the maximum predicted tide and maximum residual was larger than the minimum annual peak predicted tide at the San Francisco gage during the 105 years. Looking at the values in Table 2-1, the range of annual peak predicted tide at the San Francisco gage is 6.9 to 7.26 feet MLLW. The addition of this condition was done to reduce the previously selected 47 events to a smaller size of sample in order to minimize computation efforts for statistical analysis. The sampled events, however, had to maintain sufficient characteristics to represent the system under study.

All tide data in Table 2-2 associated with verified values below 6.9 feet MLLW was eliminated. This reduced the number of time series in Table 2-2 from 47 to 33 (Table 2-3). Three return period curves derived from the 33 verified values (Plate 2-17) were produced for comparison.

Plate 2-17 shows that the Gumbel curve fits the data well in the lower recurrent frequency range (larger return period range) and will be applied for any future related analysis. Comparison of the Gumbel curves developed from 47 events and 33 events and the stage frequency curve generated from annual peak tide (Plate 2-18) shows close alignment in the return period range of 5 to 100 years. This would confirm that the selected 33 extreme events is representative of the system.

(D) To further analyze the tide data, the phase relationship between predicted tide and residual tide time series (the positioning of the residual time series in relation to the predicted time series) was studied. Tests were done by taking a residual time series and shifting it along the predicted time series, thereby changing the phase of the residual data to observe its effects. Phase-shift decay factors (ratios of the maximum tide stage at a given phase to the maximum tide stage for all phases) were derived by creating 2-day, 3-day, 4-day, 5-day, 6-day, and 8-day synthetic residual events and phase-shifting them across real predicted tide time series, starting the peak residual of an event at a peak tide and then shifting the peak residual 3, 4, 5, 6, 7, 8, 17, 18, and 21 hours ahead along the time series (see

Plate 2-19), obtaining the maximum tide stage (sum of the predicted and residual values) at each of these phase shifts, then dividing each of these nine tide stage values by the largest tide stage value to obtain the decay factor for each phase shift (Table 2-4).

(E) The Joint Probability Method assumes that each forcing parameter in a system is independent, and that the combined probability function is equal to the product of the individual probability functions. In this study, four parameters were identified for joint probability analysis: predicted tide, residual tide, residual phase shift, and residual event duration (storm duration). This gave the joint probability for flood stage the following formula:

$$P = P_p \times P_r \times P_d \times P_s$$

Where P = joint probability for flood stage

P_p = probability for predicted tide elevation

P_r = probability for residual tide height

P_d = probability for residual event (storm event) duration

P_s = probability for residual phase shift

Using the tide data from 33 high residual events (Table 2-3), the product of probability functions for predicted tide and residual tide was computed by convolution integration (via Fast Fourier Transform, or FFT) of two Gumbel probability density functions (PDFs), one for the 33 maximum predicted values and the other for the 33 maximum residual values. The convolution result represents the statistical sum of the peak values of predicted tide and residual tide within their respective time series (i.e. $P_{p+r} = P_p \times P_r$). Thus the convolved function can be multiplied by probability functions for residual phase shift and residual event duration to obtain a resultant joint probability function of predicted tide and residual tide. The return period was calculated after applying a rate of occurrence factor to the results of the joint probability computation, to account for the less than one-to-one ratio of the number of events sampled (33) to the number of years sampled (105).

Plate 2-20 shows flood stage return period curves at the San Francisco gage determined by three methods: the annual peak sampling method, the conditional sampling method, and the joint probability method. The curves appear to be in relative proximity to each other, providing some confidence in the reliability of the joint probability method.

Analysis of Wind Data at San Francisco Airport

Statistical analysis was performed on wind data collected at San Francisco Airport (SFO). Hourly SFO wind speed and direction data between 1948 and 2007 was collected from NOAA's National Climatic Data Center website. Then the data was conditionally sampled, first by eliminating all data not occurring between November and April of any given year, then selecting speed and direction data from times at which the wind speed exceeded 35 mph. Wind events were identified by grouping together data occurring at adjacent times. The maximum wind speed and associated wind direction were recorded for each of these events. A total of 257 sets of speed and direction values were recorded.

For these 257 maximum wind speeds, the Normal, Weibull, and Gumbel PDFs and CDFs were produced (Plate 2-21), and the CDFs were used to create return period curves (Plate 2-22). A separate set of maximum wind speeds was also created, with only those speeds occurring in the northwest direction (290 to 330 degrees). Normal, Weibull, and Gumbel PDFs and CDFs were also produced for this separate set of 59 values (Plate 2-23), and the CDFs used to create another set of return period curves (Plate 2-24). The Gumbel return period curves for wind speeds in all directions and wind speeds in the northwest direction are shown in Plate 2-25.

Wind direction distribution for the maximum wind speeds in all directions was determined by creating a histogram of the 257 events of wind direction values. This histogram is shown in Plate 2-26.

3.0 Methods for Determining Dumbarton Tide Stage Frequency Curve

Because of the scarcity of tide data at the South Bay gages, it was necessary to rely on the long record of data available at the San Francisco gage and adjust it for South Bay analysis. In order to "transfer" the data from San Francisco to the gages in the South Bay, tide amplification factors were found and used. Two methods were developed to perform this transfer and derive a flood stage frequency curve at Dumbarton Bridge.

First Method: Direct Transfer/Amplification of Tide Data from Selected High Residual Events at San Francisco

A tide stage frequency curve was developed for the Dumbarton tide gage by "transferring" to that location the data for 33 high residual events (Table 2-3) observed at the San Francisco gage (see Section 2.0 (B) and (C) for a description of how the events were selected). The transfer was done specifically by amplifying predicted tide data.

First, each maximum verified tide value in Table 2-3 was "decoupled" by finding the predicted tide elevation and residual tide height corresponding to the time at which the verified maximum occurred. One time series, for February 6 to 9, 1998, was excluded from this exercise because it had an identical verified maximum value (occurring at the identical time) to the one for the time series between February 4 and 6, 1998. As a result, 32 predicted and 32 residual tide values were found for each verified maximum (Table 3-1).

Next, the zero means of the 32 predicted values were determined by subtracting 3.18 feet from each of them, a value representing the mean of predicted tide elevations at San Francisco and obtained from the NOAA website (by subtracting the station's Mean Tide Level and Mean Lower Low Water datum elevations). Then this new array of 32 zero-meaned predicted values was multiplied by 1.46, a value approximating the amplification factor of tides from San Francisco to Dumbarton and obtained from the NOAA website. Then the amplified predicted values were raised by 4.53 feet, a value for the mean of predicted tide elevations at Dumbarton, resulting in an array of 32 values for maximum predicted tide elevation relative to local MLLW at Dumbarton coinciding with 32 high residual events at San Francisco (Table 3-2, Column 7).

The maximum residual tide height at Dumbarton for each high residual event at San Francisco was assumed to be equal to the one-hour lag of (the residual value occurring one hour prior to) the decoupled residual value at San Francisco. The 32 Dumbarton residual values are shown in Table 3-3.

Finally, the 32 Dumbarton predicted values were added to the 32 Dumbarton residual values to produce 32 overall values representing maximum tide stages at Dumbarton occurring within the 32 high residual events at San Francisco (Table 3-4). These 32 values were then used to create a return period curve for Dumbarton tide stages based on Gumbel (maximum) analysis (Plate 3-1).

Second Method: Joint Probability of Four San Francisco Tide Parameters

Another tide stage frequency curve was derived for the Dumbarton tide gage by determining a joint probability of the probabilities at San Francisco for four parameters: predicted tide, residual tide, residual phase shift, and residual event duration. The following is a walkthrough of the steps involved in the joint probability procedure, followed by a description of the procedure as it was exercised.

(A) Walkthrough of the Joint Probability Procedure

Steps:

1) Assumptions: All tides are larger than neap tides. Wind statistics are for in-bay wind.

2) The following criteria apply to the selection of significant tide events: (1) predicted tide is greater than 4.5 feet MLLW, (2) residual height is greater than 1.5 feet MLLW, and (3) measured (verified) tide is greater than 6.9 feet MLLW.

3) Thirty-three events are selected based on Step 2 (See Section 2.0 (B) and (C) for discussion of how events were selected).

4) At the NOAA website, verified (measured) tide data is subtracted by predicted tide data to obtain time series of residual data.

5) The duration of residual tide, which ranges from 2 days to 8 days, is the response of storm duration in water. The phase relationship between peak tide and peak residual is measured by the phase difference, in hours, within a 24-hour interval (1-day tide cycle).

6) Peak tides range from 5.4 to 7.2 feet MLLW and peak residuals range from 1.5 to 3.1 feet in the database developed in Step 3. PDFs and CDFs of peak tide and peak residual are developed. (See Section 2.0-(C)) Further analysis will be carried out regarding the development of appropriate PDFs of tide and residual for JPM and MCS.

7) <u>Probability distribution of duration at Presidio</u>

Duration (Day)	2	3	4	5	6	8	SUM	
Without El Niño	1	6	6	3	4	2	22	
With El Niño (+0.5’)		1	1	2		1		5
With El Niño (+1.0’)		1	2	2		1		6
		3	9	10	3	6	2	33

<u>Probability distribution of phase relationship at Presidio</u>

Phase difference (Hour)	0	3	4	5	6	8	17	18	21	SUM

3	1	4	2	5	2	1	13	2	33

8) Simulation conditions of tide, residual, duration and phase are selected to establish response functions. For instance, four cases are chosen for tide (5.4, 6.0, 6.6, and 7.2 feet), four cases for residual (1.5, 2.0, 2.5, and 3.1 feet) with 2-day duration and 6.6-foot tide plus residuals with 0 phase as boundary conditions, and an additional 26 cases (8 for 2-day, 9 for 3-day, 9 for 6-day) for a total of 34 cases.

	2-day	2-day+0.5’ base	2-day+1.0’ base
Phase(hr)			
0	1	1	1
6	1	1	1
18	1	1	1

More analysis will be needed before the final selection of simulation runs.

9) Synthesized events are developed based on the combination of tide (5.4 to 7.2 feet +), residual (1.5 to 3.1 feet +), duration (2-day to 8-day, with and without El Niño effect) and phase (0 to 21 hours).

10) Establish PDF and CDF of surge elevation based on response functions developed in Step 8. This process can be simplified by convolving PDFs of peak tide and peak residual and resampling with different residual durations and phase relationship to form a new population within the range of 6.9 feet to 10.3 feet for statistical analysis.

11) Establish PDFs and CDFs of wind statistics at SFO. (See Section 2.0)

12) Require computer model simulations of long wave, short wave and wave run-up in order to establish wind set-up, wave height & period and wave run-up for carrying out the complete set of statistical analysis.

(B) Application of the Joint Probability Procedure

The following describes the application of steps 1 to 10 of the joint probability procedure outlined in part (A). Because of the availability of a long record of tide data at the San Francisco gage, step 8 was modified so that the response function was developed using actual data, rather than simulated data.

<u>Derivation of PDF/CDF for the convolution of amplified SF predicted tide PDF with SF residual tide PDF</u>

Maximum verified, predicted, and residual tide data for 33 high residual events at San Francisco were used (Table 2-3). The zero means of the predicted values were calculated by subtracting 3.18 feet from each of the 33 values (mean of San Francisco predicted tide elevations relative to MLLW). The resulting values were then multiplied by 1.46 (amplification of tides from San Francisco to Dumbarton) and then raised by 4.53 feet (mean of Dumbarton predicted tide elevations relative to local MLLW) to produce an array of 33 values representing maximum predicted tide elevations at Dumbarton occurring within the 33 high residual events at San Francisco. The maximum residual tide heights at Dumbarton were assumed to be the same as the residual tide heights at San Francisco during the 33 high residual events. Then two PDFs were created, one for the 33 Dumbarton predicted values and the other for the 33 Dumbarton residual values. The two PDFs were convolved (via FFT) to produce a PDF and a CDF at Dumbarton for 33 high residual events occurring at San Francisco (Plate 3-2).

<u>Derivation of probabilities for different combinations of synthetic residual phase shift and synthetic residual event duration</u>

Each of the 33 time series at San Francisco was examined to determine the probability for each possible residual phase shift and residual event duration shown in Table 2-4. The probabilities are shown in orange in Table 3-5, with the phase shift probabilities in the column to the right of the column of phase shifts (blue column), and the event duration probabilities in the row below the row of event durations (green rows). Probabilities were then determined for different combinations of synthetic residual phase shift and synthetic residual event duration (Table 3-5).

<u>Joint probability of Dumbarton tide stage based on probabilities for Dumbarton predicted tide elevation, residual tide height, residual phase shift, and residual event duration</u>

Using the Dumbarton PDF curve from Step 1 (Plate 3-2), probabilities for the combination of Dumbarton predicted tide elevation and residual tide height were determined at 0.2-foot intervals (Table 3-6). Then the probabilities for all combinations of Dumbarton predicted tide elevation, residual tide height, synthetic residual phase shift, and synthetic residual event duration were calculated, resulting in a column of joint probabilities (Table 3-7, Column 8). Decay factors from Table 2-4 were also applied to the tide stage intervals (Table 3-7, Column 4). The joint probabilities were sorted and grouped into intervals of tide stages (Table 3-8) and were then used to produce a return period curve (Plate 3-3).

John Cheng

Hydraulic Engineer

San Francisco District, USACE

Frank Wu, Ph.D., P.E.

Regional Technical Specialist

Estuarine Hydrodynamics

San Francisco District, USACE

Reference

Collins, J. Ian, Robert Dean and David Divoky. (2006). "South San Francisco Bay Shoreline Study Review of Proposed Technical Approach."

Knutti, Kevin. (1995). "Extreme Tide Prediction for San Francisco Bay."

McAdory, Robert. (2006). "South San Francisco Bay Shoreline Study Scope of Work and Related Documents."

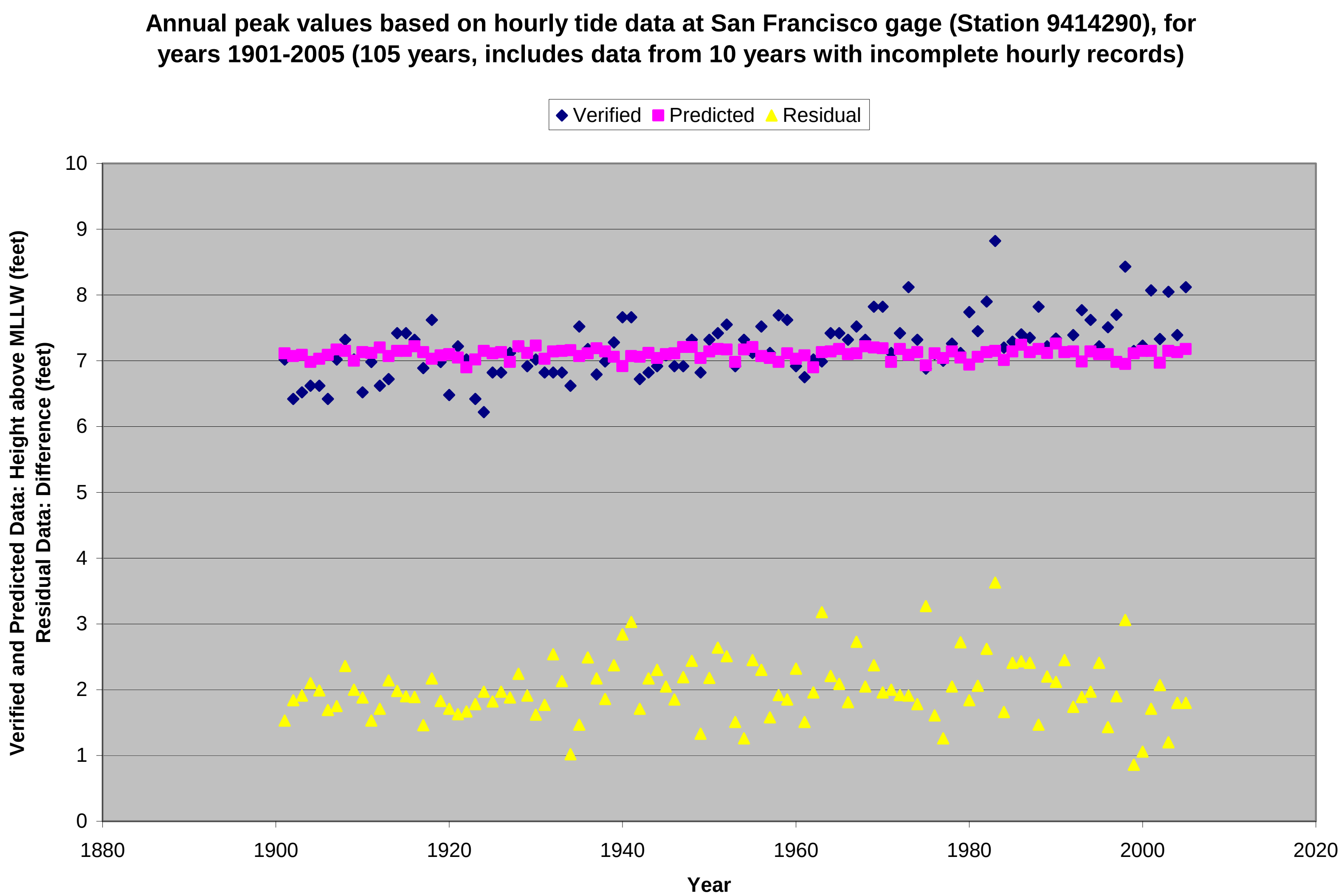
Annual peak values based on hourly tide data at San Francisco gage (Station 9414290), for years 1901-2005 (105 years, includes data from 10 years with incomplete hourly records)
Verified
Predicted
Residual
Verified and Predicted Data: Height above MLLW (feet)
Residual Data: Difference (feet)
10
9
8
7
6
5
4
3
2
1
0
1880
1900
1920
1940
1960
1980
2000
2020
Year

Plate 2-1

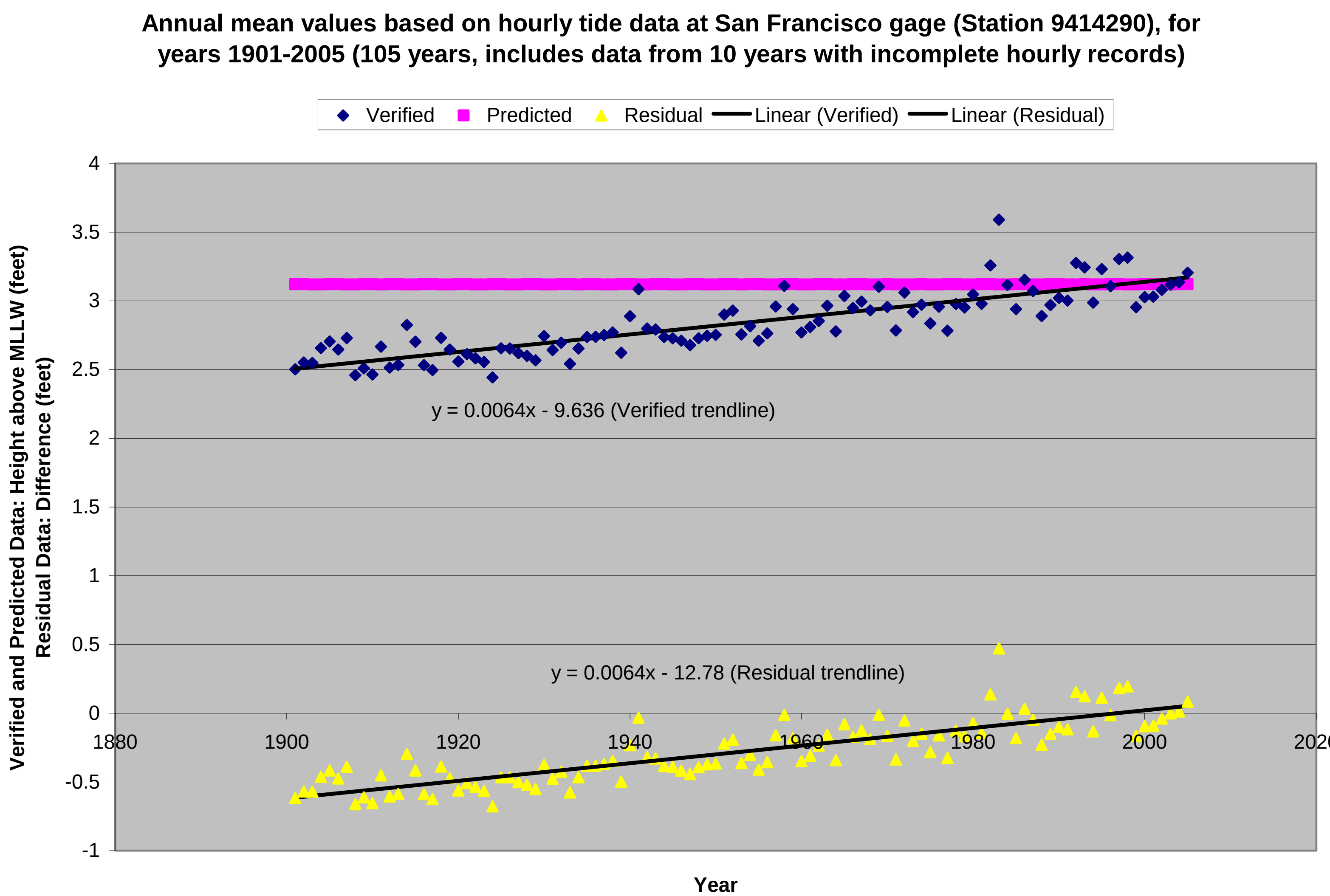
Annual mean values based on hourly tide data at San Francisco gage (Station 9414290), for years 1901-2005 (105 years, includes data from 10 years with incomplete hourly records)
Verified
Predicted
Residual
Linear (Verified)
Linear (Residual)
y = 0.0064x - 9.636 (Verified trendline)
y = 0.0064x - 12.78 (Residual trendline)
Verified and Predicted Data: Height above MLLW (feet)
Residual Data: Difference (feet)
Year
4
3.5
3
2.5
2
1.5
1
0.5
0
-0.5
-1
1880
1900
1920
1940
1960
1980
2000
2020

Plate 2-2

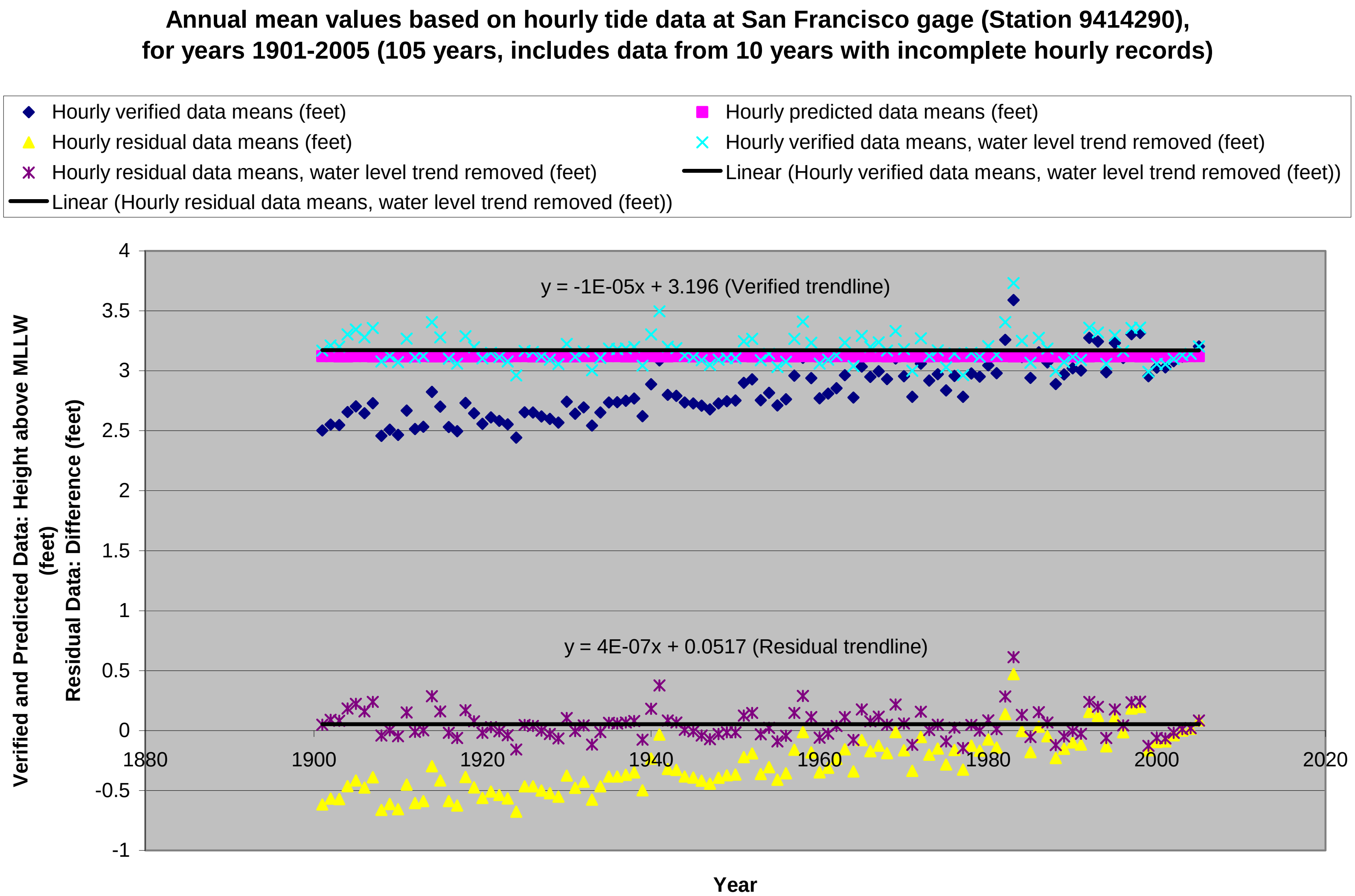

Annual mean values based on hourly tide data at San Francisco gage (Station 9414290), for years 1901-2005 (105 years, includes data from 10 years with incomplete hourly records)
Hourly verified data means (feet)
Hourly predicted data means (feet)
Hourly residual data means (feet)
Hourly verified data means, water level trend removed (feet)
Hourly residual data means, water level trend removed (feet)
Linear (Hourly verified data means, water level trend removed (feet))
Linear (Hourly residual data means, water level trend removed (feet))
y = -1E-05x + 3.196 (Verified trendline)
y = 4E-07x + 0.0517 (Residual trendline)
Verified and Predicted Data: Height above MLLW (feet)
Residual Data: Difference (feet)
Year
4
3.5
3
2.5
2
1.5
1
0.5
0
-0.5
-1
1880
1900
1920
1940
1960
1980
2000
2020

Plate 2-3

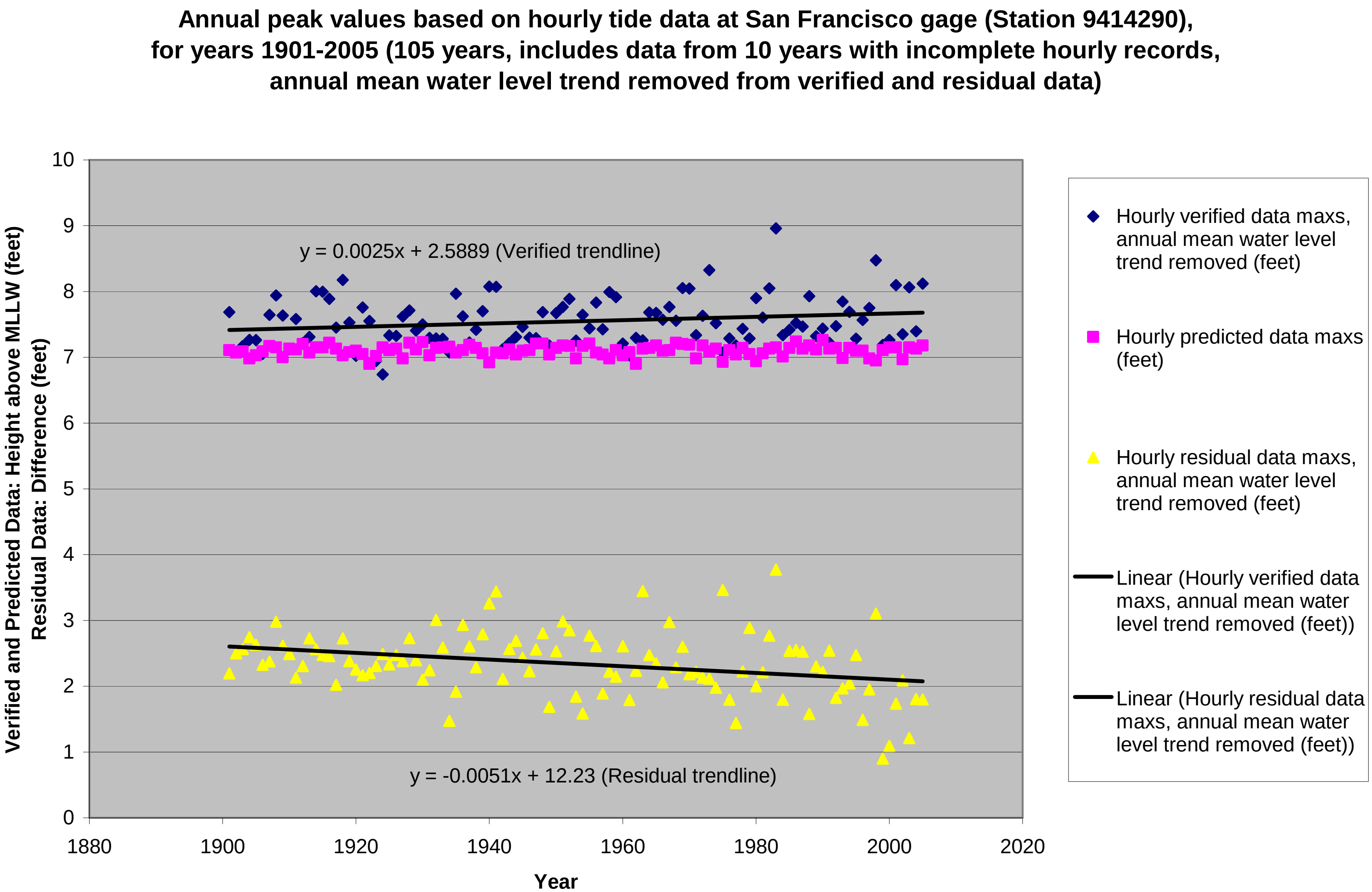

Annual peak values based on hourly tide data at San Francisco gage (Station 9414290), for years 1901-2005 (105 years, includes data from 10 years with incomplete hourly records, annual mean water level trend removed from verified and residual data)
y = 0.0025x + 2.5889 (Verified trendline)
y = -0.0051x + 12.23 (Residual trendline)
Verified and Predicted Data: Height above MLLW (feet)
Residual Data: Difference (feet)
Year
0
1
2
3
4
5
6
7
8
9
10
1880
1900
1920
1940
1960
1980
2000
2020
Hourly verified data maxs, annual mean water level trend removed (feet)
Hourly predicted data maxs (feet)
Hourly residual data maxs, annual mean water level trend removed (feet)
Linear (Hourly verified data maxs, annual mean water level trend removed (feet))
Linear (Hourly residual data maxs, annual mean water level trend removed (feet))

Plate 2-4

Year	Annual peak values of hourly verified data (feet MLLW)	Annual peak values of hourly predicted data (feet MLLW)	Annual peak values of hourly residual data (feet MLLW)	Annual adjustment in verified data mean (feet MLLW)	Annual adjustment in residual data mean (feet MLLW)	Annual peak values of hourly verified data, with annual mean water level trend removed (feet MLLW)	Annual peak values of hourly residual data, with annual mean water level trend removed (feet MLLW)
1901	7.02	7.11	1.53	0.6656	0.6656	7.6856	2.1956
1902	6.42	7.07	1.84	0.6592	0.6592	7.0792	2.4992
1903	6.52	7.09	1.91	0.6528	0.6528	7.1728	2.5628
1904	6.62	6.98	2.1	0.6464	0.6464	7.2664	2.7464
1905	6.62	7.03	1.99	0.64	0.64	7.26	2.63
1906	6.42	7.09	1.69	0.6336	0.6336	7.0536	2.3236
1907	7.02	7.17	1.75	0.6272	0.6272	7.6472	2.3772
1908	7.32	7.15	2.36	0.6208	0.6208	7.9408	2.9808
1909	7.02	7	2	0.6144	0.6144	7.6344	2.6144
1910	6.52	7.13	1.88	0.608	0.608	7.128	2.488
1911	6.98	7.12	1.53	0.6016	0.6016	7.5816	2.1316
1912	6.62	7.2	1.71	0.5952	0.5952	7.2152	2.3052
1913	6.72	7.07	2.14	0.5888	0.5888	7.3088	2.7288
1914	7.42	7.15	1.98	0.5824	0.5824	8.0024	2.5624
1915	7.42	7.15	1.9	0.576	0.576	7.996	2.476
1916	7.32	7.22	1.89	0.5696	0.5696	7.8896	2.4596
1917	6.89	7.13	1.46	0.5632	0.5632	7.4532	2.0232
1918	7.62	7.03	2.17	0.5568	0.5568	8.1768	2.7268
1919	6.98	7.08	1.83	0.5504	0.5504	7.5304	2.3804
1920	6.48	7.1	1.71	0.544	0.544	7.024	2.254
1921	7.22	7.05	1.63	0.5376	0.5376	7.7576	2.1676
1922	7.02	6.9	1.67	0.5312	0.5312	7.5512	2.2012
1923	6.42	7.02	1.78	0.5248	0.5248	6.9448	2.3048
1924	6.22	7.15	1.97	0.5184	0.5184	6.7384	2.4884
1925	6.82	7.11	1.82	0.512	0.512	7.332	2.332
1926	6.82	7.13	1.97	0.5056	0.5056	7.3256	2.4756

1927	7.12	6.98	1.88	0.4992	0.4992	7.6192	2.3792
1928	7.22	7.22	2.24	0.4928	0.4928	7.7128	2.7328
1929	6.92	7.12	1.91	0.4864	0.4864	7.4064	2.3964
1930	7.02	7.23	1.62	0.48	0.48	7.5	2.1
1931	6.82	7.03	1.77	0.4736	0.4736	7.2936	2.2436
1932	6.82	7.14	2.54	0.4672	0.4672	7.2872	3.0072
1933	6.82	7.15	2.13	0.4608	0.4608	7.2808	2.5908
1934	6.62	7.16	1.02	0.4544	0.4544	7.0744	1.4744
1935	7.52	7.07	1.47	0.448	0.448	7.968	1.918
1936	7.18	7.11	2.49	0.4416	0.4416	7.6216	2.9316
1937	6.79	7.19	2.17	0.4352	0.4352	7.2252	2.6052
1938	6.99	7.14	1.86	0.4288	0.4288	7.4188	2.2888
1939	7.28	7.06	2.37	0.4224	0.4224	7.7024	2.7924
1940	7.66	6.92	2.84	0.416	0.416	8.076	3.256

Table 2-1: Annual peak tide values selected, adjustments to peak values, and adjusted annual peak tide values

Year	Annual peak values of hourly verified data (feet MLLW)	Annual peak values of hourly predicted data (feet MLLW)	Annual peak values of hourly residual data (feet MLLW)	Annual adjustment in verified data mean (feet MLLW)	Annual adjustment in residual data mean (feet MLLW)	Annual peak values of hourly verified data, with annual mean water level trend removed (feet MLLW)	Annual peak values of hourly residual data, with annual mean water level trend removed (feet MLLW)
1941	7.66	7.07	3.03	0.4096	0.4096	8.0696	3.4396
1942	6.72	7.06	1.71	0.4032	0.4032	7.1232	2.1132
1943	6.82	7.12	2.17	0.3968	0.3968	7.2168	2.5668
1944	6.92	7.04	2.3	0.3904	0.3904	7.3104	2.6904
1945	7.08	7.1	2.05	0.384	0.384	7.464	2.434
1946	6.92	7.11	1.85	0.3776	0.3776	7.2976	2.2276
1947	6.92	7.21	2.19	0.3712	0.3712	7.2912	2.5612
1948	7.32	7.21	2.44	0.3648	0.3648	7.6848	2.8048
1949	6.82	7.04	1.33	0.3584	0.3584	7.1784	1.6884
1950	7.32	7.14	2.18	0.352	0.352	7.672	2.532
1951	7.42	7.18	2.64	0.3456	0.3456	7.7656	2.9856
1952	7.55	7.17	2.51	0.3392	0.3392	7.8892	2.8492
1953	6.92	6.98	1.51	0.3328	0.3328	7.2528	1.8428
1954	7.32	7.17	1.26	0.3264	0.3264	7.6464	1.5864
1955	7.12	7.21	2.45	0.32	0.32	7.44	2.77
1956	7.52	7.07	2.3	0.3136	0.3136	7.8336	2.6136
1957	7.12	7.04	1.58	0.3072	0.3072	7.4272	1.8872
1958	7.69	6.98	1.92	0.3008	0.3008	7.9908	2.2208
1959	7.62	7.11	1.85	0.2944	0.2944	7.9144	2.1444
1960	6.92	7.03	2.32	0.288	0.288	7.208	2.608
1961	6.75	7.08	1.51	0.2816	0.2816	7.0316	1.7916
1962	7.02	6.9	1.96	0.2752	0.2752	7.2952	2.2352
1963	6.99	7.13	3.18	0.2688	0.2688	7.2588	3.4488
1964	7.42	7.14	2.21	0.2624	0.2624	7.6824	2.4724
1965	7.42	7.18	2.09	0.256	0.256	7.676	2.346
1966	7.32	7.1	1.81	0.2496	0.2496	7.5696	2.0596

1967	7.52	7.11	2.73	0.2432	0.2432	7.7632	2.9732
1968	7.32	7.22	2.05	0.2368	0.2368	7.5568	2.2868
1969	7.82	7.2	2.37	0.2304	0.2304	8.0504	2.6004
1970	7.82	7.19	1.96	0.224	0.224	8.044	2.184
1971	7.12	6.98	2	0.2176	0.2176	7.3376	2.2176
1972	7.42	7.18	1.92	0.2112	0.2112	7.6312	2.1312
1973	8.12	7.09	1.91	0.2048	0.2048	8.3248	2.1148
1974	7.32	7.13	1.78	0.1984	0.1984	7.5184	1.9784
1975	6.88	6.93	3.27	0.192	0.192	7.072	3.462
1976	7.1	7.11	1.61	0.1856	0.1856	7.2856	1.7956
1977	7	7.04	1.26	0.1792	0.1792	7.1792	1.4392
1978	7.26	7.14	2.05	0.1728	0.1728	7.4328	2.2228
1979	7.12	7.05	2.72	0.1664	0.1664	7.2864	2.8864
1980	7.74	6.94	1.84	0.16	0.16	7.9	2

Table 2-1 (continued): Annual peak tide values selected, adjustments to peak values, and adjusted annual peak tide values

Year	Annual peak values of hourly verified data (feet MLLW)	Annual peak values of hourly predicted data (feet MLLW)	Annual peak values of hourly residual data (feet MLLW)	Annual adjustment in verified data mean (feet MLLW)	Annual adjustment in residual data mean (feet MLLW)	Annual peak values of hourly verified data, with annual mean water level trend removed (feet MLLW)	Annual peak values of hourly residual data, with annual mean water level trend removed (feet MLLW)
1981	7.45	7.06	2.06	0.1536	0.1536	7.6036	2.2136
1982	7.9	7.13	2.62	0.1472	0.1472	8.0472	2.7672
1983	8.82	7.15	3.63	0.1408	0.1408	8.9608	3.7708
1984	7.2	7.01	1.66	0.1344	0.1344	7.3344	1.7944
1985	7.29	7.14	2.41	0.128	0.128	7.418	2.538
1986	7.4	7.24	2.43	0.1216	0.1216	7.5216	2.5516
1987	7.35	7.13	2.41	0.1152	0.1152	7.4652	2.5252
1988	7.82	7.18	1.47	0.1088	0.1088	7.9288	1.5788
1989	7.22	7.12	2.2	0.1024	0.1024	7.3224	2.3024
1990	7.34	7.26	2.12	0.096	0.096	7.436	2.216
1991	7.13	7.13	2.45	0.0896	0.0896	7.2196	2.5396
1992	7.39	7.14	1.74	0.0832	0.0832	7.4732	1.8232
1993	7.77	6.99	1.89	0.0768	0.0768	7.8468	1.9668
1994	7.62	7.14	1.97	0.0704	0.0704	7.6904	2.0404
1995	7.22	7.1	2.41	0.064	0.064	7.284	2.474
1996	7.51	7.1	1.43	0.0576	0.0576	7.5676	1.4876
1997	7.7	6.98	1.9	0.0512	0.0512	7.7512	1.9512
1998	8.43	6.95	3.06	0.0448	0.0448	8.4748	3.1048
1999	7.15	7.11	0.86	0.0384	0.0384	7.1884	0.8984
2000	7.23	7.15	1.06	0.032	0.032	7.262	1.092
2001	8.07	7.15	1.71	0.0256	0.0256	8.0956	1.7356
2002	7.33	6.97	2.07	0.0192	0.0192	7.3492	2.0892
2003	8.05	7.15	1.2	0.0128	0.0128	8.0628	1.2128
2004	7.39	7.13	1.8	0.0064	0.0064	7.3964	1.8064
2005	8.12	7.18	1.8	0	0	8.12	1.8

Table 2-1 (continued): Annual peak tide values selected, adjustments to peak values, and adjusted annual peak tide value

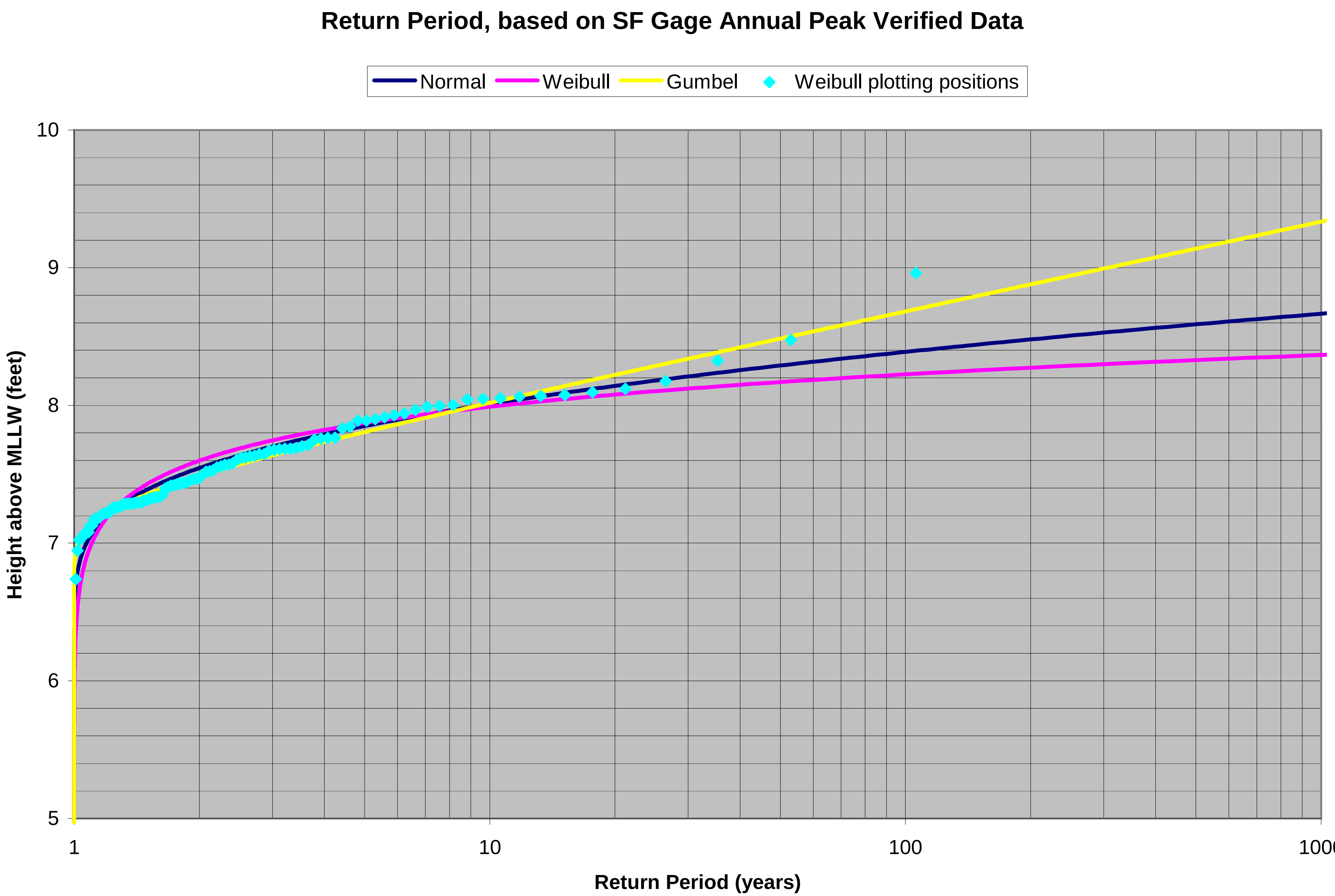

Return Period, based on SF Gage Annual Peak Verified Data
Normal
Weibull
Gumbel
Weibull plotting positions
10
9
8
7
6
5
Height above MLLW (feet)
1
10
100
1000
Return Period (years)

Plate 2-5

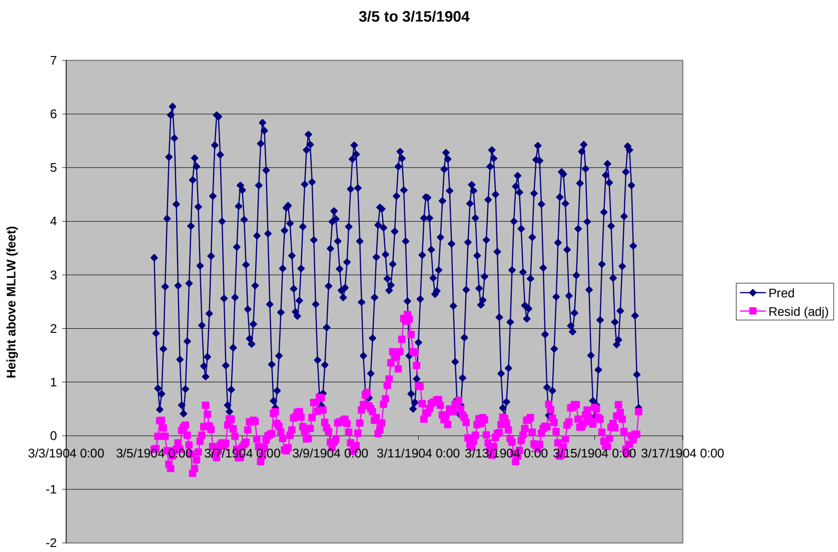
3/5 to 3/15/1904
Height above MLLW (feet)
7
6
5
4
3
2
1
0
-1
-2
3/3/1904 0:00
3/5/1904 0:00
3/7/1904 0:00
3/9/1904 0:00
3/11/1904 0:00
3/13/1904 0:00
3/15/1904 0:00
3/17/1904 0:00
Pred
Resid (adj)

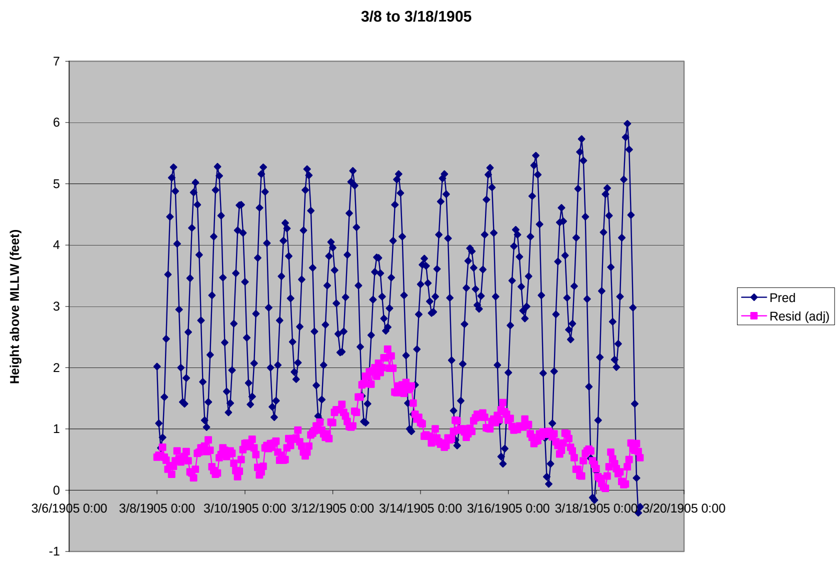
3/8 to 3/18/1905
Height above MLLW (feet)
7
6
5
4
3
2
1
0
-1
3/6/1905 0:00
3/8/1905 0:00
3/10/1905 0:00
3/12/1905 0:00
3/14/1905 0:00
3/16/1905 0:00
3/18/1905 0:00
3/20/1905 0:00
Pred
Resid (adj)

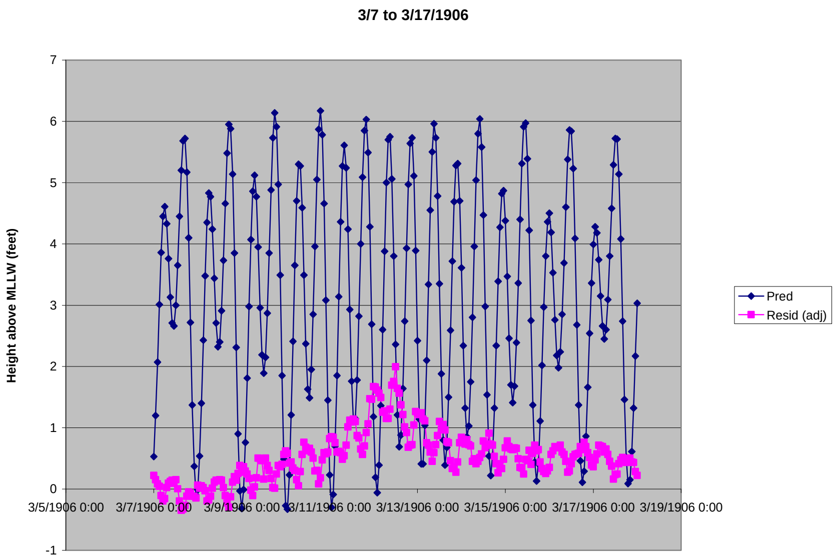

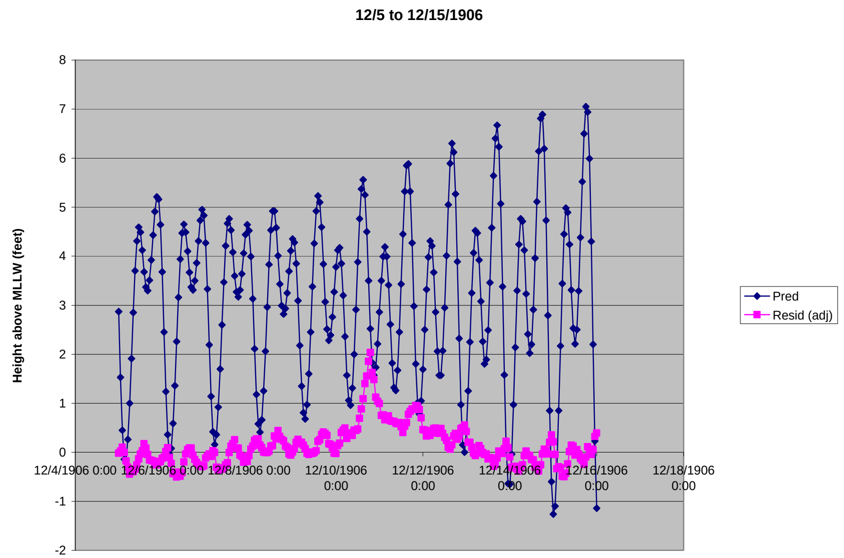

Plate 2-6: Time series of predicted and residual tide data

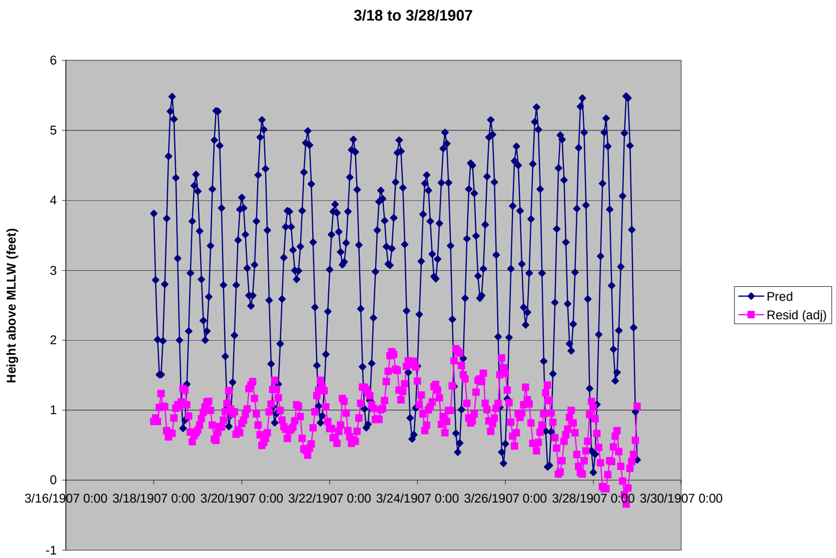

3/18 to 3/28/1907
Height above MLLW (feet)
6
5
4
3
2
1
0
-1
3/16/1907 0:00
3/18/1907 0:00
3/20/1907 0:00
3/22/1907 0:00
3/24/1907 0:00
3/26/1907 0:00
3/28/1907 0:00
3/30/1907 0:00
Pred
Resid (adj)

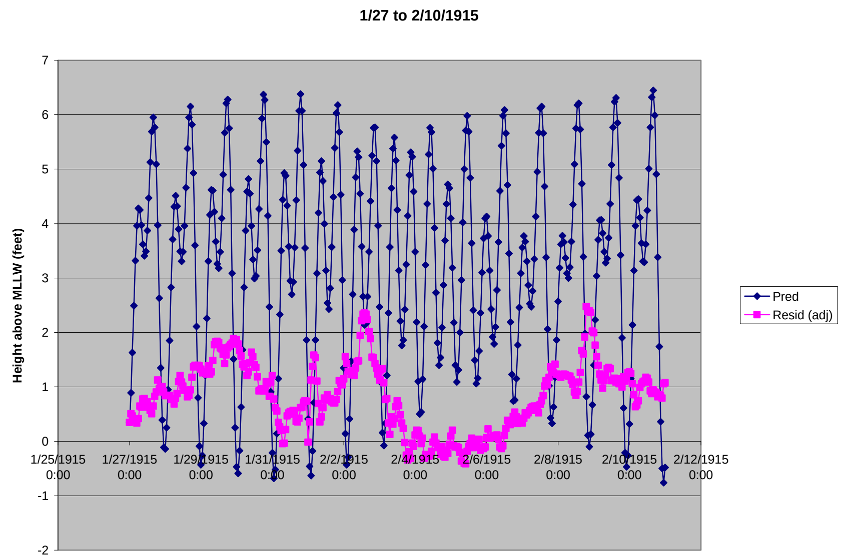

1/27 to 2/10/1915
Height above MLLW (feet)
7
6
5
4
3
2
1
0
-1
-2
1/25/1915 0:00
1/27/1915 0:00
1/29/1915 0:00
1/31/1915 0:00
2/2/1915 0:00
2/4/1915 0:00
2/6/1915 0:00
2/8/1915 0:00
2/10/1915 0:00
2/12/1915 0:00
Pred
Resid (adj)

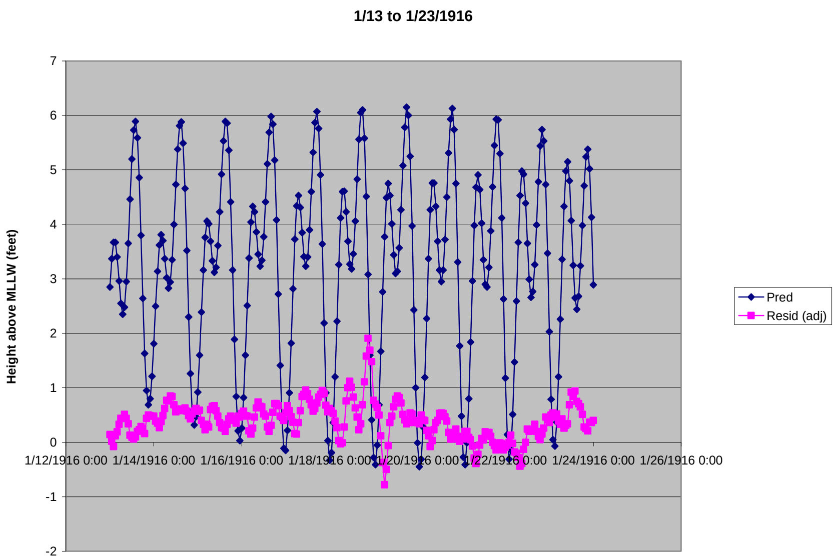

1/13 to 1/23/1916
Height above MLLW (feet)
7
6
5
4
3
2
1
0
-1
-2
1/12/1916 0:00
1/14/1916 0:00
1/16/1916 0:00
1/18/1916 0:00
1/20/1916 0:00
1/22/1916 0:00
1/24/1916 0:00
1/26/1916 0:00
Pred
Resid (adj)

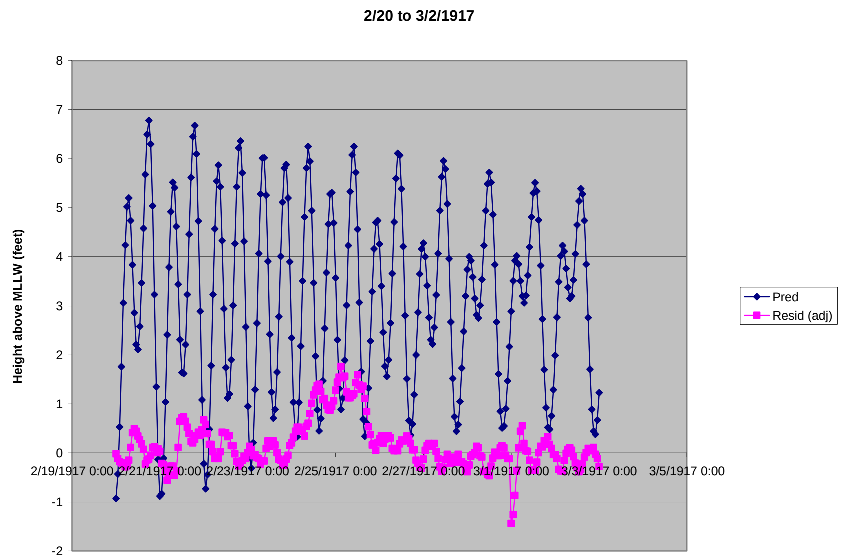

2/20 to 3/2/1917
Height above MLLW (feet)
8
7
6
5
4
3
2
1
0
-1
-2
2/19/1917 0:00
2/21/1917 0:00
2/23/1917 0:00
2/25/1917 0:00
2/27/1917 0:00
3/1/1917 0:00
3/3/1917 0:00
3/5/1917 0:00
Pred
Resid (adj)

Plate 2-7: Time series of predicted and residual tide data

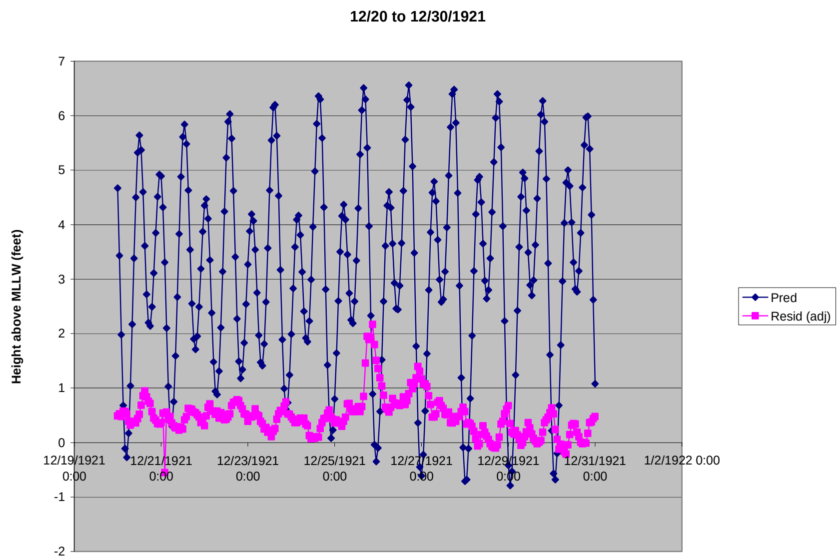

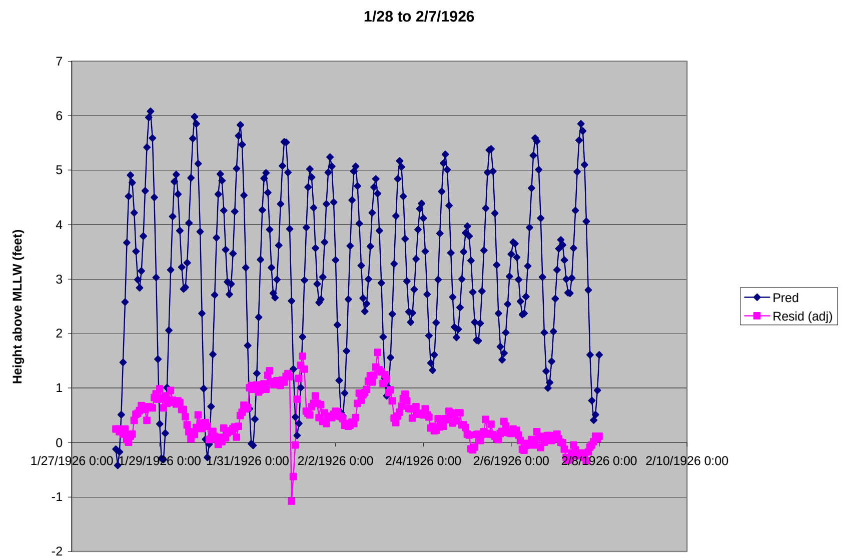

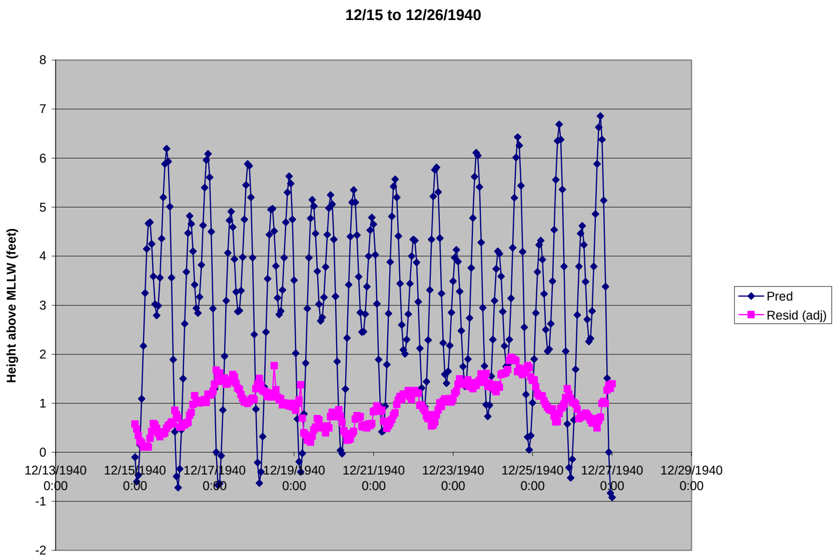

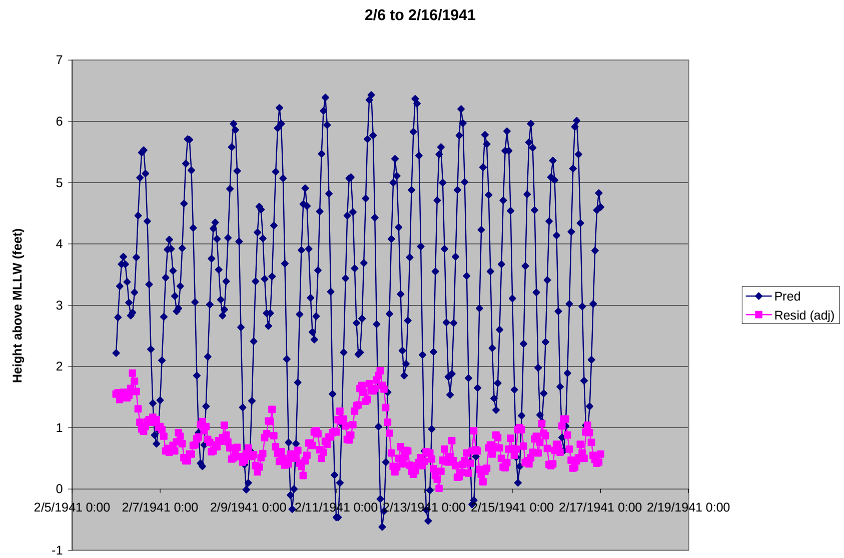

Plate 2-8: Time series of predicted and residual tide data

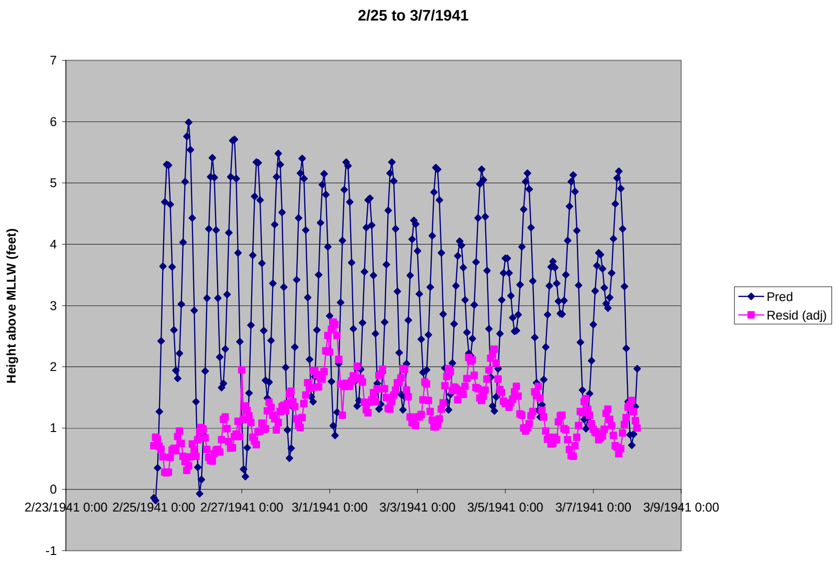

2/25 to 3/7/1941
Height above MLLW (feet)
7
6
5
4
3
2
1
0
-1
2/23/1941 0:00
2/25/1941 0:00
2/27/1941 0:00
3/1/1941 0:00
3/3/1941 0:00
3/5/1941 0:00
3/7/1941 0:00
3/9/1941 0:00
Pred
Resid (adj)

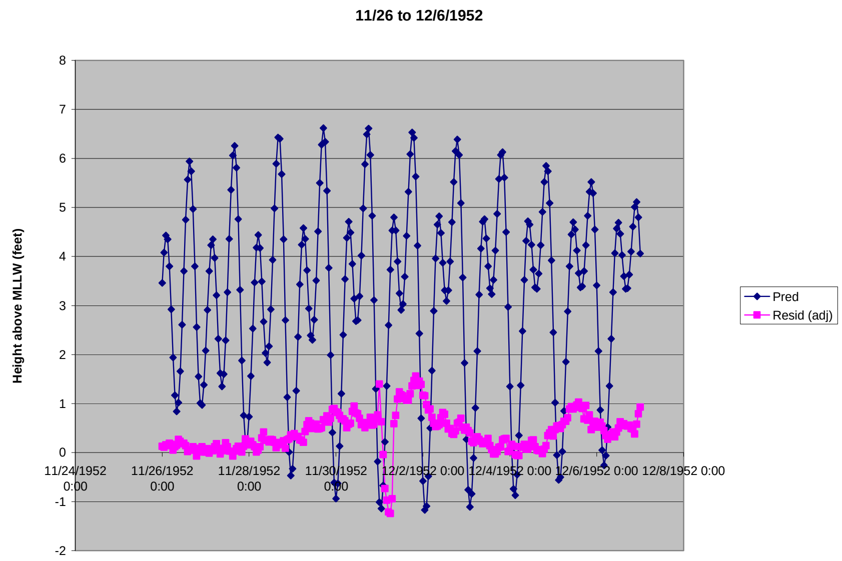

11/26 to 12/6/1952
Height above MLLW (feet)
8
7
6
5
4
3
2
1
0
-1
-2
11/24/1952 0:00
11/26/1952 0:00
11/28/1952 0:00
11/30/1952 0:00
12/2/1952 0:00
12/4/1952 0:00
12/6/1952 0:00
12/8/1952 0:00
Pred
Resid (adj)

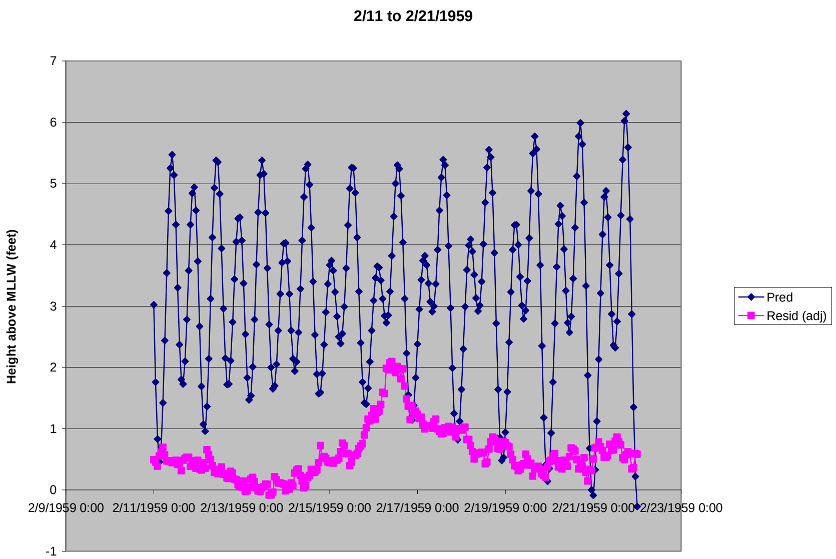

2/11 to 2/21/1959
Height above MLLW (feet)
7
6
5
4
3
2
1
0
-1
2/9/1959 0:00
2/11/1959 0:00
2/13/1959 0:00
2/15/1959 0:00
2/17/1959 0:00
2/19/1959 0:00
2/21/1959 0:00
2/23/1959 0:00
Pred
Resid (adj)

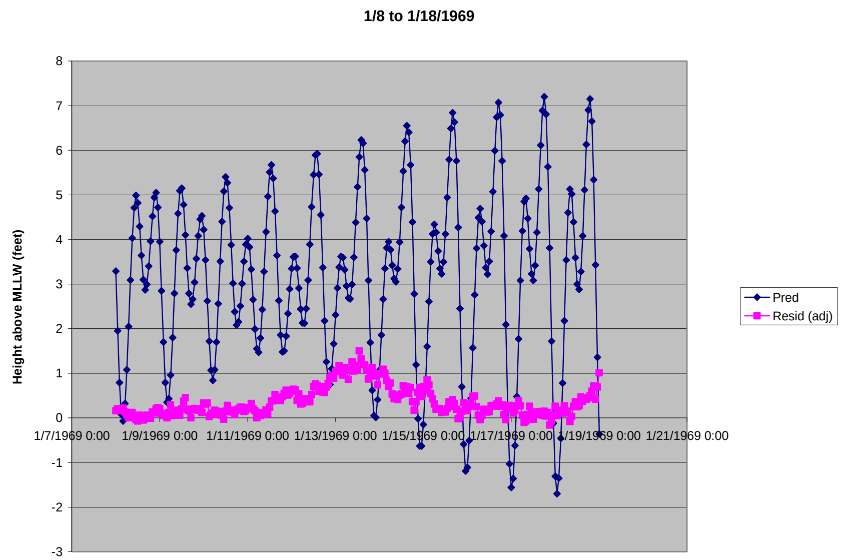

1/8 to 1/18/1969
Height above MLLW (feet)
8
7
6
5
4
3
2
1
0
-1
-2
-3
1/7/1969 0:00
1/9/1969 0:00
1/11/1969 0:00
1/13/1969 0:00
1/15/1969 0:00
1/17/1969 0:00
1/19/1969 0:00
1/21/1969 0:00
Pred
Resid (adj)

Plate 2-9: Time series of predicted and residual tide data

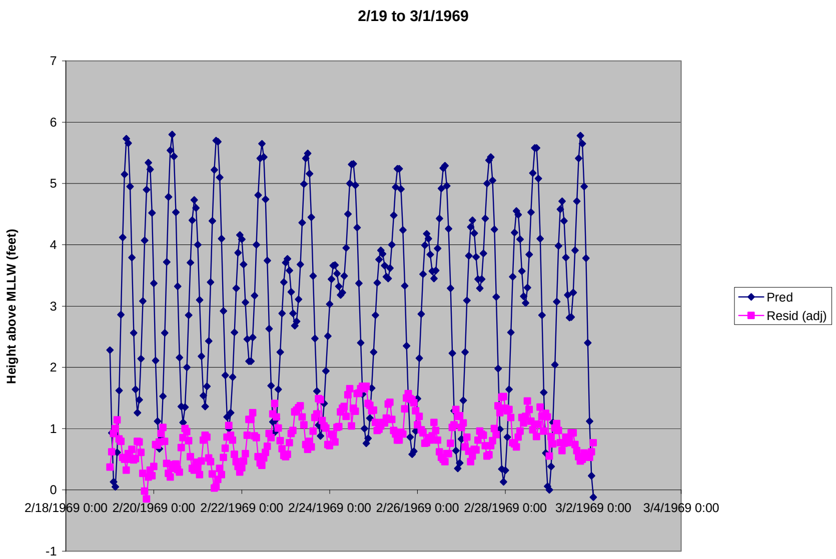

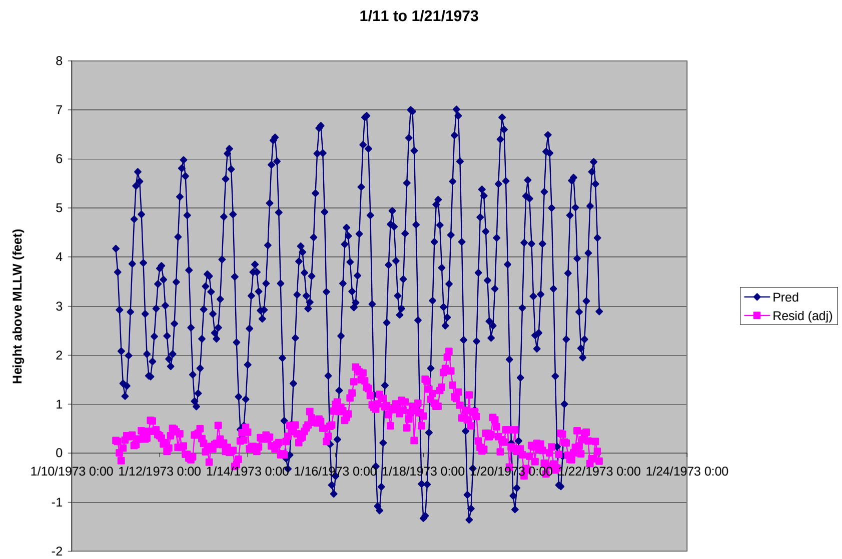

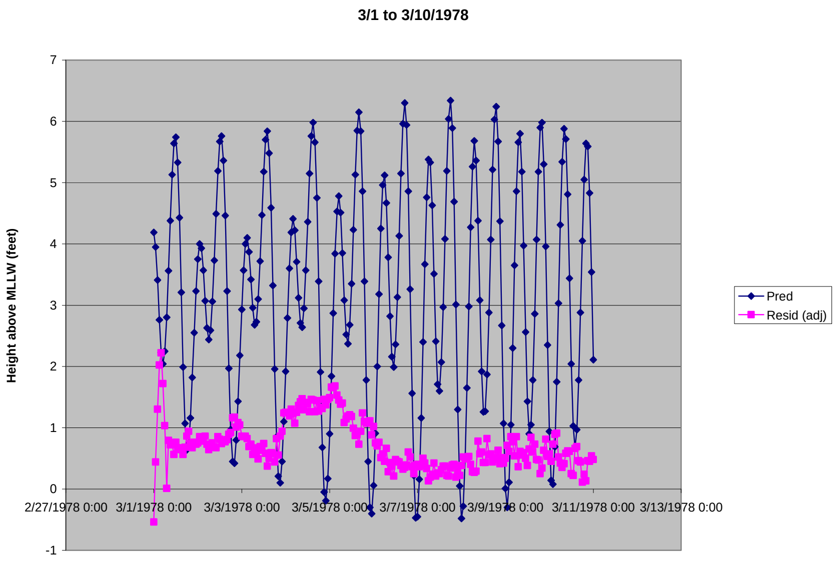

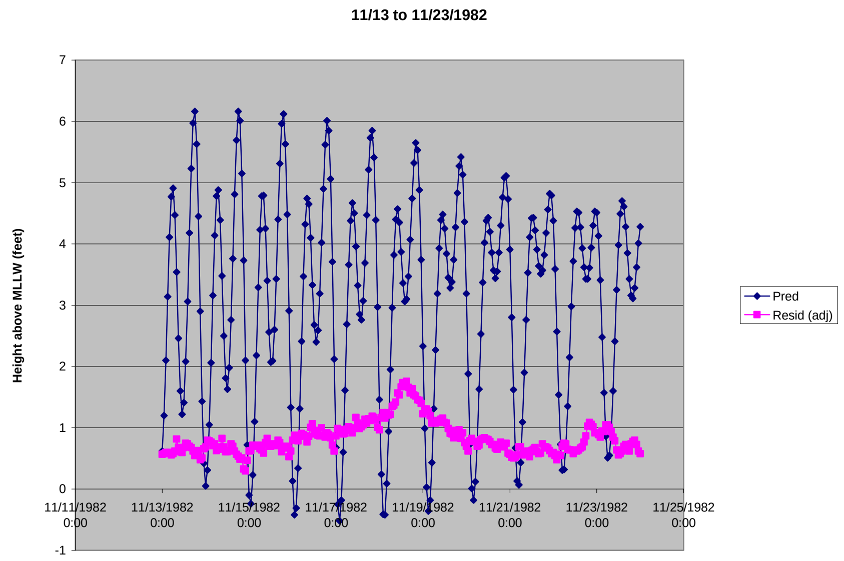

Plate 2-10: Time series of predicted and residual tide data

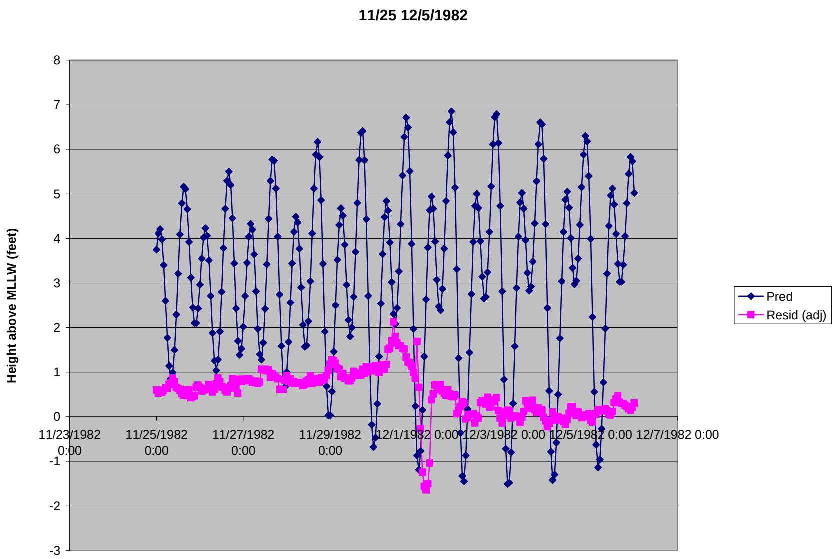

11/25 12/5/1982
Height above MLLW (feet)
8
7
6
5
4
3
2
1
0
-1
-2
-3
11/23/1982 0:00
11/25/1982 0:00
11/27/1982 0:00
11/29/1982 0:00
12/1/1982 0:00
12/3/1982 0:00
12/5/1982 0:00
12/7/1982 0:00
Pred
Resid (adj)

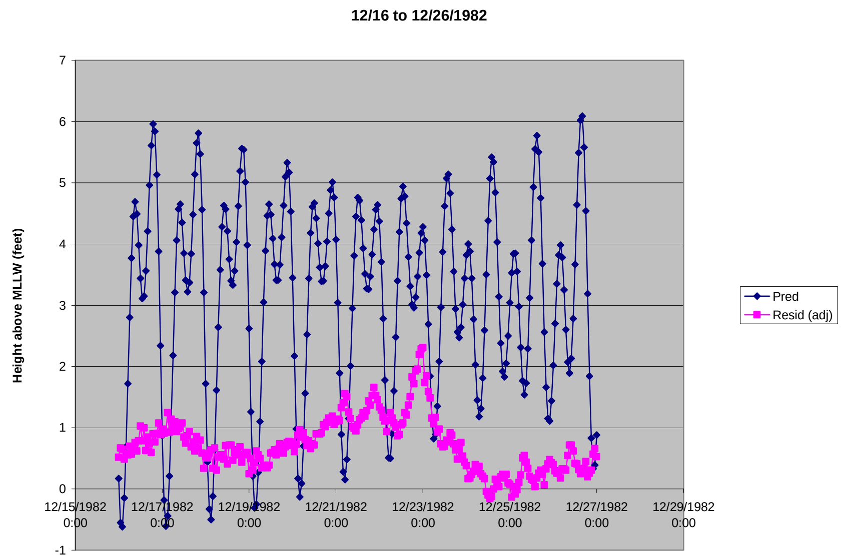

12/16 to 12/26/1982
Height above MLLW (feet)
7
6
5
4
3
2
1
0
-1
12/15/1982 0:00
12/17/1982 0:00
12/19/1982 0:00
12/21/1982 0:00
12/23/1982 0:00
12/25/1982 0:00
12/27/1982 0:00
12/29/1982 0:00
Pred
Resid (adj)

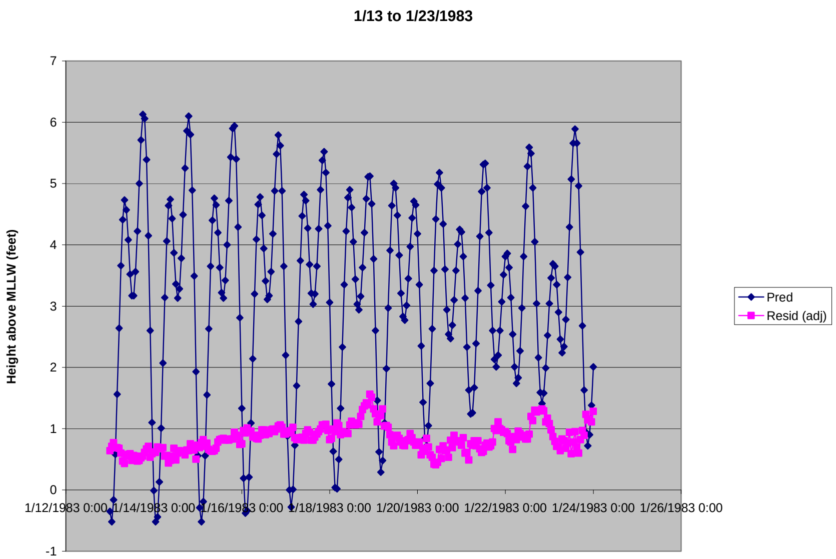

1/13 to 1/23/1983
Height above MLLW (feet)
7
6
5
4
3
2
1
0
-1
1/12/1983 0:00
1/14/1983 0:00
1/16/1983 0:00
1/18/1983 0:00
1/20/1983 0:00
1/22/1983 0:00
1/24/1983 0:00
1/26/1983 0:00
Pred
Resid (adj)

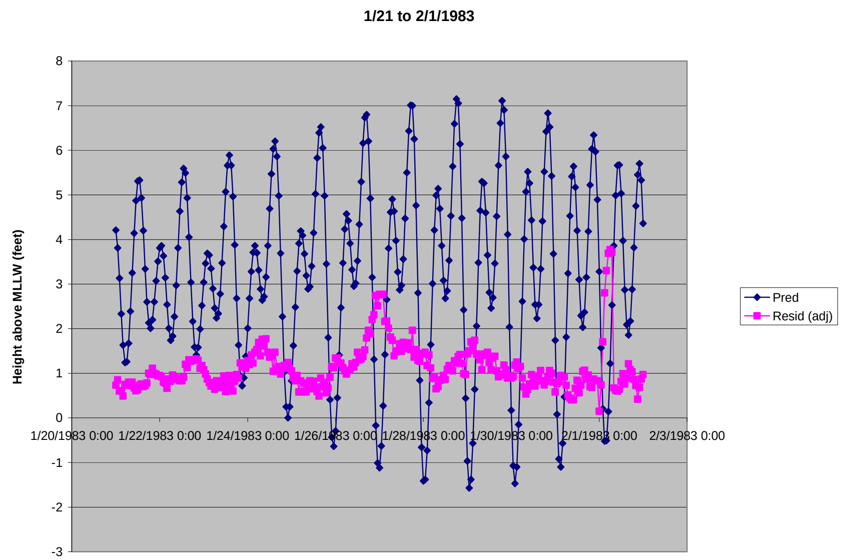

1/21 to 2/1/1983
Height above MLLW (feet)
8
7
6
5
4
3
2
1
0
-1
-2
-3
1/20/1983 0:00
1/22/1983 0:00
1/24/1983 0:00
1/26/1983 0:00
1/28/1983 0:00
1/30/1983 0:00
2/1/1983 0:00
2/3/1983 0:00
Pred
Resid (adj)

Plate 2-11: Time series of predicted and residual tide data

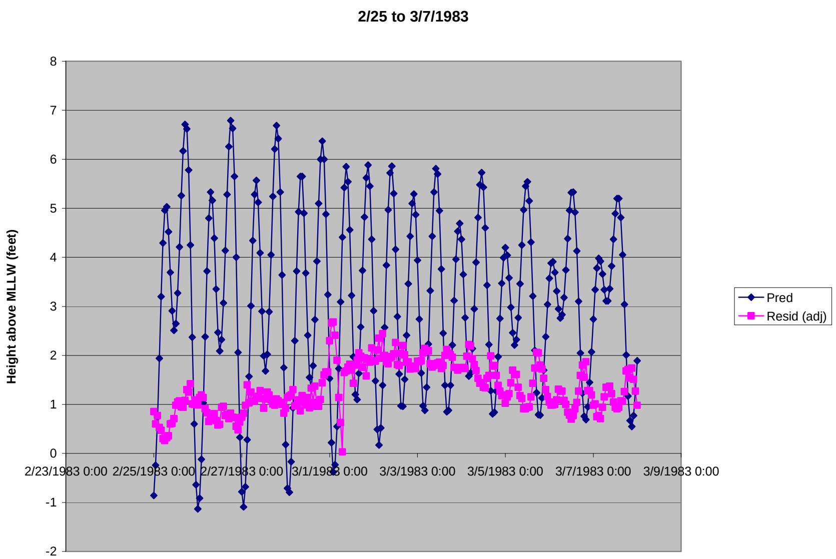

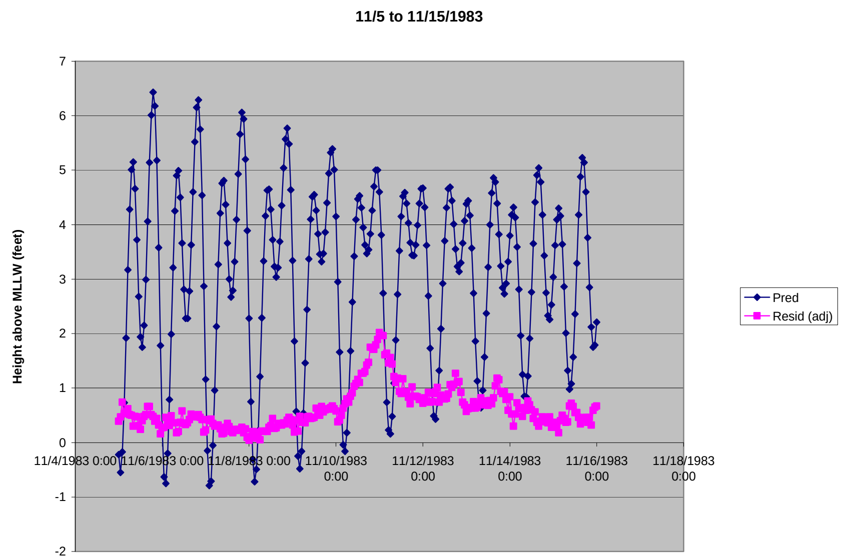

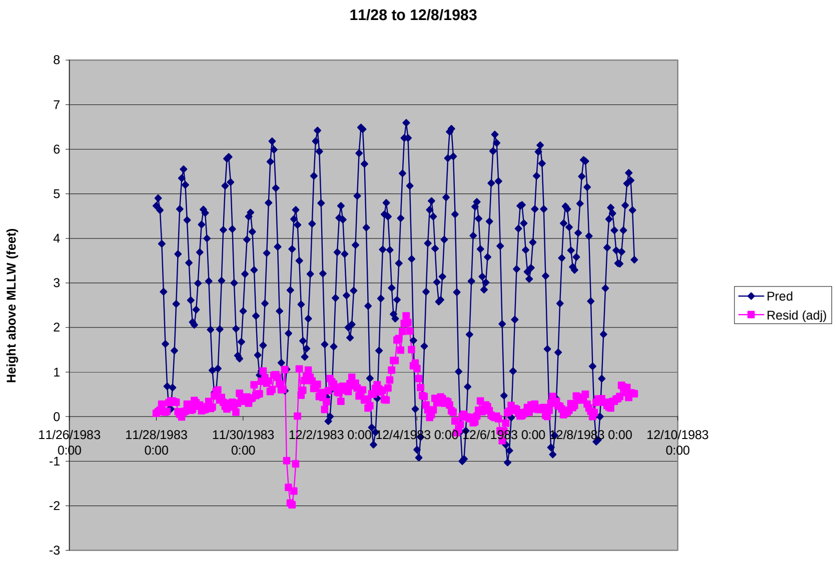

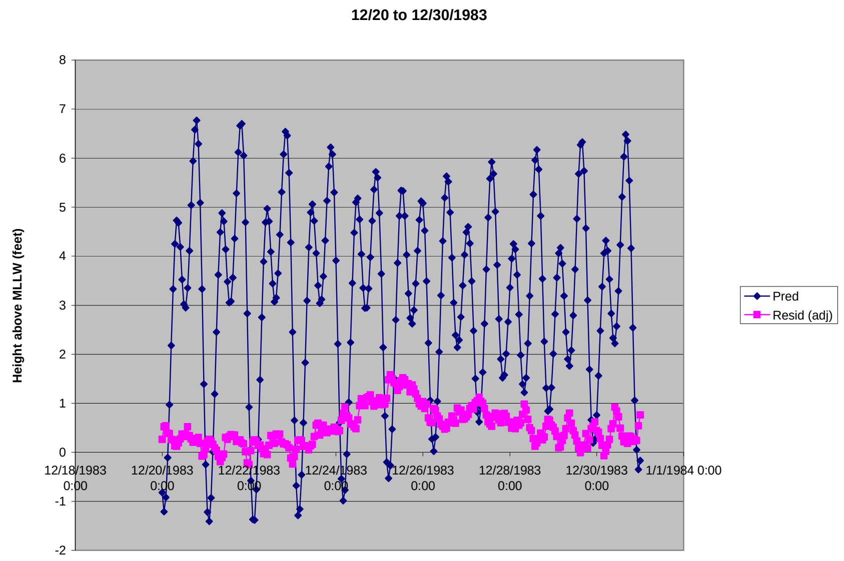

Plate 2-12: Time series of predicted and residual tide data

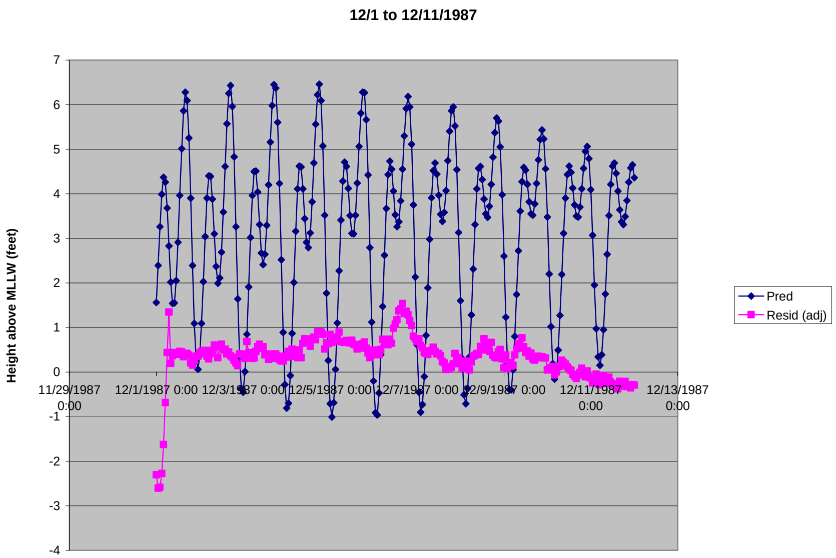
12/1 to 12/11/1987
Height above MLLW (feet)
7
6
5
4
3
2
1
0
-1
-2
-3
-4
11/29/1987 0:00
12/1/1987 0:00
12/3/1987 0:00
12/5/1987 0:00
12/7/1987 0:00
12/9/1987 0:00
12/11/1987 0:00
12/13/1987 0:00
Pred
Resid (adj)

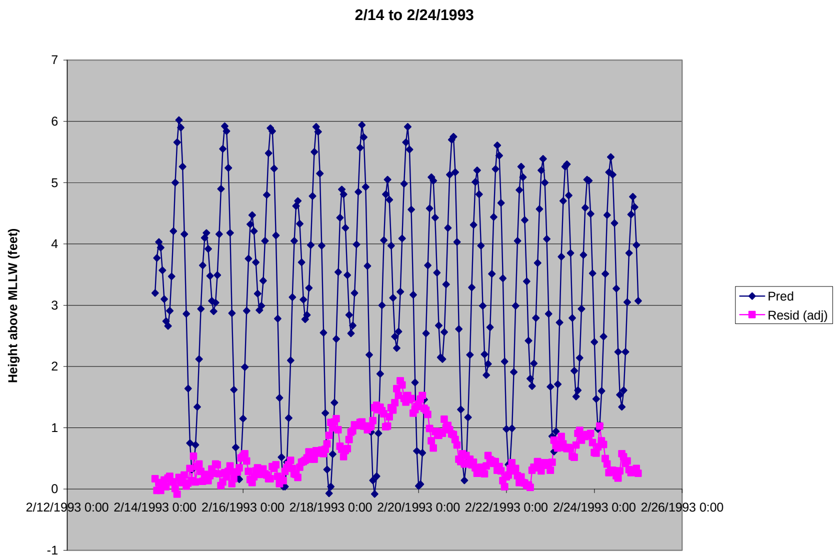
2/14 to 2/24/1993
Height above MLLW (feet)
7
6
5
4
3
2
1
0
-1
2/12/1993 0:00
2/14/1993 0:00
2/16/1993 0:00
2/18/1993 0:00
2/20/1993 0:00
2/22/1993 0:00
2/24/1993 0:00
2/26/1993 0:00
Pred
Resid (adj)

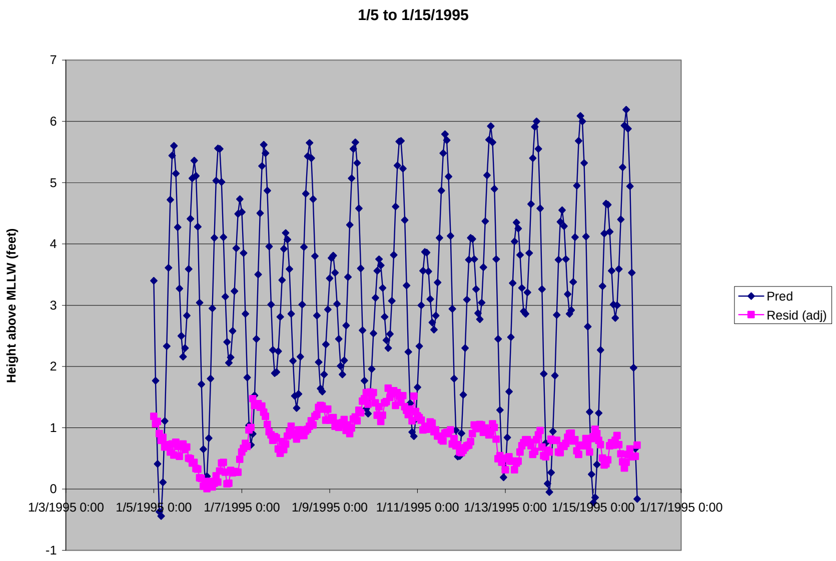

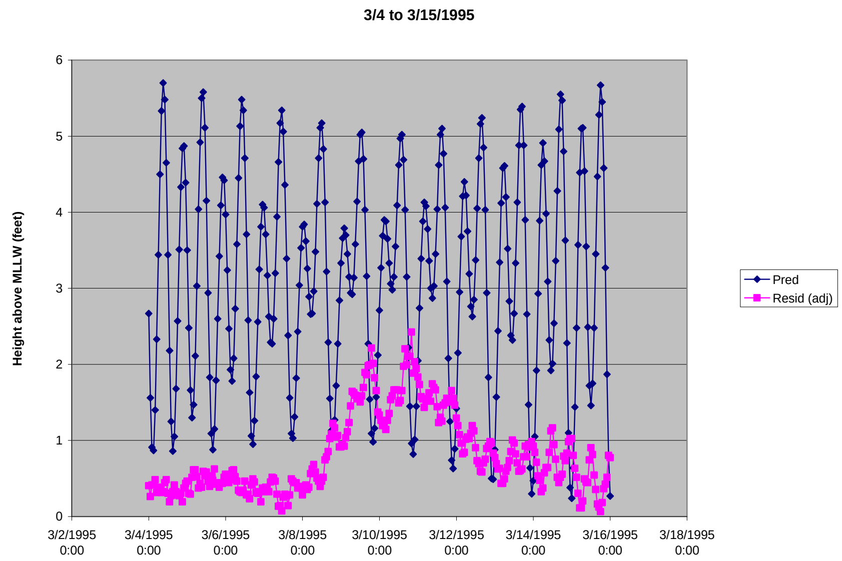

Plate 2-13: Time series of predicted and residual tide data

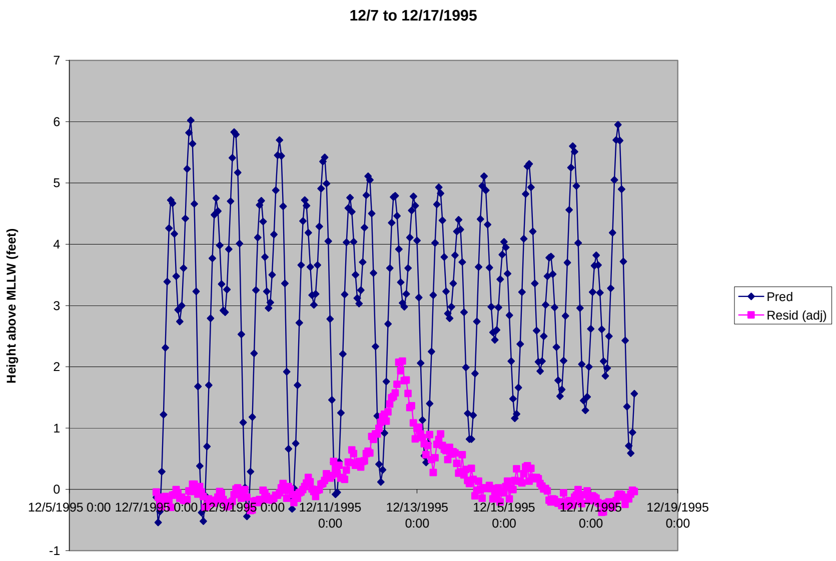
12/7 to 12/17/1995
Height above MLLW (feet)
Pred
Resid (adj)

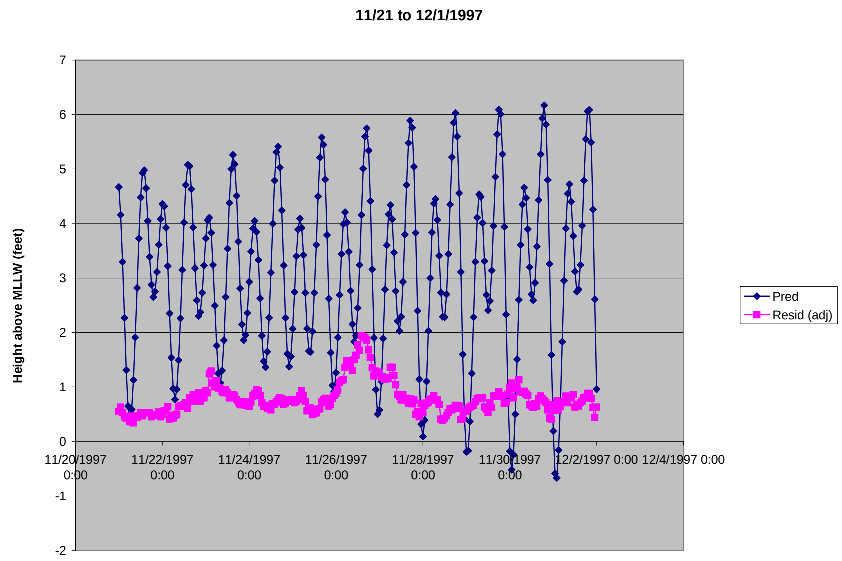
11/21 to 12/1/1997
Height above MLLW (feet)
Pred
Resid (adj)

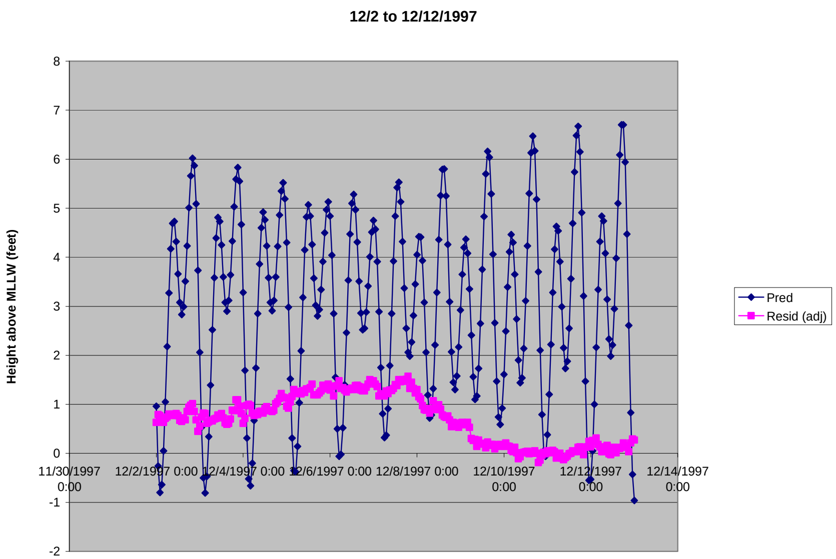
12/2 to 12/12/1997
Height above MLLW (feet)
Pred
Resid (adj)

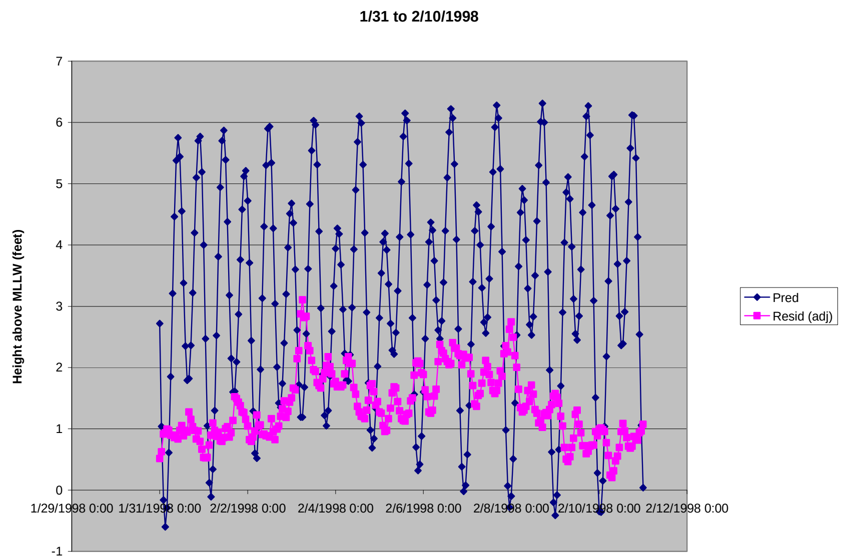
1/31 to 2/10/1998
Height above MLLW (feet)
Pred
Resid (adj)

Plate 2-14: Time series of predicted and residual tide data

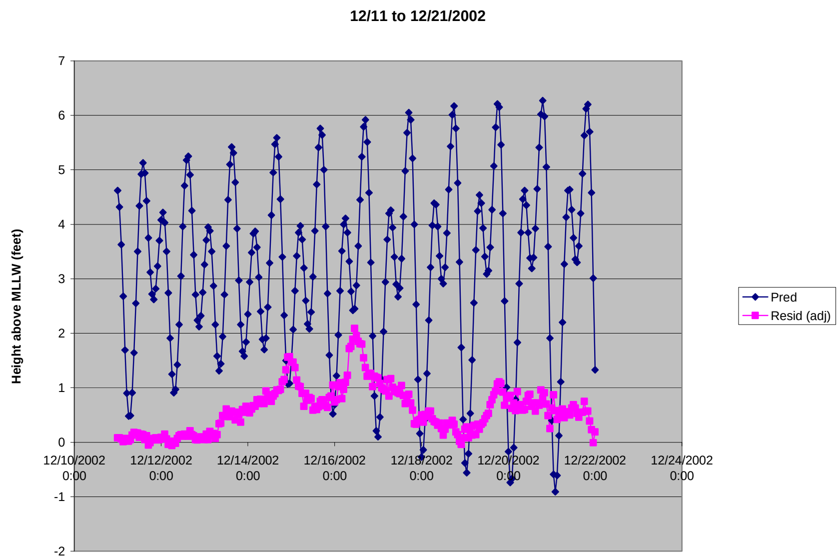

Plate 2-15: Time series of predicted and residual tide data

47 Time Series with High Residual Events				
Beginning of Time Series	End of Time Series	Maximum predicted tide data value during time series (feet MLLW)	Maximum verified tide data value during time series, adjusted for sea level rise (feet MLLW)	Maximum residual tide data value during time series, adjusted for sea level rise (feet MLLW)
3/9/1904 0:00	3/12/1904 0:00	5.42	6.97	2.26
3/12/1905 0:00	3/15/1905 0:00	5.21	6.86	2.30
3/11/1906 0:00	3/14/1906 0:00	6.03	7.05	1.99
12/10/1906 0:00	12/13/1906 0:00	6.3	6.65	2.03
3/23/1907 0:00	3/26/1907 0:00	5.15	6.25	1.88
1/28/1915 0:00	1/31/1915 0:00	6.37	8.00	1.89
2/1/1915 0:00	2/4/1915 0:00	6.18	7.30	2.36
2/7/1915 0:00	2/10/1915 0:00	6.31	7.40	2.48
1/17/1916 0:00	1/20/1916 0:00	6.15	6.79	1.91
2/23/1917 0:00	2/26/1917 0:00	6.25	7.45	1.76
12/25/1921 0:00	12/28/1921 0:00	6.56	7.76	2.17
1/30/1926 0:00	2/2/1926 0:00	5.83	6.73	1.59
2/2/1926 0:00	2/5/1926 0:00	5.29	6.23	1.66
12/16/1940 0:00	12/19/1940 0:00	6.09	7.28	1.77
12/23/1940 0:00	12/26/1940 0:00	6.69	8.08	1.94
2/10/1941 0:00	2/13/1941 0:00	6.43	8.07	1.93
2/28/1941 0:00	3/3/1941 0:00	5.4	7.07	2.73
3/3/1941 0:00	3/6/1941 0:00	5.25	6.67	2.29
11/30/1952 0:00	12/3/1952 0:00	6.61	7.89	1.56
2/15/1959 0:00	2/18/1959 0:00	5.39	7.31	2.09
1/12/1969 0:00	1/15/1969 0:00	6.55	7.55	1.50
2/23/1969 0:00	2/26/1969 0:00	5.49	6.65	1.69
1/15/1973 0:00	1/18/1973 0:00	7	8.32	1.75
1/17/1973 0:00	1/20/1973 0:00	7.01	8.12	2.07
3/3/1978 0:00	3/6/1978 0:00	6.15	7.43	1.68
11/17/1982 0:00	11/20/1982 0:00	5.85	7.17	1.76
11/29/1982 0:00	12/2/1982 0:00	6.85	8.05	2.13
12/21/1982 0:00	12/24/1982 0:00	5.14	6.59	2.31
1/17/1983 0:00	1/20/1983 0:00	5.52	6.68	1.56
1/22/1983 0:00	1/25/1983 0:00	6.2	7.67	1.77
1/26/1983 0:00	1/29/1983 0:00	7.15	8.96	2.77
1/28/1983 0:00	1/31/1983 0:00	7.15	8.42	1.74
3/1/1983 0:00	3/4/1983 0:00	5.88	7.83	2.68
11/10/1983 0:00	11/13/1983 0:00	5	6.89	2.02
12/2/1983 0:00	12/5/1983 0:00	6.59	8.85	2.26
12/24/1983 0:00	12/27/1983 0:00	5.72	6.85	1.58
12/5/1987 0:00	12/8/1987 0:00	6.28	7.47	1.54
2/18/1993 0:00	2/21/1993 0:00	5.94	7.44	1.77
1/8/1995 0:00	1/11/1995 0:00	5.68	7.19	1.64
3/9/1995 0:00	3/12/1995 0:00	5.1	6.67	2.42
12/11/1995 0:00	12/14/1995 0:00	5.11	6.36	2.09
11/25/1997 0:00	11/28/1997 0:00	5.89	7.61	1.94
12/5/1997 0:00	12/8/1997 0:00	5.53	7.03	1.57
2/2/1998 0:00	2/5/1998 0:00	6.1	7.99	3.10
2/4/1998 0:00	2/7/1998 0:00	6.22	8.47	2.40
2/6/1998 0:00	2/9/1998 0:00	6.31	8.47	2.74
12/14/2002 0:00	12/17/2002 0:00	5.92	7.34	2.09

Table 2-2. Selected events based on conditions applied to predicted and residual data

33 Time Series with High Residual Events				
Beginning of Time Series	End of Time Series	Maximum predicted tide data value during time series (feet MLLW)	Maximum verified tide data value during time series, adjusted for sea level rise (feet MLLW)	Maximum residual tide data value during time series, adjusted for sea level rise (feet MLLW)
3/9/1904 0:00	3/12/1904 0:00	5.42	6.9664	2.2564
3/11/1906 0:00	3/14/1906 0:00	6.03	7.0536	1.9936
1/28/1915 0:00	1/31/1915 0:00	6.37	7.996	1.886
2/1/1915 0:00	2/4/1915 0:00	6.18	7.296	2.356
2/7/1915 0:00	2/10/1915 0:00	6.31	7.396	2.476
2/23/1917 0:00	2/26/1917 0:00	6.25	7.4532	1.7632
12/25/1921 0:00	12/28/1921 0:00	6.56	7.7576	2.1676
12/16/1940 0:00	12/19/1940 0:00	6.09	7.276	1.766
12/23/1940 0:00	12/26/1940 0:00	6.69	8.076	1.936
2/10/1941 0:00	2/13/1941 0:00	6.43	8.0696	1.9296
2/28/1941 0:00	3/3/1941 0:00	5.4	7.0696	2.7296
11/30/1952 0:00	12/3/1952 0:00	6.61	7.8892	1.5592
2/15/1959 0:00	2/18/1959 0:00	5.39	7.3144	2.0944
1/12/1969 0:00	1/15/1969 0:00	6.55	7.5504	1.5004
1/15/1973 0:00	1/18/1973 0:00	7	8.3248	1.7548
1/17/1973 0:00	1/20/1973 0:00	7.01	8.1248	2.0748
3/3/1978 0:00	3/6/1978 0:00	6.15	7.4328	1.6828
11/17/1982 0:00	11/20/1982 0:00	5.85	7.1672	1.7572
11/29/1982 0:00	12/2/1982 0:00	6.85	8.0472	2.1272
1/22/1983 0:00	1/25/1983 0:00	6.2	7.6708	1.7708
1/26/1983 0:00	1/29/1983 0:00	7.15	8.9608	2.7708
1/28/1983 0:00	1/31/1983 0:00	7.15	8.4208	1.7408
3/1/1983 0:00	3/4/1983 0:00	5.88	7.8308	2.6808
12/2/1983 0:00	12/5/1983 0:00	6.59	8.8508	2.2608
12/5/1987 0:00	12/8/1987 0:00	6.28	7.4652	1.5352
2/18/1993 0:00	2/21/1993 0:00	5.94	7.4368	1.7668
1/8/1995 0:00	1/11/1995 0:00	5.68	7.194	1.644
11/25/1997 0:00	11/28/1997 0:00	5.89	7.6112	1.9412
12/5/1997 0:00	12/8/1997 0:00	5.53	7.0312	1.5712
2/2/1998 0:00	2/5/1998 0:00	6.1	7.9948	3.1048
2/4/1998 0:00	2/7/1998 0:00	6.22	8.4748	2.4048
2/6/1998 0:00	2/9/1998 0:00	6.31	8.4748	2.7448
12/14/2002 0:00	12/17/2002 0:00	5.92	7.3392	2.0892

Table 2-3. Selected events based on conditions applied to predicted and residual data

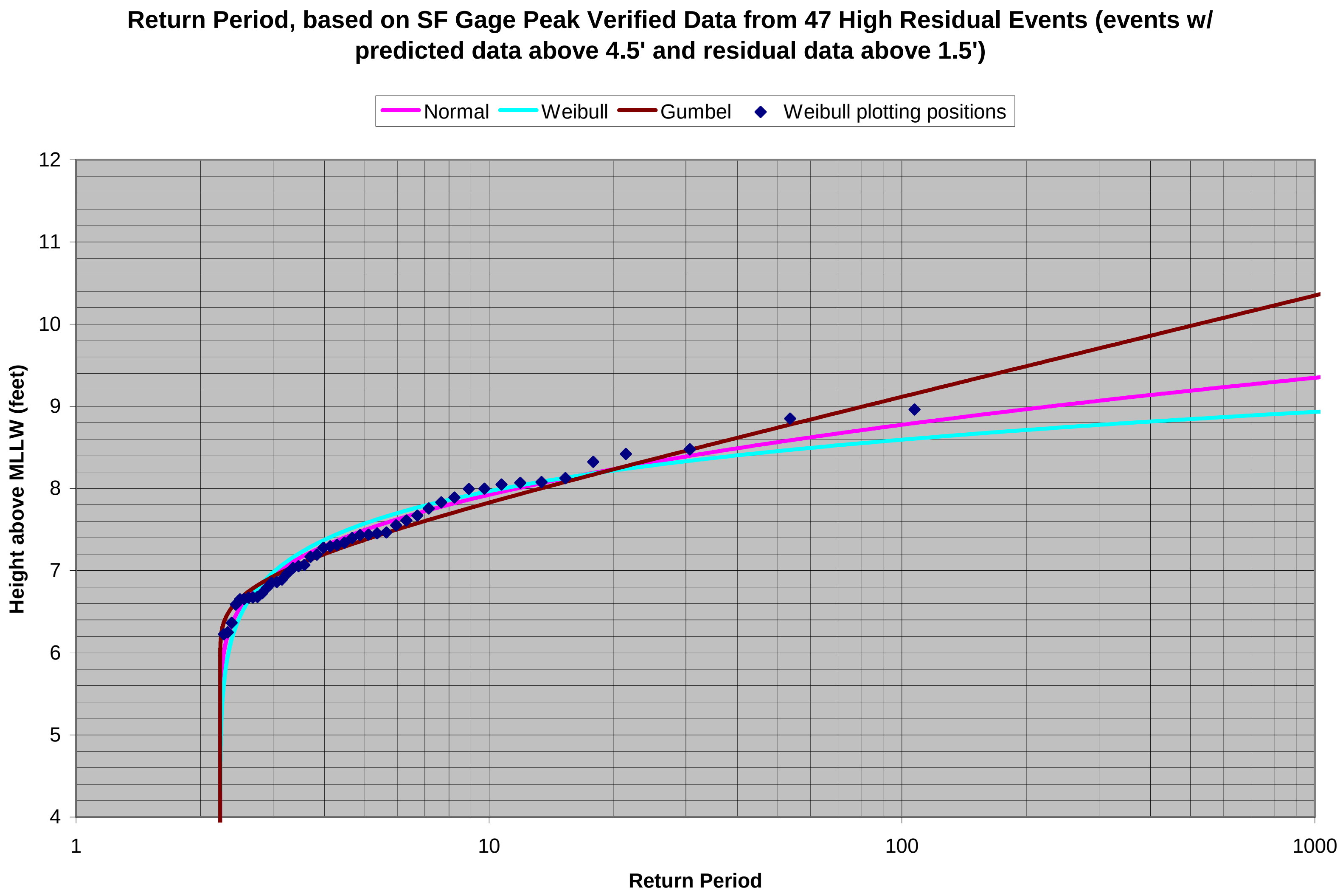

Return Period, based on SF Gage Peak Verified Data from 47 High Residual Events (events w/ predicted data above 4.5' and residual data above 1.5')
Normal
Weibull
Gumbel
Weibull plotting positions
Height above MLLW (feet)
12
11
10
9
8
7
6
5
4
1
10
100
1000
Return Period

Plate 2-16

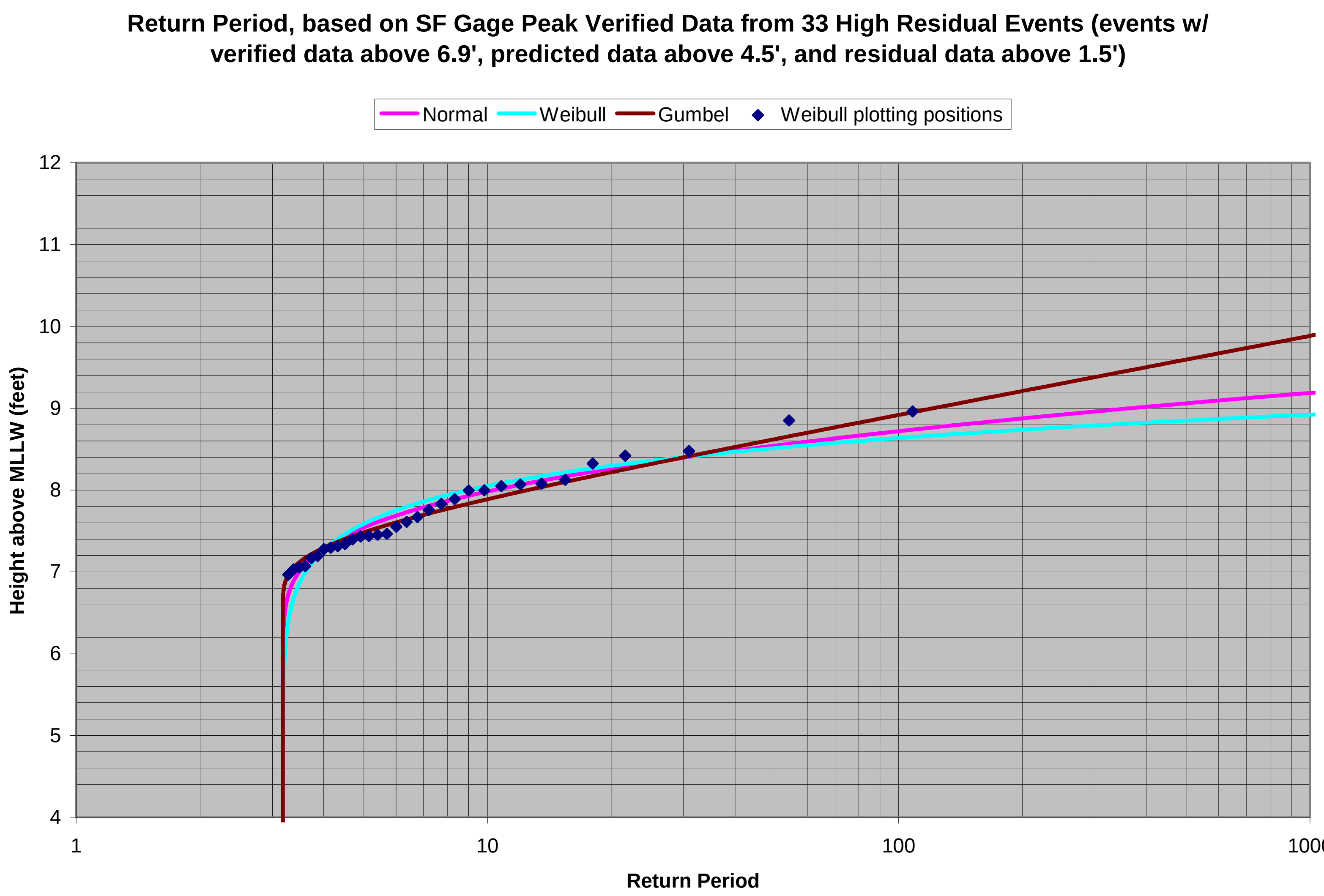
Return Period, based on SF Gage Peak Verified Data from 33 High Residual Events (events w/ verified data above 6.9', predicted data above 4.5', and residual data above 1.5')
Normal
Weibull
Gumbel
Weibull plotting positions
Height above MLLW (feet)
12
11
10
9
8
7
6
5
4
1
10
100
1000
Return Period

Plate 2-17

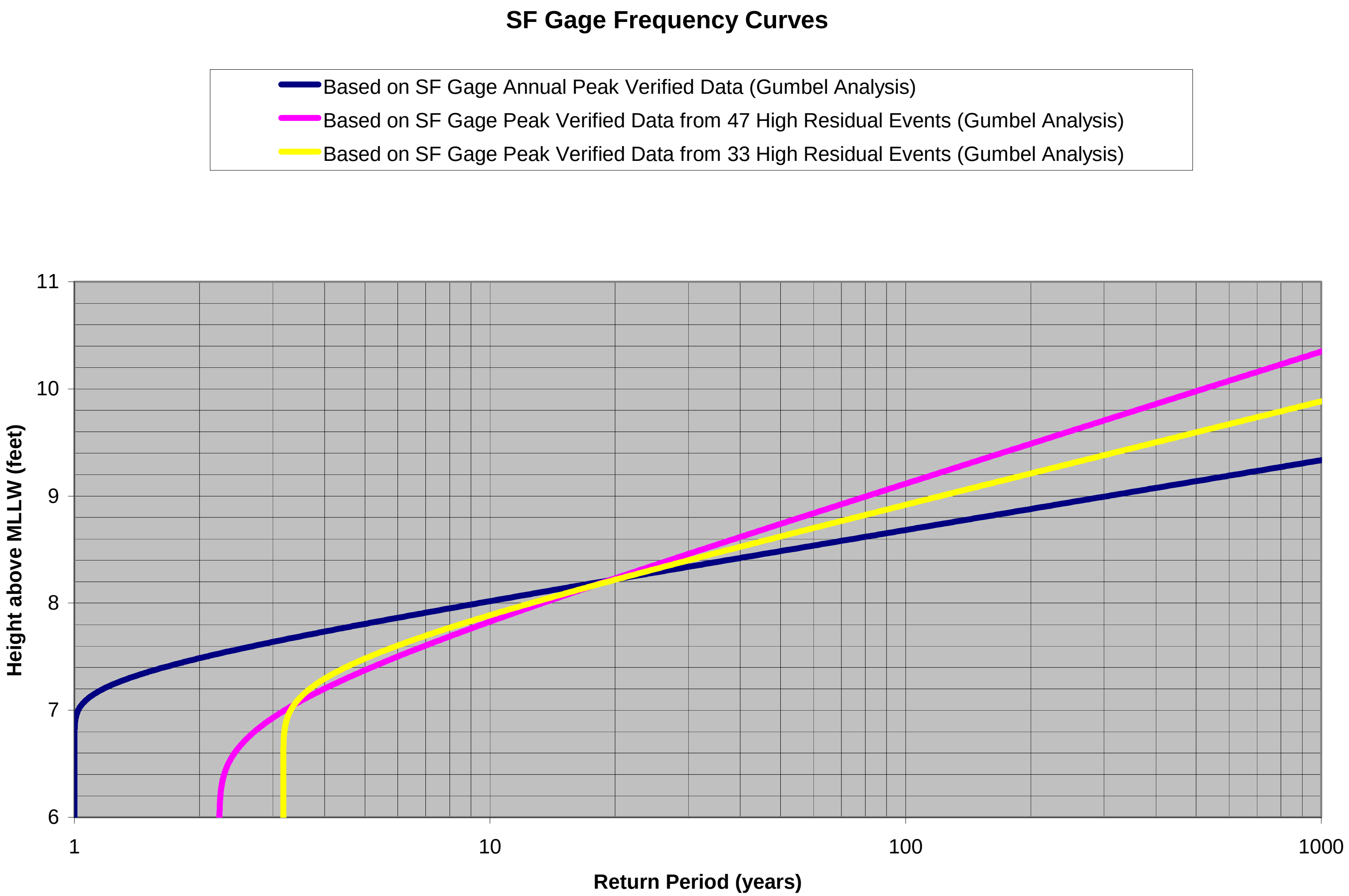
SF Gage Frequency Curves
Based on SF Gage Annual Peak Verified Data (Gumbel Analysis)
Based on SF Gage Peak Verified Data from 47 High Residual Events (Gumbel Analysis)
Based on SF Gage Peak Verified Data from 33 High Residual Events (Gumbel Analysis)
Height above MLLW (feet)
11
10
9
8
7
6
1
10
100
1000
Return Period (years)

Plate 2-18

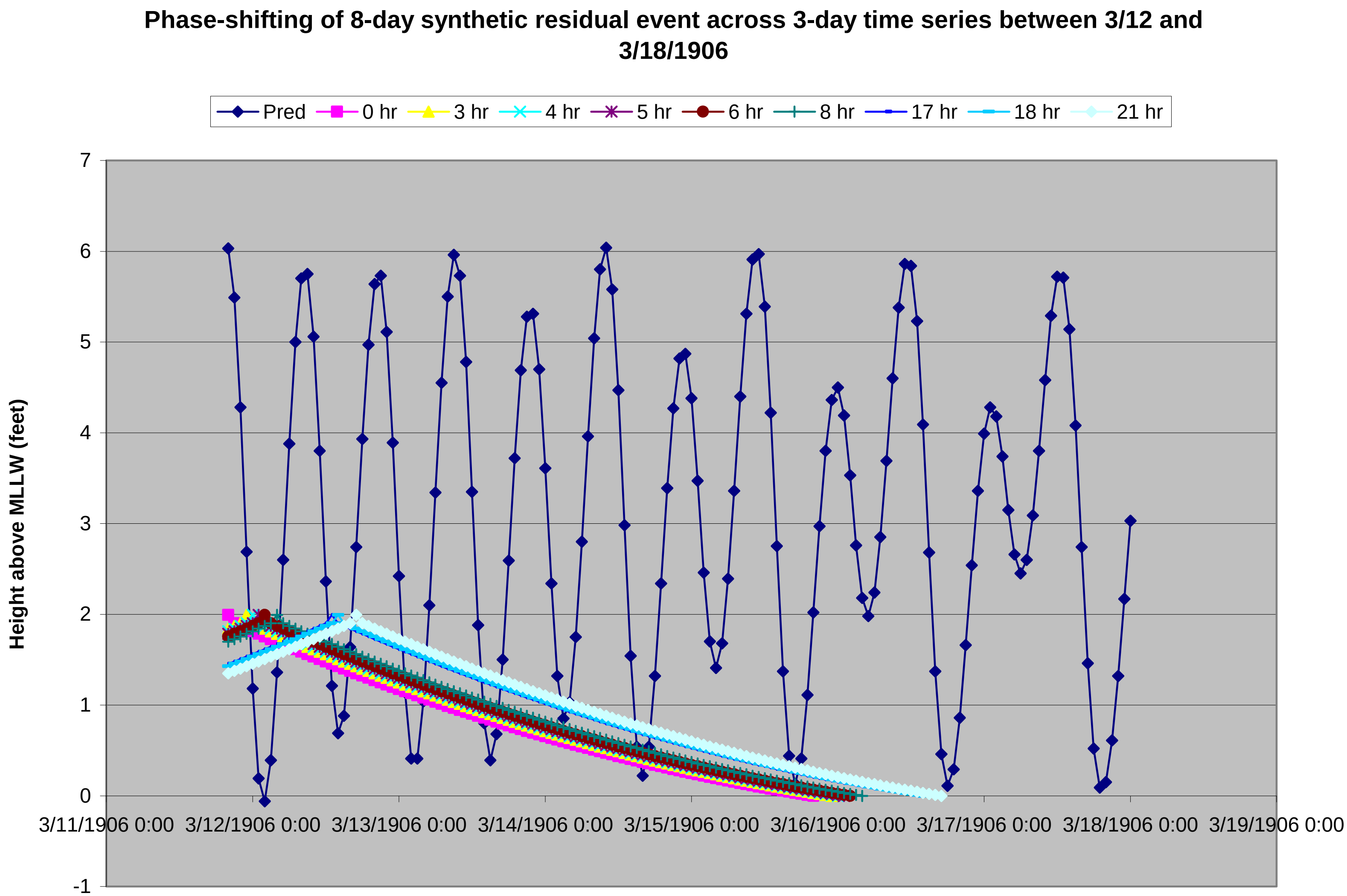
Phase-shifting of 8-day synthetic residual event across 3-day time series between 3/12 and 3/18/1906
Pred
0 hr
3 hr
4 hr
5 hr
6 hr
8 hr
17 hr
18 hr
21 hr
Height above MLLW (feet)
7
6
5
4
3
2
1
0
-1
3/11/1906 0:00
3/12/1906 0:00
3/13/1906 0:00
3/14/1906 0:00
3/15/1906 0:00
3/16/1906 0:00
3/17/1906 0:00
3/18/1906 0:00
3/19/1906 0:00

Plate 2-19

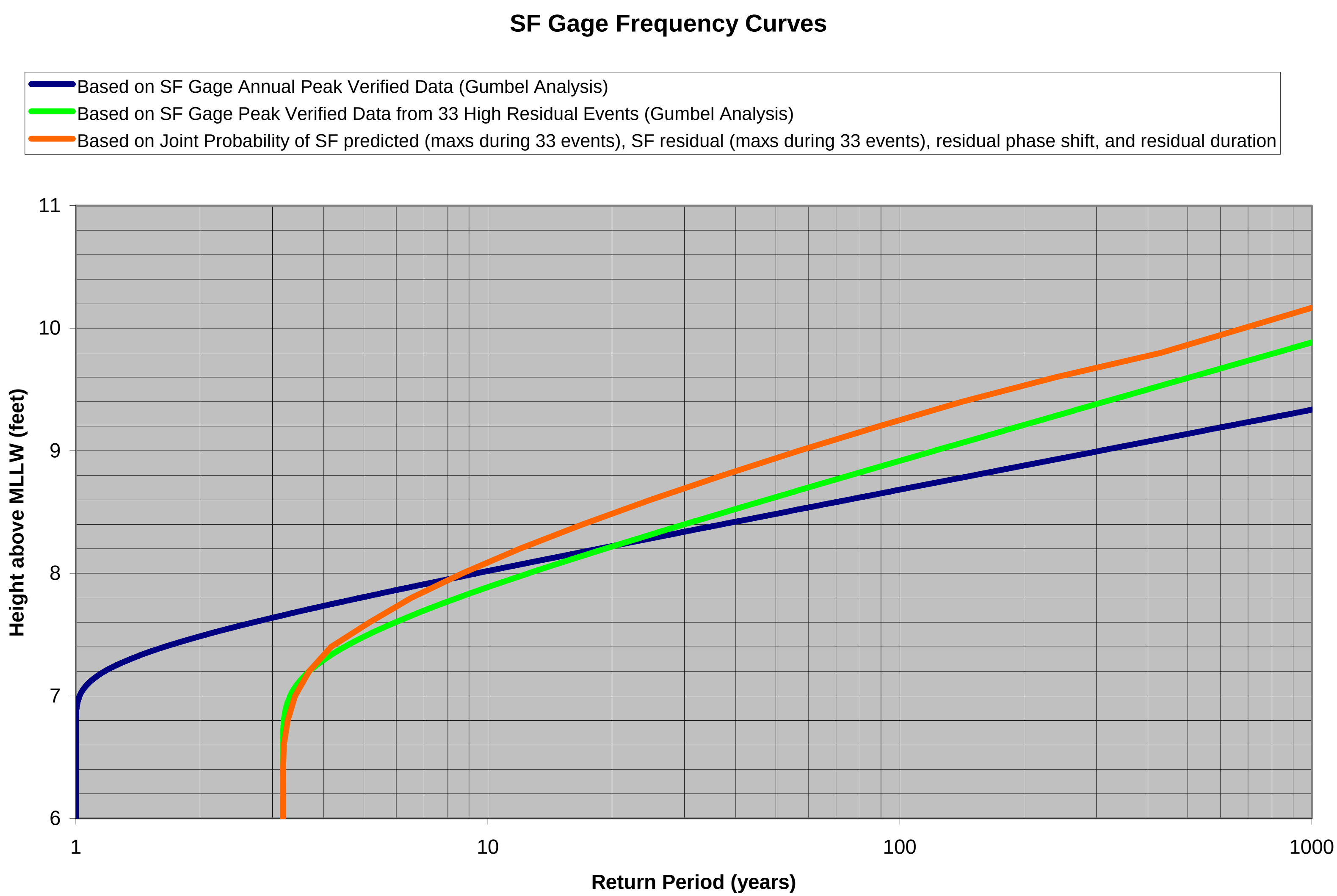
SF Gage Frequency Curves
Based on SF Gage Annual Peak Verified Data (Gumbel Analysis)
Based on SF Gage Peak Verified Data from 33 High Residual Events (Gumbel Analysis)
Based on Joint Probability of SF predicted (maxs during 33 events), SF residual (maxs during 33 events), residual phase shift, and residual duration
Height above MLLW (feet)
11
10
9
8
7
6
1
10
100
1000
Return Period (years)

Plate 2-20

phase (hours)	Synthetic residual event duration									
	2-day (12/6/1987)	3-day (3/10/1904)	3-day (12/3/1983)	4-day (2/2/1915)	4-day (1/13/1969)	5-day (12/2/1952)	5-day (2/19/1993)	6-day (2/9/1915)	8-day (3/12/1906)	8-day (12/24/1940)
0	1	1	1	1	1	1	1	1	1	1
3	0.9734	0.9657	0.96948	0.9791	0.9703	0.98623	0.9823	0.99298	0.981	0.987202
4	0.9605	0.9549	0.96014	0.9709	0.9703	0.9817	0.9771	0.98738	0.9774	0.983952
5	0.9481	0.9443	0.95095	0.9628	0.9703	0.97723	0.972	0.9818	0.9738	0.98072
6	0.9362	0.9339	0.94192	0.9548	0.9703	0.9728	0.9669	0.97633	0.9703	0.977504
8	0.91375	0.9136	0.92434	0.9391	0.9703	0.9641	0.957	0.96546	0.9632	0.983056
17	0.89176	0.898	0.9105	0.8977	0.98766	0.94679	0.9531	0.97697	0.9425	1.010897
18	0.90224	0.908	0.9193	0.9056	0.99353	0.95112	0.958	0.98239	0.9389	1.014078
21	0.93657	0.9393	0.94688	0.9299	1.01181	0.9644	0.9732	0.99889	0.94	1.023724

phase (hours)	Synthetic residual event duration (with 0.5' base residual)		
	2-day (1/29/1983)	3-day (1/27/1983)	6-day (11/18/1982)
0	1	1	1
3	0.9748	0.96962	0.9907
4	0.9675	0.96101	0.9876
5	0.9605	0.95254	0.9845
6	0.9536	0.94423	0.9814
8	0.94034	0.92803	0.9752
17	0.93584	0.958	0.952
18	0.94237	0.9662	0.9551
21	0.96302	0.99156	0.9645

phase (hours	Synthetic residual event duration with 1.0' base residual		
	2-day (2/8/1998)	3-day (2/3/1998)	4-day (3/2/1983)
0	1	1	1
3	0.9677	0.9745	0.9749
4	0.9574	0.9654	0.9703
5	0.9473	0.9564	0.9658
6	0.9375	0.9477	0.9614
8	0.9187	0.9307	0.9526
17	0.922	0.9501	0.9153
18	0.9313	0.9587	0.9114
21	0.9607	0.9856	0.9162

Table 2-4. Decay factor due to phase shift between predicted tide and residual tide for various residual durations

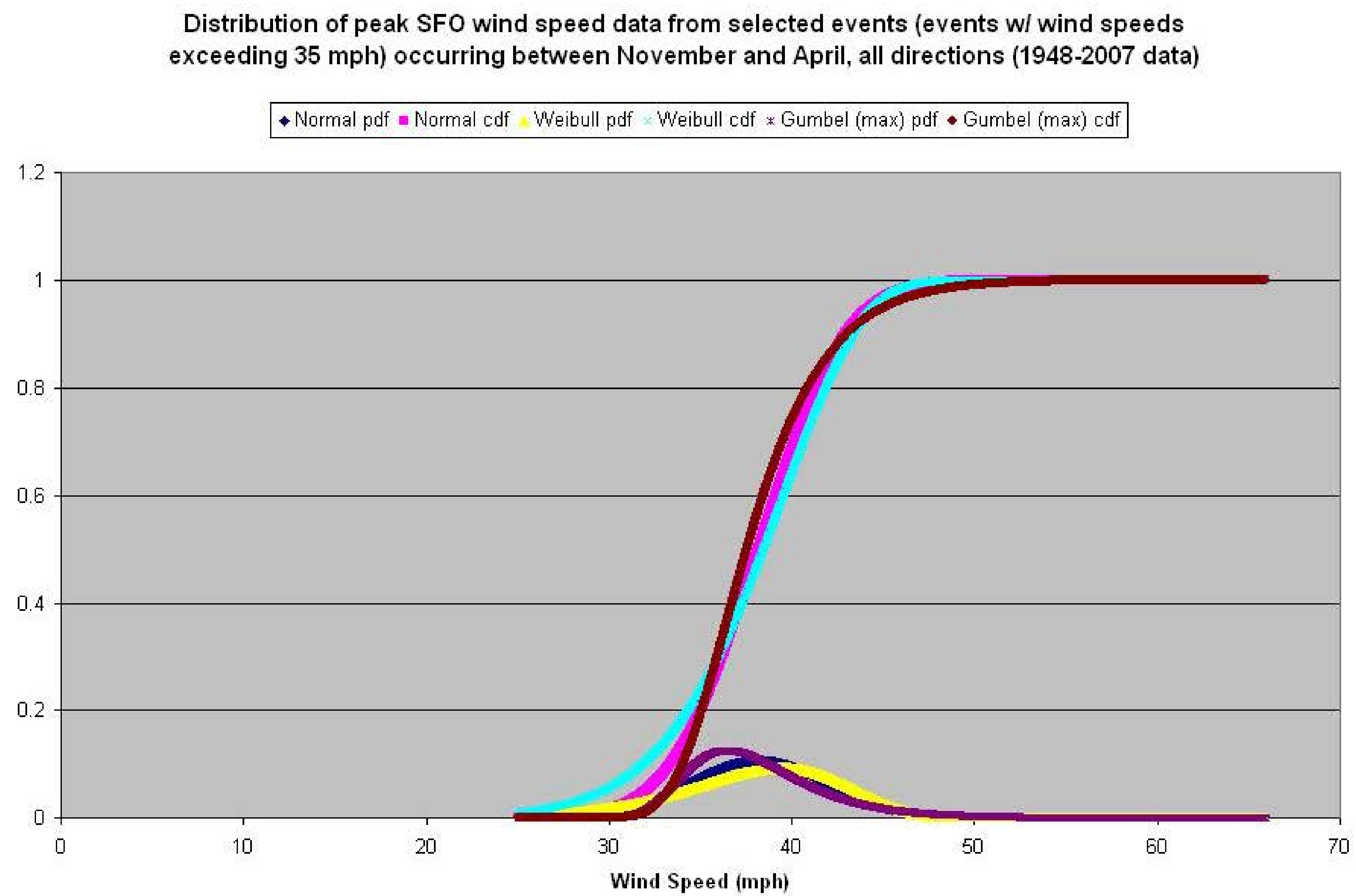
Distribution of peak SFO wind speed data from selected events (events w/ wind speeds exceeding 35 mph) occurring between November and April, all directions (1948-2007 data)
Normal pdf
Normal cdf
Weibull pdf
Weibull cdf
Gumbel (max) pdf
Gumbel (max) cdf
1.2
1
0.8
0.6
0.4
0.2
0
0
10
20
30
40
50
60
70
Wind Speed (mph)

Plate 2-21

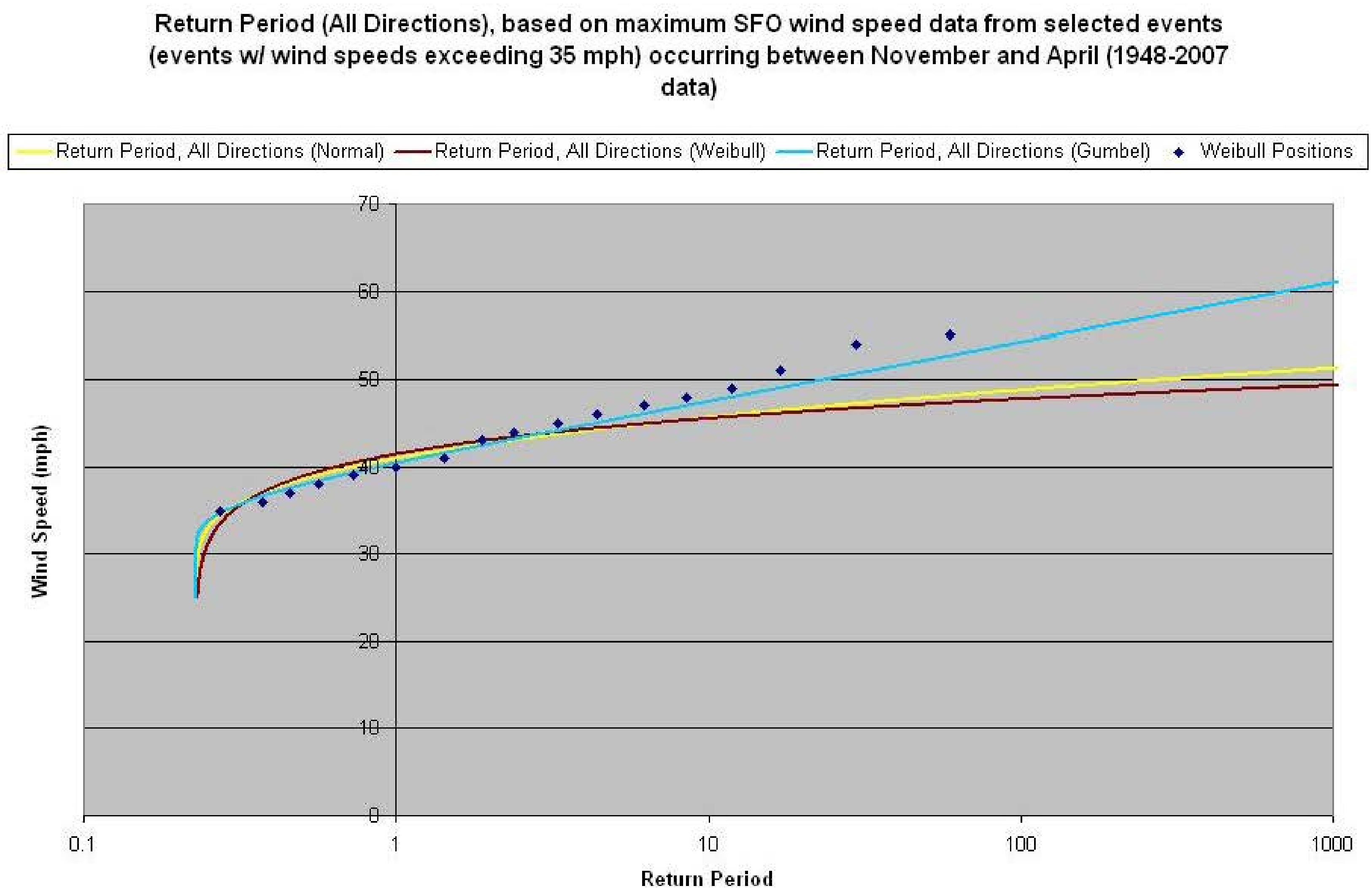

Return Period (All Directions), based on maximum SFO wind speed data from selected events (events w/ wind speeds exceeding 35 mph) occurring between November and April (1948-2007 data)
Return Period, All Directions (Normal)
Return Period, All Directions (Weibull)
Return Period, All Directions (Gumbel)
Weibull Positions
Wind Speed (mph)
70
60
50
40
30
20
10
0
0.1
1
10
100
1000
Return Period

Plate 2-22

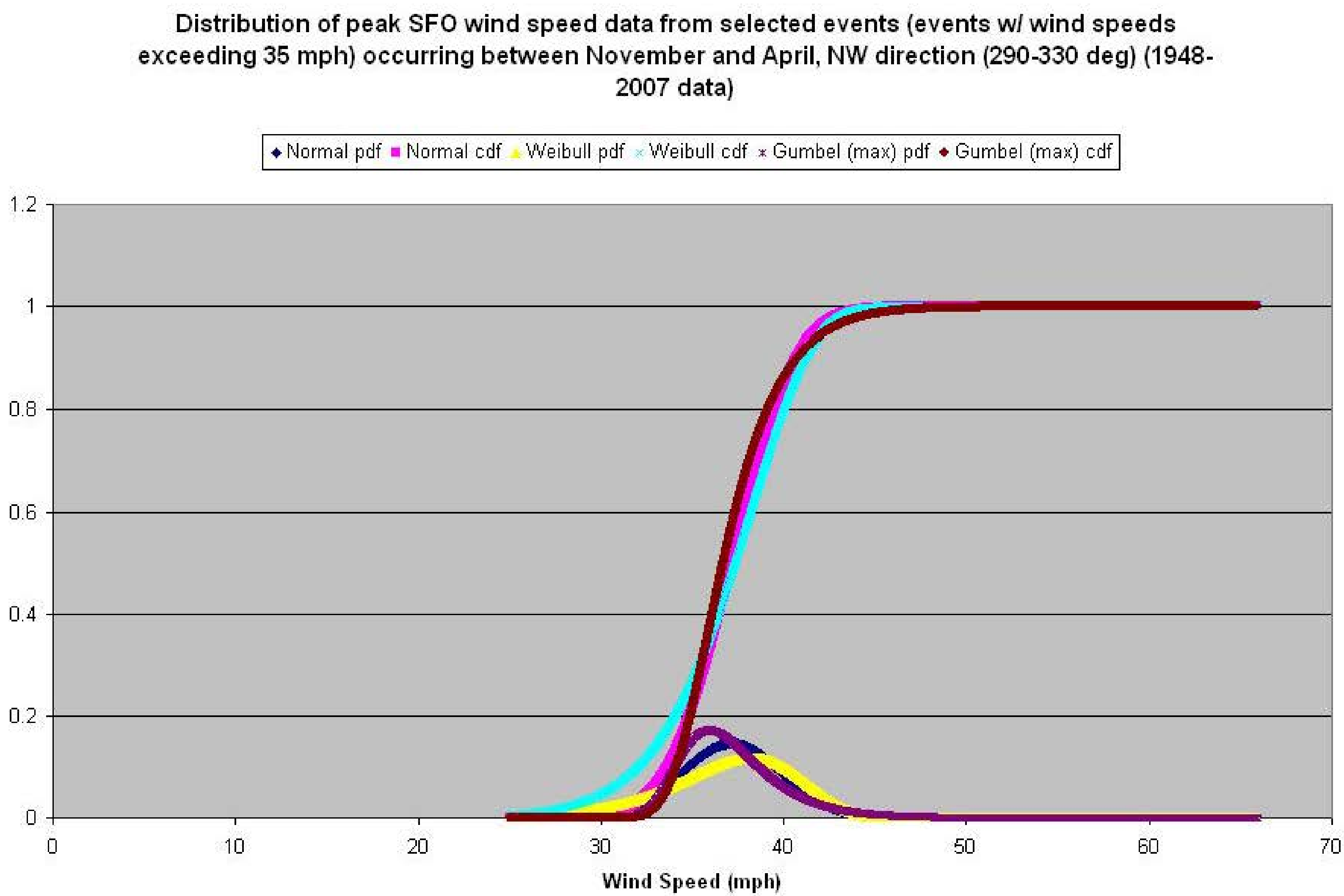

Distribution of peak SFO wind speed data from selected events (events w/ wind speeds exceeding 35 mph) occurring between November and April, NW direction (290-330 deg) (1948-2007 data)
Normal pdf
Normal cdf
Weibull pdf
Weibull cdf
Gumbel (max) pdf
Gumbel (max) cdf
1.2
1
0.8
0.6
0.4
0.2
0
0
10
20
30
40
50
60
70
Wind Speed (mph)

Plate 2-23

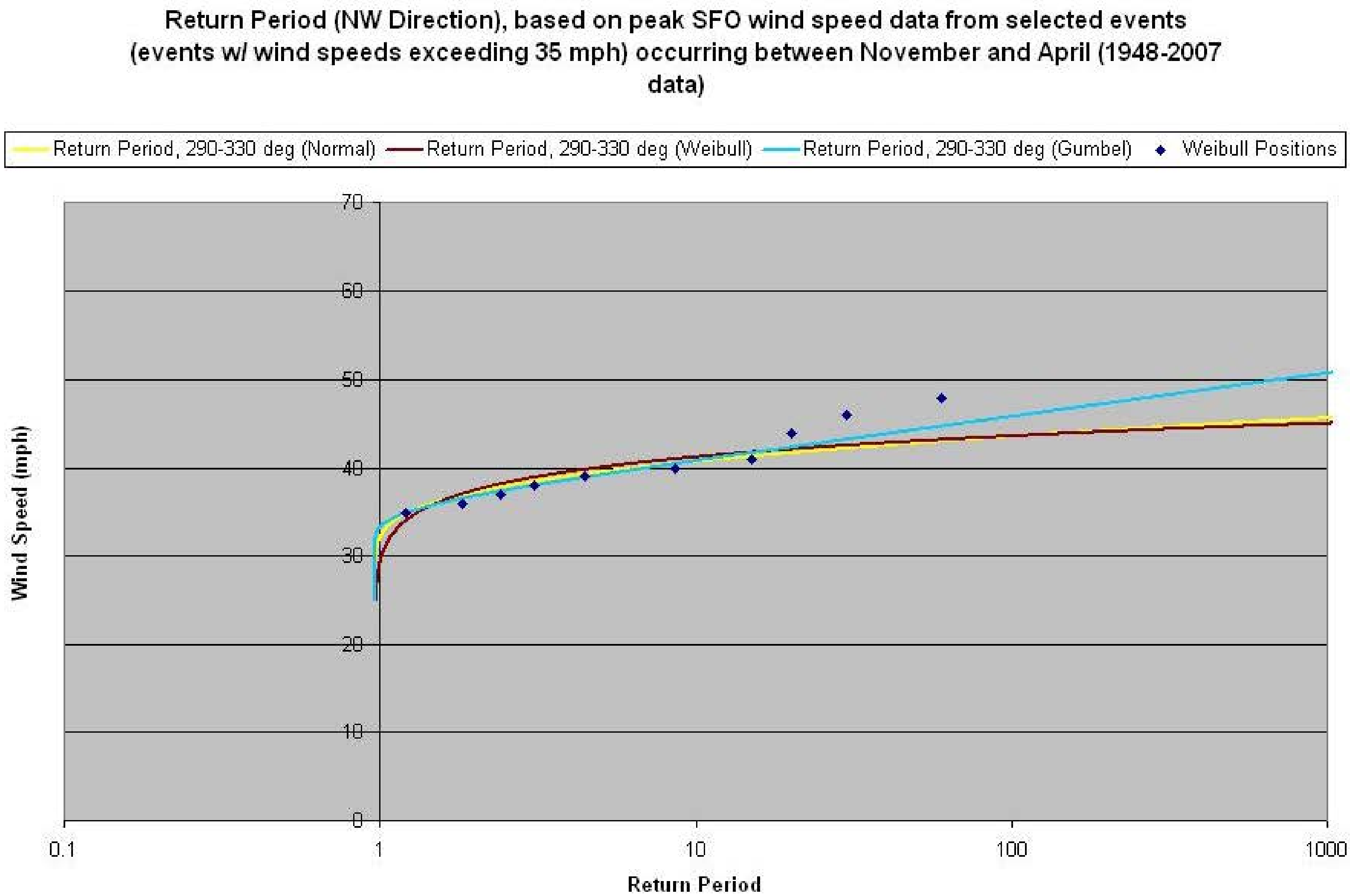

Return Period (NW Direction), based on peak SFO wind speed data from selected events (events w/ wind speeds exceeding 35 mph) occurring between November and April (1948-2007 data)
Return Period, 290-330 deg (Normal)
Return Period, 290-330 deg (Weibull)
Return Period, 290-330 deg (Gumbel)
Weibull Positions
Wind Speed (mph)
70
60
50
40
30
20
10
0
0.1
1
10
100
1000
Return Period

Plate 2-24


Return Period, based on peak SFO wind speed data from selected events (events w/ wind speeds exceeding 35 mph) occurring between November and April (1948-2007 data)
Return Period, All Directions (Gumbel)
Return Period, 290-330 deg (Gumbel)
Wind Speed (mph)
70
60
50
40
30
20
10
0
0.1
1
10
100
1000
Return Period

Plate 2-25

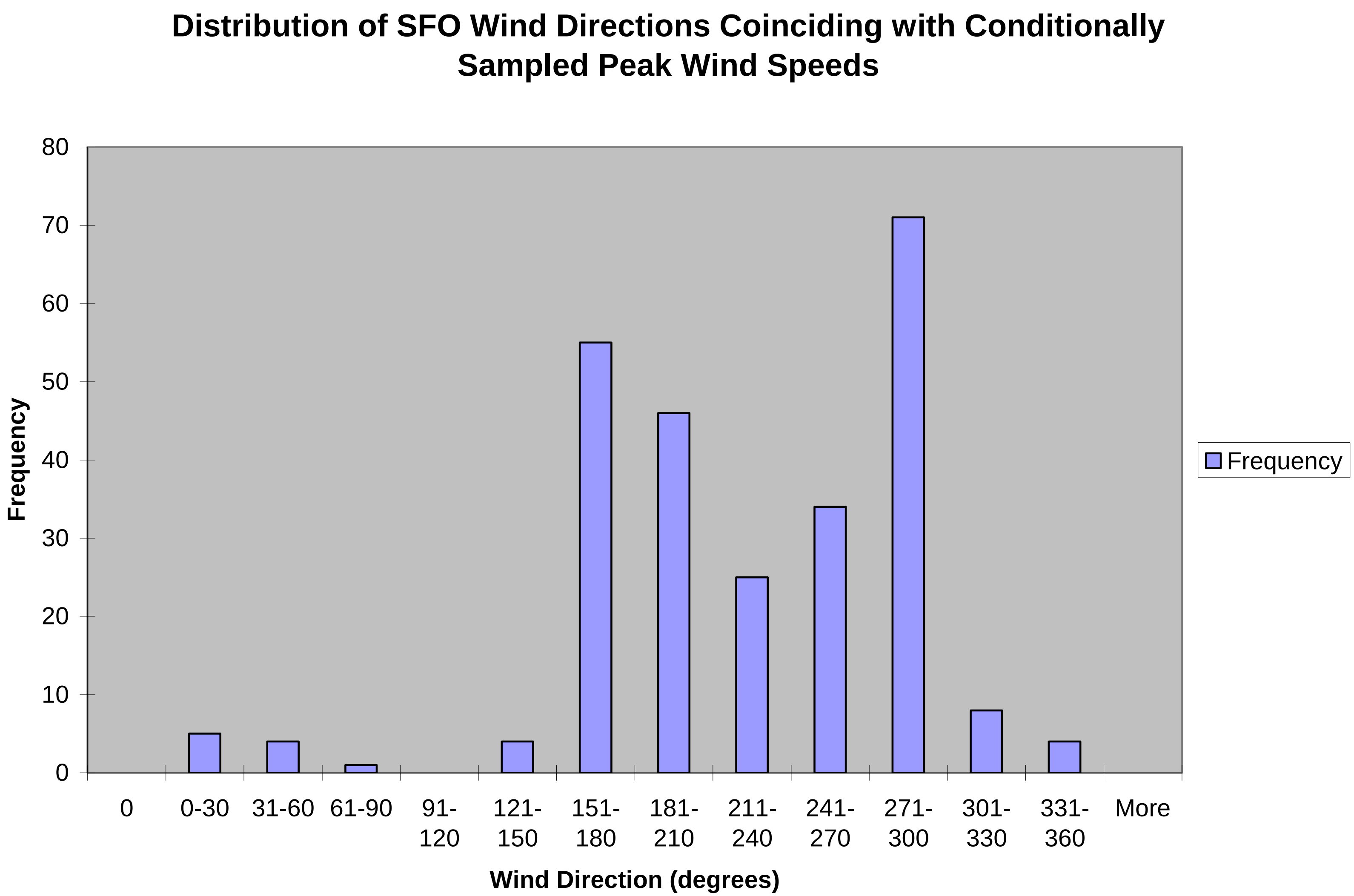
Distribution of SFO Wind Directions Coinciding with Conditionally Sampled Peak Wind Speeds
Frequency
80
70
60
50
40
30
20
10
0
0
0-30
31-60
61-90
91-120
121-150
151-180
181-210
211-240
241-270
271-300
301-330
331-360
More
Wind Direction (degrees)
Frequency

Plate 2-26

Tide Data at San Francisco for 32 Time Series with High Residual Events					
Begin Date	**End Date**	**Maximum verified data value, adjusted for sea level rise (feet MLLW)**	**Time at which maximum verified value occurred**	**Predicted data value at this time (feet MLLW)**	**Residual data value at this time, adjusted for sea level rise (feet MLLW)**
3/9/1904 0:00	3/12/1904 0:00	6.9664	3/10/1904 15:00	5.17	1.7964
3/11/1906 0:00	3/14/1906 0:00	7.0536	3/12/1906 9:00	5.75	1.3036
1/28/1915 0:00	1/31/1915 0:00	7.996	1/29/1915 18:00	6.28	1.716
2/1/1915 0:00	2/4/1915 0:00	7.296	2/2/1915 20:00	5.76	1.536
2/7/1915 0:00	2/10/1915 0:00	7.396	2/9/1915 14:00	6.24	1.156
2/23/1917 0:00	2/26/1917 0:00	7.4532	2/25/1917 10:00	6.25	1.2032
12/25/1921 0:00	12/28/1921 0:00	7.7576	12/25/1921 17:00	6.3	1.4576
12/16/1940 0:00	12/19/1940 0:00	7.276	12/16/1940 20:00	6.09	1.186
12/23/1940 0:00	12/26/1940 0:00	8.076	12/24/1940 15:00	6.43	1.646
2/10/1941 0:00	2/13/1941 0:00	8.0696	2/11/1941 18:00	6.35	1.7196
2/28/1941 0:00	3/3/1941 0:00	7.0696	2/28/1941 21:00	5.15	1.9196
11/30/1952 0:00	12/3/1952 0:00	7.8892	12/1/1952 18:00	6.53	1.3592
2/15/1959 0:00	2/18/1959 0:00	7.3144	2/16/1959 13:00	5.3	2.0144
1/12/1969 0:00	1/15/1969 0:00	7.5504	1/13/1969 14:00	6.23	1.3204
1/15/1973 0:00	1/18/1973 0:00	8.3248	1/16/1973 16:00	6.85	1.4748
1/17/1973 0:00	1/20/1973 0:00	8.1248	1/18/1973 18:00	7.01	1.1148
3/3/1978 0:00	3/6/1978 0:00	7.4328	3/4/1978 15:00	5.98	1.4528
11/17/1982 0:00	11/20/1982 0:00	7.1672	11/18/1982 20:00	5.65	1.5172
11/29/1982 0:00	12/2/1982 0:00	8.0472	11/30/1982 18:00	6.71	1.3372
1/22/1983 0:00	1/25/1983 0:00	7.6708	1/24/1983 15:00	6.2	1.4708
1/26/1983 0:00	1/29/1983 0:00	8.9608	1/27/1983 18:00	7	1.9608
1/28/1983 0:00	1/31/1983 0:00	8.4208	1/28/1983 19:00	7.05	1.3708
3/1/1983 0:00	3/4/1983 0:00	7.8308	3/2/1983 10:00	5.86	1.9708
12/2/1983 0:00	12/5/1983 0:00	8.8508	12/3/1983 18:00	6.59	2.2608
12/5/1987 0:00	12/8/1987 0:00	7.4652	12/6/1987 19:00	6.18	1.2852
2/18/1993 0:00	2/21/1993 0:00	7.4368	2/19/1993 18:00	5.91	1.5268
1/8/1995 0:00	1/11/1995 0:00	7.194	1/10/1995 14:00	5.67	1.524
11/25/1997 0:00	11/28/1997 0:00	7.6112	11/26/1997 17:00	5.75	1.8612
12/5/1997 0:00	12/8/1997 0:00	7.0312	12/7/1997 14:00	5.53	1.5012
2/2/1998 0:00	2/5/1998 0:00	7.9948	2/3/1998 12:00	6.03	1.9648
2/4/1998 0:00	2/7/1998 0:00	8.4748	2/6/1998 16:00	6.07	2.4048
12/14/2002 0:00	12/17/2002 0:00	7.3392	12/16/2002 16:00	5.79	1.5492

Table 3-1

Calculation of Dumbarton Predicted Tide Levels for 32 Time Series with High Residual Events at San Francisco						
1	**2**	**3**	**4**	**5**	**6**	**7**
Begin Date	**End Date**	**Time at which maximum verified value occurred**	**Predicted data value at this time (feet MLLW)**	**Zero mean of predicted SF value [(Column 4) - 3.18] (feet MLLW)**	**Amplification to Dumbarton of SF zero mean predicted [(Column 5) x 1.46] (feet MLLW)**	**Dumbarton predicted data values [(Column 6) + 4.53] (feet MLLW)**
3/9/1904 0:00	3/12/1904 0:00	3/10/1904 15:00	5.17	1.99	2.9054	7.4354
3/11/1906 0:00	3/14/1906 0:00	3/12/1906 9:00	5.75	2.57	3.7522	8.2822
1/28/1915 0:00	1/31/1915 0:00	1/29/1915 18:00	6.28	3.1	4.526	9.056
2/1/1915 0:00	2/4/1915 0:00	2/2/1915 20:00	5.76	2.58	3.7668	8.2968
2/7/1915 0:00	2/10/1915 0:00	2/9/1915 14:00	6.24	3.06	4.4676	8.9976
2/23/1917 0:00	2/26/1917 0:00	2/25/1917 10:00	6.25	3.07	4.4822	9.0122
12/25/1921 0:00	12/28/1921 0:00	12/25/1921 17:00	6.3	3.12	4.5552	9.0852
12/16/1940 0:00	12/19/1940 0:00	12/16/1940 20:00	6.09	2.91	4.2486	8.7786
12/23/1940 0:00	12/26/1940 0:00	12/24/1940 15:00	6.43	3.25	4.745	9.275
2/10/1941 0:00	2/13/1941 0:00	2/11/1941 18:00	6.35	3.17	4.6282	9.1582
2/28/1941 0:00	3/3/1941 0:00	2/28/1941 21:00	5.15	1.97	2.8762	7.4062
11/30/1952 0:00	12/3/1952 0:00	12/1/1952 18:00	6.53	3.35	4.891	9.421
2/15/1959 0:00	2/18/1959 0:00	2/16/1959 13:00	5.3	2.12	3.0952	7.6252
1/12/1969 0:00	1/15/1969 0:00	1/13/1969 14:00	6.23	3.05	4.453	8.983
1/15/1973 0:00	1/18/1973 0:00	1/16/1973 16:00	6.85	3.67	5.3582	9.8882
1/17/1973 0:00	1/20/1973 0:00	1/18/1973 18:00	7.01	3.83	5.5918	10.1218
3/3/1978 0:00	3/6/1978 0:00	3/4/1978 15:00	5.98	2.8	4.088	8.618
11/17/1982 0:00	11/20/1982 0:00	11/18/1982 20:00	5.65	2.47	3.6062	8.1362
11/29/1982 0:00	12/2/1982 0:00	11/30/1982 18:00	6.71	3.53	5.1538	9.6838
1/22/1983 0:00	1/25/1983 0:00	1/24/1983 15:00	6.2	3.02	4.4092	8.9392
1/26/1983 0:00	1/29/1983 0:00	1/27/1983 18:00	7	3.82	5.5772	10.1072
1/28/1983 0:00	1/31/1983 0:00	1/28/1983 19:00	7.05	3.87	5.6502	10.1802
3/1/1983 0:00	3/4/1983 0:00	3/2/1983 10:00	5.86	2.68	3.9128	8.4428
12/2/1983 0:00	12/5/1983 0:00	12/3/1983 18:00	6.59	3.41	4.9786	9.5086
12/5/1987 0:00	12/8/1987 0:00	12/6/1987 19:00	6.18	3	4.38	8.91
2/18/1993 0:00	2/21/1993 0:00	2/19/1993 18:00	5.91	2.73	3.9858	8.5158
1/8/1995 0:00	1/11/1995 0:00	1/10/1995 14:00	5.67	2.49	3.6354	8.1654
11/25/1997 0:00	11/28/1997 0:00	11/26/1997 17:00	5.75	2.57	3.7522	8.2822
12/5/1997 0:00	12/8/1997 0:00	12/7/1997 14:00	5.53	2.35	3.431	7.961
2/2/1998 0:00	2/5/1998 0:00	2/3/1998 12:00	6.03	2.85	4.161	8.691
2/4/1998 0:00	2/7/1998 0:00	2/6/1998 16:00	6.07	2.89	4.2194	8.7494
12/14/2002 0:00	12/17/2002 0:00	12/16/2002 16:00	5.79	2.61	3.8106	8.3406

Table 3-2

One-Hour Residual Lag for 32 Time Series with High Residual Events at San Francisco					
Begin Date	**End Date**	**Time at which maximum verified value occurred**	**Residual data value at this time, adjusted for sea level rise (feet MLLW)**	**Time corresponding to one-hour residual tide phase lag**	**Residual data value at one-hour lag, adjusted for sea level rise (feet MLLW)**
3/9/1904 0:00	3/12/1904 0:00	3/10/1904 15:00	1.7964	3/10/1904 14:00	1.5664
3/11/1906 0:00	3/14/1906 0:00	3/12/1906 9:00	1.3036	3/12/1906 8:00	1.1536
1/28/1915 0:00	1/31/1915 0:00	1/29/1915 18:00	1.716	1/29/1915 17:00	1.586
2/1/1915 0:00	2/4/1915 0:00	2/2/1915 20:00	1.536	2/2/1915 19:00	1.546
2/7/1915 0:00	2/10/1915 0:00	2/9/1915 14:00	1.156	2/9/1915 13:00	1.126
2/23/1917 0:00	2/26/1917 0:00	2/25/1917 10:00	1.2032	2/25/1917 9:00	1.1732
12/25/1921 0:00	12/28/1921 0:00	12/25/1921 17:00	1.4576	12/25/1921 16:00	0.8476
12/16/1940 0:00	12/19/1940 0:00	12/16/1940 20:00	1.186	12/16/1940 19:00	1.016
12/23/1940 0:00	12/26/1940 0:00	12/24/1940 15:00	1.646	12/24/1940 14:00	1.866
2/10/1941 0:00	2/13/1941 0:00	2/11/1941 18:00	1.7196	2/11/1941 17:00	1.4596
2/28/1941 0:00	3/3/1941 0:00	2/28/1941 21:00	1.9196	2/28/1941 20:00	1.7996
11/30/1952 0:00	12/3/1952 0:00	12/1/1952 18:00	1.3592	12/1/1952 17:00	1.1992
2/15/1959 0:00	2/18/1959 0:00	2/16/1959 13:00	2.0144	2/16/1959 12:00	1.9144
1/12/1969 0:00	1/15/1969 0:00	1/13/1969 14:00	1.3204	1/13/1969 13:00	1.5004
1/15/1973 0:00	1/18/1973 0:00	1/16/1973 16:00	1.4748	1/16/1973 15:00	1.6348
1/17/1973 0:00	1/20/1973 0:00	1/18/1973 18:00	1.1148	1/18/1973 17:00	1.1448
3/3/1978 0:00	3/6/1978 0:00	3/4/1978 15:00	1.4528	3/4/1978 14:00	1.4628
11/17/1982 0:00	11/20/1982 0:00	11/18/1982 20:00	1.5172	11/18/1982 19:00	1.5372
11/29/1982 0:00	12/2/1982 0:00	11/30/1982 18:00	1.3372	11/30/1982 17:00	1.5172
1/22/1983 0:00	1/25/1983 0:00	1/24/1983 15:00	1.4708	1/24/1983 14:00	1.0408
1/26/1983 0:00	1/29/1983 0:00	1/27/1983 18:00	1.9608	1/27/1983 17:00	1.5308
1/28/1983 0:00	1/31/1983 0:00	1/28/1983 19:00	1.3708	1/28/1983 18:00	1.2308
3/1/1983 0:00	3/4/1983 0:00	3/2/1983 10:00	1.9708	3/2/1983 9:00	1.9508
12/2/1983 0:00	12/5/1983 0:00	12/3/1983 18:00	2.2608	12/3/1983 17:00	2.0908
12/5/1987 0:00	12/8/1987 0:00	12/6/1987 19:00	1.2852	12/6/1987 18:00	1.3652
2/18/1993 0:00	2/21/1993 0:00	2/19/1993 18:00	1.5268	2/19/1993 17:00	1.4168
1/8/1995 0:00	1/11/1995 0:00	1/10/1995 14:00	1.524	1/10/1995 13:00	1.574
11/25/1997 0:00	11/28/1997 0:00	11/26/1997 17:00	1.8612	11/26/1997 16:00	1.9012
12/5/1997 0:00	12/8/1997 0:00	12/7/1997 14:00	1.5012	12/7/1997 13:00	1.3812
2/2/1998 0:00	2/5/1998 0:00	2/3/1998 12:00	1.9648	2/3/1998 11:00	2.1148
2/4/1998 0:00	2/7/1998 0:00	2/6/1998 16:00	2.4048	2/6/1998 15:00	2.0648
12/14/2002 0:00	12/17/2002 0:00	12/16/2002 16:00	1.5492	12/16/2002 15:00	1.7992

Table 3-3

Maximum Tide Stage at Dumbarton for 32 Time Series with High Residual Events at San Francisco				
Begin Date	**End Date**	**Predicted tide elevations from Table III-2 (feet MLLW)**	**Residual Tide Heights from Table III-3 (feet MLLW)**	**Dumbarton Tidal Stage (feet MLLW)**
3/9/1904 0:00	3/12/1904 0:00	7.4354	1.5664	9.0018
3/11/1906 0:00	3/14/1906 0:00	8.2822	1.1536	9.4358
1/28/1915 0:00	1/31/1915 0:00	9.056	1.586	10.642
2/1/1915 0:00	2/4/1915 0:00	8.2968	1.546	9.8428
2/7/1915 0:00	2/10/1915 0:00	8.9976	1.126	10.1236
2/23/1917 0:00	2/26/1917 0:00	9.0122	1.1732	10.1854
12/25/1921 0:00	12/28/1921 0:00	9.0852	0.8476	9.9328
12/16/1940 0:00	12/19/1940 0:00	8.7786	1.016	9.7946
12/23/1940 0:00	12/26/1940 0:00	9.275	1.866	11.141
2/10/1941 0:00	2/13/1941 0:00	9.1582	1.4596	10.6178
2/28/1941 0:00	3/3/1941 0:00	7.4062	1.7996	9.2058
11/30/1952 0:00	12/3/1952 0:00	9.421	1.1992	10.6202
2/15/1959 0:00	2/18/1959 0:00	7.6252	1.9144	9.5396
1/12/1969 0:00	1/15/1969 0:00	8.983	1.5004	10.4834
1/15/1973 0:00	1/18/1973 0:00	9.8882	1.6348	11.523
1/17/1973 0:00	1/20/1973 0:00	10.1218	1.1448	11.2666
3/3/1978 0:00	3/6/1978 0:00	8.618	1.4628	10.0808
11/17/1982 0:00	11/20/1982 0:00	8.1362	1.5372	9.6734
11/29/1982 0:00	12/2/1982 0:00	9.6838	1.5172	11.201
1/22/1983 0:00	1/25/1983 0:00	8.9392	1.0408	9.98
1/26/1983 0:00	1/29/1983 0:00	10.1072	1.5308	11.638
1/28/1983 0:00	1/31/1983 0:00	10.1802	1.2308	11.411
3/1/1983 0:00	3/4/1983 0:00	8.4428	1.9508	10.3936
12/2/1983 0:00	12/5/1983 0:00	9.5086	2.0908	11.5994
12/5/1987 0:00	12/8/1987 0:00	8.91	1.3652	10.2752
2/18/1993 0:00	2/21/1993 0:00	8.5158	1.4168	9.9326
1/8/1995 0:00	1/11/1995 0:00	8.1654	1.574	9.7394
11/25/1997 0:00	11/28/1997 0:00	8.2822	1.9012	10.1834
12/5/1997 0:00	12/8/1997 0:00	7.961	1.3812	9.3422
2/2/1998 0:00	2/5/1998 0:00	8.691	2.1148	10.8058
2/4/1998 0:00	2/7/1998 0:00	8.7494	2.0648	10.8142
12/14/2002 0:00	12/17/2002 0:00	8.3406	1.7992	10.1398

Table 3-4

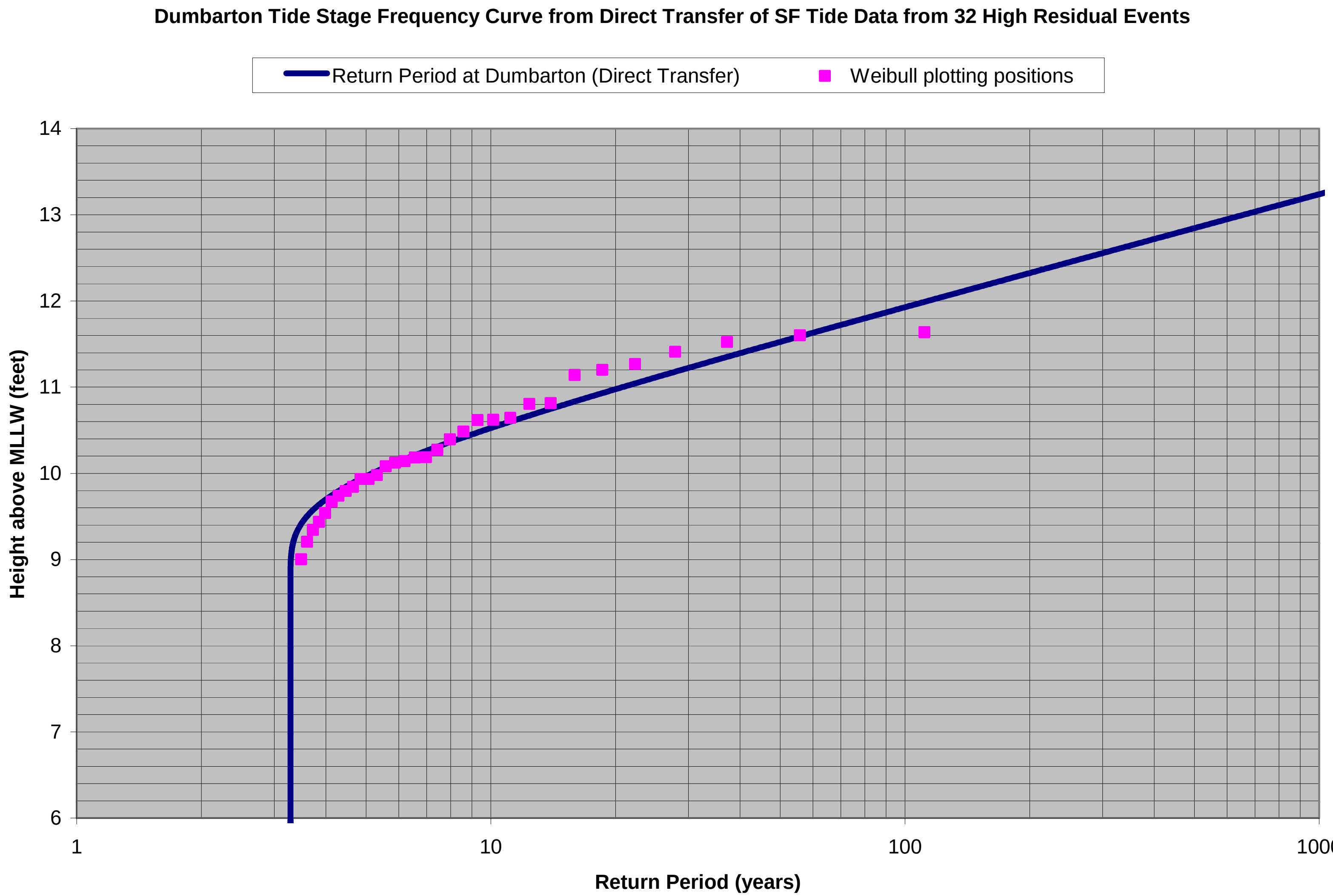
Dumbarton Tide Stage Frequency Curve from Direct Transfer of SF Tide Data from 32 High Residual Events
Return Period at Dumbarton (Direct Transfer)
Weibull plotting positions
Height above MLLW (feet)
14
13
12
11
10
9
8
7
6
1
10
100
1000
Return Period (years)

Plate 3-1

Statistical distribution of the convolution of amplified SF predicted tide and SF residual tide from 33 high residual events

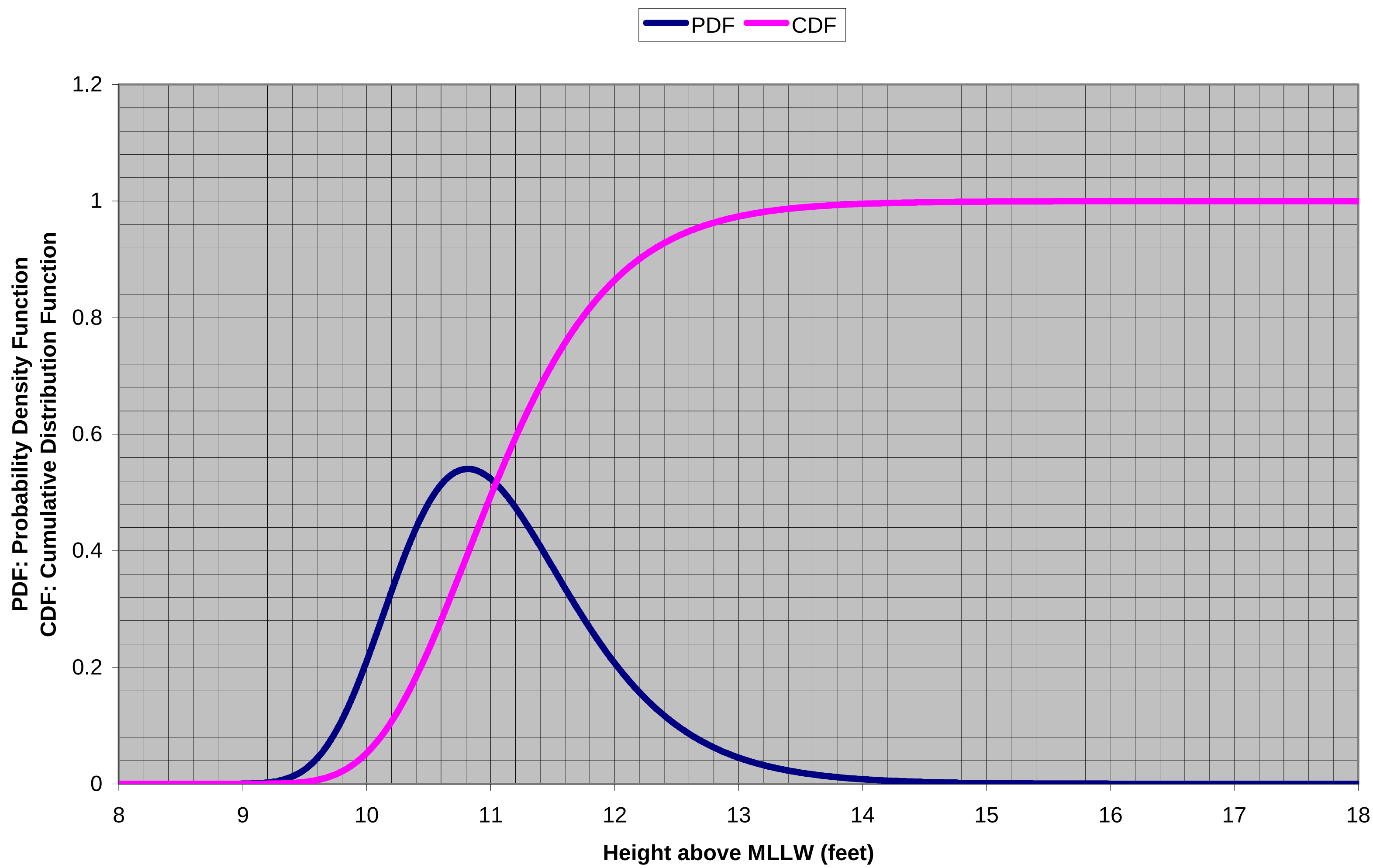

Plate 3-2

Probabilities for different combinations of synthetic residual phase shift and synthetic residual event duration																
Phase		**Event Duration (days)**														
Shift		**2**	**3**	**4**	**5**	**6**	**8**	**2'**	**3'**	**4'**	**6'**	**2"**	**3"**	**4"**	**6"**	
(hours)	**probability**	**1/33**	**6/33**	**6/33**	**3/33**	**4/33**	**2/33**	**1/33**	**1/33**	**2/33**	**1/33**	**1/33**	**2/33**	**2/33**	**1/33**	**33/33**
0	**3/33**	3/1089	18/1089	18/1089	9/1089	12/1089	6/1089	3/1089	3/1089	6/1089	3/1089	3/1089	6/1089	6/1089	3/1089	
3	**1/33**	1/1089	6/1089	6/1089	3/1089	4/1089	2/1089	1/1089	1/1089	2/1089	1/1089	1/1089	2/1089	2/1089	1/1089	
4	**4/33**	4/1089	24/1089	24/1089	12/1089	16/1089	8/1089	4/1089	4/1089	8/1089	4/1089	4/1089	8/1089	8/1089	4/1089	
5	**2/33**	2/1089	12/1089	12/1089	6/1089	8/1089	4/1089	2/1089	2/1089	4/1089	2/1089	2/1089	4/1089	4/1089	2/1089	
6	**5/33**	5/1089	30/1089	30/1089	15/1089	20/1089	10/1089	5/1089	5/1089	10/1089	5/1089	5/1089	10/1089	10/1089	5/1089	
8	**2/33**	2/1089	12/1089	12/1089	6/1089	8/1089	4/1089	2/1089	2/1089	4/1089	2/1089	2/1089	4/1089	4/1089	2/1089	
17	**1/33**	1/1089	6/1089	6/1089	3/1089	4/1089	2/1089	1/1089	1/1089	2/1089	1/1089	1/1089	2/1089	2/1089	1/1089	
18	**13/33**	13/1089	78/1089	78/1089	39/1089	52/1089	26/1089	13/1089	13/1089	26/1089	13/1089	13/1089	26/1089	26/1089	13/1089	
21	**2/33**	2/1089	12/1089	12/1089	6/1089	8/1089	4/1089	2/1089	2/1089	4/1089	2/1089	2/1089	4/1089	4/1089	2/1089	
	33/33															

' = add 0.5 feet to residual tide data
" = add 1 foot to residual tide data

Table 3-5

Dumbarton Probabilities for the Convolution of Amplified SF Predicted Tide and SF Residual Tide		
1	**2**	**3**
Elevation (feet MLLW)	**Probability value read from Dumbarton pdf in Plate III-2**	**Probability at this elevation [(Column 2) x 0.2]**
8.1	0	0
8.3	2.97427E-10	5.94853E-11
8.5	5.48082E-08	1.09616E-08
8.7	3.24191E-06	6.48383E-07
8.9	7.76332E-05	1.55266E-05
9.1	0.000905275	0.000181055
9.3	0.005953936	0.001190787
9.5	0.024824115	0.004964823
9.7	0.072005405	0.014401081
9.9	0.156456654	0.031291331
10.1	0.270087989	0.054017598
10.3	0.388164758	0.077632952
10.5	0.482043661	0.096408732
10.7	0.532807483	0.106561497
10.9	0.536654418	0.107330884
11.1	0.501878645	0.100375729
11.3	0.442347228	0.088469446
11.5	0.371837037	0.074367407
11.7	0.300943642	0.060188728
11.9	0.236291816	0.047258363
12.1	0.181080089	0.036216018
12.3	0.136098525	0.027219705
12.5	0.100711825	0.020142365
12.7	0.073603999	0.0147208
12.9	0.053259707	0.010651941
13.1	0.038233244	0.007646649
13.3	0.027272534	0.005454507
13.5	0.01935579	0.003871158
13.7	0.013681873	0.002736375
13.9	0.009640251	0.00192805
14.1	0.006775267	0.001355053
14.3	0.004752138	0.000950428
14.5	0.003327814	0.000665563
14.7	0.002327459	0.000465492
14.9	0.001626199	0.00032524
15.1	0.001135339	0.000227068
15.3	0.000792156	0.000158431
15.5	0.000552441	0.000110488
15.7	0.000385121	7.70242E-05
15.9	0.000268398	5.36797E-05
16.1	0.000187009	3.74017E-05
16.3	0.000130276	2.60552E-05
16.5	9.07416E-05	1.81483E-05
16.7	6.31976E-05	1.26395E-05
16.9	4.40106E-05	8.80211E-06
17.1	3.06468E-05	6.12935E-06
17.3	2.13398E-05	4.26795E-06
17.5	1.48586E-05	2.97172E-06
17.7	1.03455E-05	2.0691E-06

Table 3-6

1	2	3	4	5	6	7	8
Dumbarton tide stage (w/o decay factor)	**Probability for the convolution of amplified SF predicted tide and SF residual tide (from Table III-6)**	**Decay factor**	**Dumbarton stage (w/ decay factor)**	**Duration (days)**	**Phase shift (hours)**	**Prob(Duration) x Prob(Phase) (from Table III-5)**	**Joint probability of amplified SF predicted tide, SF residual tide, synthetic residual phase shift, and synthetic residual event duration [(Column 2) x (Column 7)]**
10.7	0.106561497	1	10.7	3"	0	6/1089	0.000587116
10.7	0.106561497	0.97	10.379	3"	3	2/1089	0.000195705
10.7	0.106561497	0.97	10.379	3"	4	8/1089	0.000782821
10.7	0.106561497	0.96	10.272	3"	5	4/1089	0.00039141
10.7	0.106561497	0.95	10.165	3"	6	10/1089	0.000978526
10.7	0.106561497	0.93	9.951	3"	8	4/1089	0.00039141
10.7	0.106561497	0.95	10.165	3"	17	2/1089	0.000195705
10.7	0.106561497	0.96	10.272	3"	18	26/1089	0.002544168
10.7	0.106561497	0.98	10.486	3"	21	4/1089	0.00039141
10.7	0.106561497	1	10.7	4"	0	6/1089	0.000587116
10.7	0.106561497	0.97	10.379	4"	3	2/1089	0.000195705
10.7	0.106561497	0.97	10.379	4"	4	8/1089	0.000782821
10.7	0.106561497	0.97	10.379	4"	5	4/1089	0.00039141
10.7	0.106561497	0.96	10.272	4"	6	10/1089	0.000978526
10.7	0.106561497	0.95	10.165	4"	8	4/1089	0.00039141
10.7	0.106561497	0.92	9.844	4"	17	2/1089	0.000195705
10.7	0.106561497	0.91	9.737	4"	18	26/1089	0.002544168
10.7	0.106561497	0.92	9.844	4"	21	4/1089	0.00039141
10.7	0.106561497	1	10.7	6"	0	3/1089	0.000293558
10.7	0.106561497	0.98	10.486	6"	3	1/1089	9.78526E-05
10.7	0.106561497	0.98	10.486	6"	4	4/1089	0.00039141
10.7	0.106561497	0.98	10.486	6"	5	2/1089	0.000195705
10.7	0.106561497	0.97	10.379	6"	6	5/1089	0.000489263
10.7	0.106561497	0.97	10.379	6"	8	2/1089	0.000195705
10.7	0.106561497	0.96	10.272	6"	17	1/1089	9.78526E-05
10.7	0.106561497	0.96	10.272	6"	18	13/1089	0.001272084
10.7	0.106561497	0.96	10.272	6"	21	2/1089	0.000195705
10.9	0.107330884	1	10.9	2	0	3/1089	0.000295677
10.9	0.107330884	0.97	10.573	2	3	1/1089	9.85591E-05
10.9	0.107330884	0.96	10.464	2	4	4/1089	0.000394236
10.9	0.107330884	0.95	10.355	2	5	2/1089	0.000197118
10.9	0.107330884	0.94	10.246	2	6	5/1089	0.000492796
10.9	0.107330884	0.91	9.919	2	8	2/1089	0.000197118
10.9	0.107330884	0.89	9.701	2	17	1/1089	9.85591E-05
10.9	0.107330884	0.9	9.81	2	18	13/1089	0.001281269
10.9	0.107330884	0.94	10.246	2	21	2/1089	0.000197118
10.9	0.107330884	1	10.9	3	0	18/1089	0.001774064
10.9	0.107330884	0.97	10.573	3	3	6/1089	0.000591355
10.9	0.107330884	0.96	10.464	3	4	24/1089	0.002365419
10.9	0.107330884	0.95	10.355	3	5	12/1089	0.001182709

Table 3-7. Partial table demonstrating the calculation of joint probabilities for Dumbarton tide stage

Dumbarton Tide Stage Return Period from Joint Probability of Amplified SF Predicted Tide, SF Residual Tide, Synthetic Residual Phase Shift, and Synthetic Residual Event Duration					
Elevation Range	**Elevation**	**PDF**	**CDF**	**Exceedance Probability**	**Return Period**
7.1-7.3	7.2	0	0	1	3.181818182
7.3-7.5	7.4	7.64733E-13	7.64733E-13	1	3.181818182
7.5-7.7	7.6	1.48186E-10	1.48951E-10	1	3.181818182
7.7-7.9	7.8	9.68944E-09	9.83839E-09	0.99999999	3.181818213
7.9-8.1	8	9.43944E-07	9.53782E-07	0.999999046	3.181821217
8.1-8.3	8.2	1.07475E-05	1.17013E-05	0.999988299	3.181855414
8.3-8.5	8.4	7.94625E-05	9.11639E-05	0.999908836	3.182108275
8.5-8.7	8.6	0.000404481	0.000495644	0.999504356	3.183396014
8.7-8.9	8.8	0.001530922	0.002026566	0.997973434	3.188279441
8.9-9.1	9	0.005201633	0.007228199	0.992771801	3.204984447
9.1-9.3	9.2	0.016277134	0.023505333	0.976494667	3.258408151
9.3-9.5	9.4	0.028108332	0.051613666	0.948386334	3.354981052
9.5-9.7	9.6	0.051722701	0.103336367	0.896663633	3.548508118
9.7-9.9	9.8	0.075524678	0.178861045	0.821138955	3.874883978
9.9-10.1	10	0.087322177	0.266183222	0.733816778	4.335984508
10.1-10.3	10.2	0.101560688	0.36774391	0.63225609	5.032483251
10.3-10.5	10.4	0.102019486	0.469763396	0.530236604	6.00075166
10.5-10.7	10.6	0.099598661	0.569362057	0.430637943	7.388615501
10.7-10.9	10.8	0.089311501	0.658673558	0.341326442	9.321921147
10.9-11.1	11	0.076515152	0.73518871	0.26481129	12.01541738
11.1-11.3	11.2	0.063309623	0.798498333	0.201501667	15.79053029
11.3-11.5	11.4	0.059012506	0.857510839	0.142489161	22.33024717
11.5-11.7	11.6	0.037321293	0.894832132	0.105167868	30.2546609
11.7-11.9	11.8	0.028385684	0.923217816	0.076782184	41.43953748
11.9-12.1	12	0.021213967	0.944431783	0.055568217	57.25967778
12.1-12.3	12.2	0.015751837	0.96018362	0.03981638	79.91229157
12.3-12.5	12.4	0.01135094	0.97153456	0.02846544	111.7782895
12.5-12.7	12.6	0.008433354	0.979967914	0.020032086	158.8360884
12.7-12.9	12.8	0.005799931	0.985767845	0.014232155	223.5654537
12.9-13.1	13	0.004647	0.990414845	0.009585155	331.95272
13.1-13.3	13.2	0.002793948	0.993208793	0.006791207	468.5202723
13.3-13.5	13.4	0.001955583	0.995164376	0.004835624	657.9953989
13.5-13.7	13.6	0.001376448	0.996540825	0.003459175	919.8198325
13.7-13.9	13.8	0.000987223	0.997528047	0.002471953	1287.16801
13.9-14.1	14	0.000671275	0.998199322	0.001800678	1767.011249
14.1-14.3	14.2	0.000472253	0.998671575	0.001328425	2395.180415
14.3-14.5	14.4	0.000366567	0.999038142	0.000961858	3307.990815
14.5-14.7	14.6	0.000217219	0.999255361	0.000744639	4272.965608
14.7-14.9	14.8	0.000151595	0.999406956	0.000593044	5365.227444
14.9-15.1	15	0.000105749	0.999512705	0.000487295	6529.552333
15.1-15.3	15.2	8.0468E-05	0.999593173	0.000406827	7821.059816
15.3-15.5	15.4	4.93548E-05	0.999642528	0.000357472	8900.882374
15.5-15.7	15.6	3.5124E-05	0.999677652	0.000322348	9870.749325
15.7-15.9	15.8	2.37396E-05	0.999701391	0.000298609	10655.48046
15.9-16.1	16	1.688E-05	0.999718271	0.000281729	11293.91427
16.1-16.3	16.2	1.13951E-05	0.999729667	0.000270333	11769.97417
16.3-16.5	16.4	7.75996E-06	0.999737426	0.000262574	12117.81763
16.5-16.7	16.6	5.37875E-06	0.999742805	0.000257195	12371.23946
16.7-16.9	16.8	3.66209E-06	0.999746467	0.000253533	12549.933
16.9-17.1	17	2.29066E-06	0.999748758	0.000251242	12664.35502
17.1-17.3	17.2	1.35154E-06	0.99975011	0.00024989	12732.8508
17.3-17.5	17.4	7.49223E-07	0.999750859	0.000249141	12771.14131
17.5-17.7	17.6	2.584E-07	0.999751117	0.000248883	12784.4008

Table 3-8

Dumbarton Tide Stage Frequency Curve from Joint Probability of Amplified SF Predicted Tide, SF Residual Tide, Synthetic Residual Phase Shift, and Synthetic Residual Event Duration

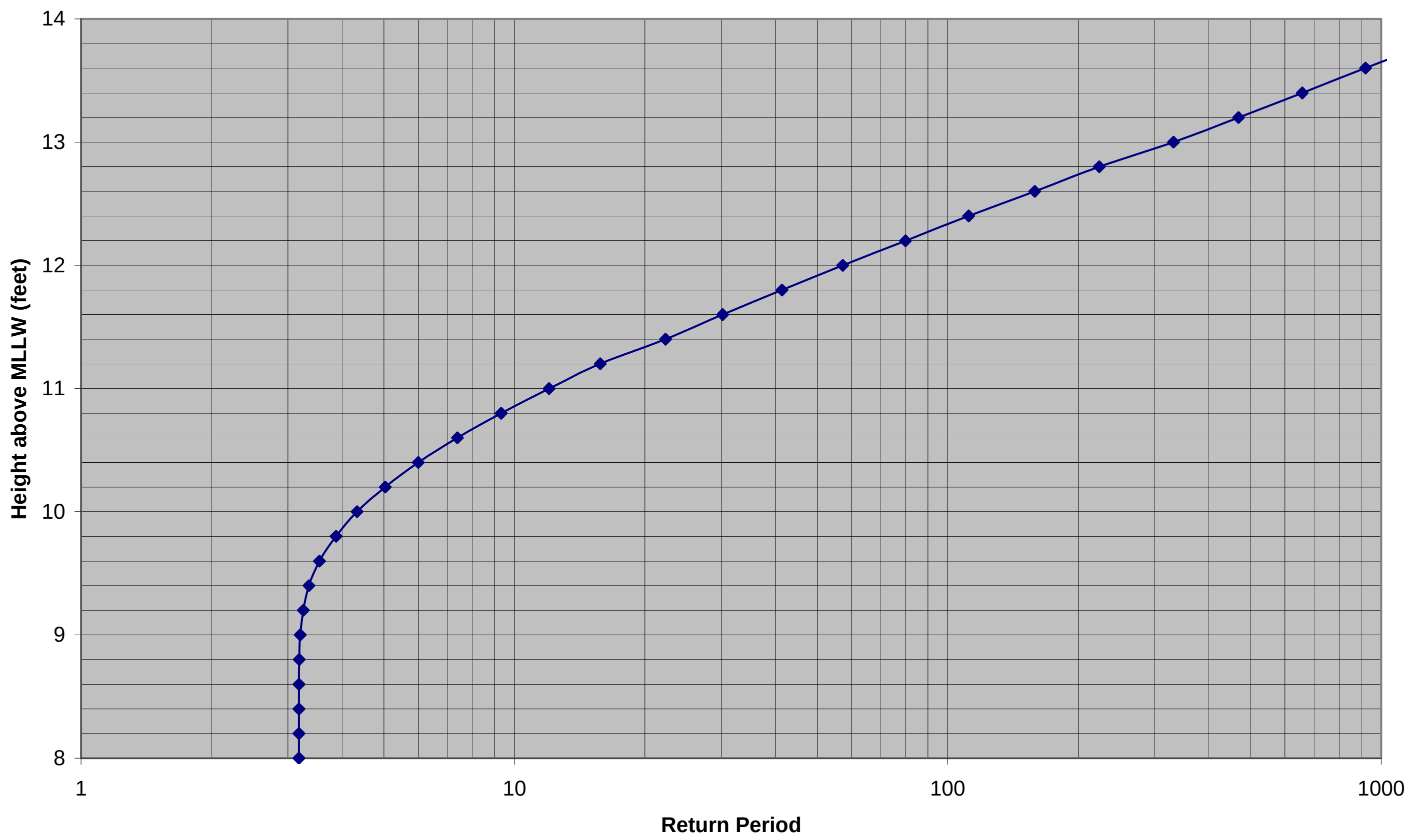

Plate 3-3

ANNEX 3: SOUTH SAN FRANCISCO BAY LONG WAVE MODELING REPORT

SOUTH SAN FRANCISCO BAY SHORELINE STUDY

South San Francisco Bay Long Wave Modeling Report

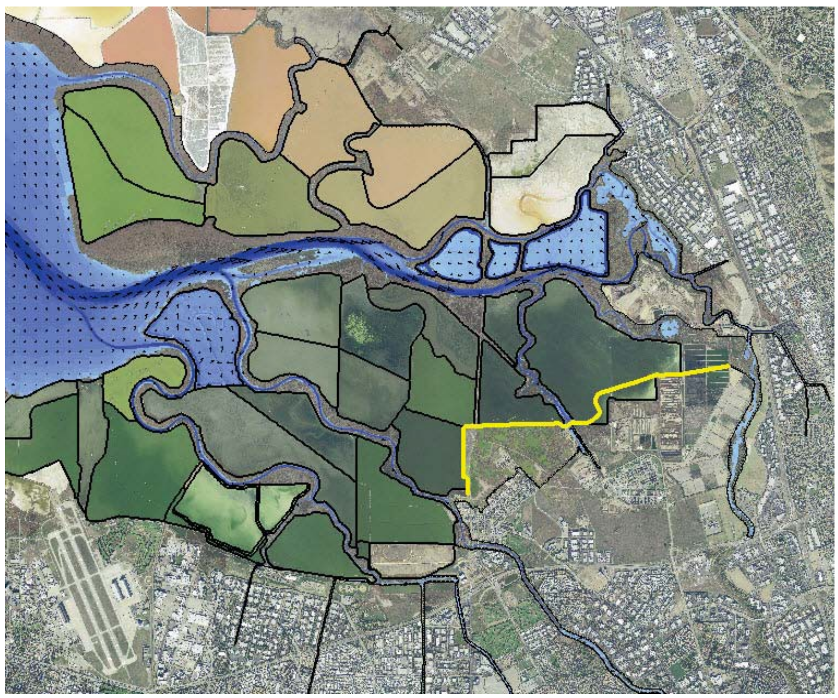

Prepared For:

U.S. Army Corps of Engineers
San Francisco District

Prepared By:

Michael L. MacWilliams, Ph.D., Nina E. Kilham, Ph.D., Aaron J. Bever, Ph.D.

DELTA MODELING ASSOCIATES

Due to its large size, Annex 3 of Appendix E of the South San Francisco Bay Shoreline Study, Phase 1, Alviso Economic Impact Area report, will be provided under its own separate cover.

ANNEX 4: MONTE CARLO SIMULATION REPORT

Monte Carlo Simulation Under With Project Conditions For South San Francisco Bay Shoreline Study

Final Summary Report

Prepared For:
U.S. Army Corps of Engineers
San Francisco District

Prepared By:
Noble Consultants, Inc.

July 2012

Due to its large size, Annex 4 of Appendix E of the South San Francisco Bay Shoreline Study, Phase 1, Alviso Economic Impact Area report, will be provided under its own separate cover.

REPORT DOCUMENTATION PAGE	*Form Approved*

The public reporting burden for this collection of information is estimated to average 1 hour per response, including the time for reviewing instructions, searching existing data sources, gathering and maintaining the data needed, and completing and reviewing the collection of information. Send comments regarding this burden estimate or any other aspect of this collection of information, including suggestions for reducing the burden, to the Department of Defense, Executive Service Directorate (0704-0188). Respondents should be aware that notwithstanding any other provision of law, no person shall be subject to any penalty for failing to comply with a collection of information if it does not display a currently valid OMS control number.

1. REPORT DATE *(00-MM-YYYY)* ,2. REPORT TYPE	3. DATES COVERED *(From- To)*
4. TITLE AND SUBTITLE South San Francisco Bay Shoreline Study, Phase 1, Alviso Economic Impact Area; Appendix E: Water Resources Engineering	5a. CONTRACT NUMBER 5b. GRANT NUMBER 5c. PROGRAM ELEMENT NUMBER
6. AUTHOR(S) Lisa Andes, Craig Conner, Patrick O'Brien, Benjamin Snyder, and Frank Wu	5d. PROJECT NUMBER 5e. TASK NUMBER 5f. WORK UNIT NUMBER
7. PERFORMING ORGANIZATION NAME(S) AND ADDRESS(ES) U.S. Army Corps of Engineers, San Francisco District 1455 Market Street San Francisco, CA 94103, USA	8. PERFORMING ORGANIZATION REPORT NUMBER
9. SPONSORING/MONITORING AGENCY NAME(S) AND ADDRESS(ES) U.S. Army Corps of Engineers, San Francisco District 1455 Market Street	10. SPONSOR/MONITOR'S ACRONYM(S) 11. SPONSOR/MONITOR'S REPORT NUMBER(S)

12. DISTRIBUTION/AVAILABILITY STATEMENT

13. SUPPLEMENTARY NOTES

14. ABSTRACT

15. SUBJECT TERMS

16. SECURITY CLASSIFICATION OF: a. REPORT	b. ABSTRACT	c. THIS PAGE	17. LIMITATION OF ABSTRACT	18. NUMBER OF PAGES	19a. NAME OF RESPONSIBLE PERSON 19b. TELEPHONE NUMBER *(Include area code)*
				124	